Commun. Math. Phys. 332, 117–188 (2014)
Digital Object Identifier (DOI) 10.1007/s00220-014-2142-6

Communications in
Mathematical Physics

Renormalizable Models in Rank $d \geq 2$ Tensorial Group Field Theory

Joseph Ben Geloun[1,2]

[1] Perimeter Institute for Theoretical Physics, 31 Caroline St, Waterloo, ON, Canada.
E-mail: jobengeloun@gmail.com
[2] International Chair in Mathematical Physics and Applications, ICMPA-UNESCO Chair,
072BP50 Cotonou, Republic of Benin

Received: 10 June 2013 / Accepted: 10 June 2014
Published online: 23 August 2014 – © Springer-Verlag Berlin Heidelberg 2014

Abstract: Classes of renormalizable models in the Tensorial Group Field Theory framework are investigated. The rank d tensor fields are defined over d copies of a group manifold $G_D = U(1)^D$ or $G_D = SU(2)^D$ with no symmetry and no gauge invariance assumed on the fields. In particular, we explore the space of renormalizable models endowed with a kinetic term corresponding to a sum of momenta of the form $p^{2a}, a \in (0, 1]$. This study is tailored for models equipped with Laplacian dynamics on G_D (case $a = 1$) but also for more exotic nonlocal models in quantum topology (case $0 < a < 1$). A generic model can be written $({}_{\dim G_D}\Phi^k_d, a)$, where k is the maximal valence of its interactions. Using a multi-scale analysis for the generic situation, we identify several classes of renormalizable actions, including matrix model actions. In this specific instance, we find a tower of renormalizable matrix models parametrized by $k \geq 4$. In a second part of this work, we study the UV behavior of the models up to maximal valence of interaction $k = 6$. All rank $d \geq 3$ tensor models proved renormalizable are asymptotically free in the UV. All matrix models with $k = 4$ have a vanishing β-function at one-loop and, very likely, reproduce the same feature of the Grosse–Wulkenhaar model (Commun Math Phys 256:305, 2005).

Contents

1. Introduction

In attempts to generalize in higher dimensions matrix model results on 2D quantum gravity (QG) [1], tensor models have been examined since the early 90s [2–4]. These models stem from the idea that the classical geometry of some manifold could emerge from the statistical sum of random triangulations of manifolds of the same dimension. They might also pertain to a broader proposal that gravity originates from more fundamental (quantum) objects and laws [5]. The special case of matrices provides one of the most compelling results in that direction. Indeed, the Feynman integral of matrix models generates ribbon graphs organized in a $1/N$ (or genus) expansion [6] so that this statistical sum is well controlled through only analytical tools. The real beauty of these models reveals itself after a phase transition [7,8]: the resulting model maps to a 2D theory of gravity coupled with a Liouville conformal field [9–12]. From the study of matrix models, important developments on integrable systems and statistical mechanics followed [1]. The framework of random matrices still attracts a lot of attention in both physicist and mathematician communities [13–18].

For higher rank tensor models, the story turns out to be a far greater challenge [2,3]. The crucial $1/N$ expansion leading to the understanding and control of the partition function in the case of matrix models has been missing for a long time. The attempt to understand analytically the partition function of tensor models was abandoned and, until recently, computations in theories implementing a discrete version of QG in higher dimension rested on numerics. With somehow a different perspective and still in the same period, Boulatov showed that the amplitudes of a simplicial theory of 3D complexes made of tensors equipped with a particular invariance reproduce several features of amplitudes of a lattice gauge theory [19,20]. The type of invariance of the Boulatov model turned out to be interesting on its own and lead to several connections with other QG approaches [21,22].

Concerning analytical calculations, the interest in tensor models could have been certainly and significantly improved if these were provided with an appropriate notion of $1/N$-expansion. This was indeed what happened after the spotless discovery by Gurau

of a genuine notion of large N-expansion for a particular class of random tensor models [23–25]. This particular class, the colored tensor models, proves to be associated with triangulations of simplicial pseudo-manifolds in any dimension [26–29]. The critical behavior for this class of tensor models has been investigated. They are found to undergo a phase transition towards the so-called branched polymer phase [30–32]. More results provide answers to longstanding questions on statistical mechanics on random lattices [33,34] and mathematical physics [35–37]. Another profound result is that there exists an extension of the universality and Wigner-Dyson law valid for tensors [38] (for more results in a short review, see either [39] or [40]).

It is reasonable to expect that more will be unraveled from such developments. Indeed, the $1/N$-expansion revealed a basis of unitary trace invariants for (unsymmetrized) tensors [36,37,41]. In simple words, these extend the unitary trace invariants $\mathrm{tr}[(M^\dagger M)^p]$, for $p \geq 0$, built from matrices M themselves generalizing the unique unitary invariant built from vectors $|\vec{\phi}|^2$. Unitary tensor invariants had been studied long ago by mathematicians [42,43]. The interest of the aforementioned works comes from the fact that all these unitary tensor invariants are captured by a path integral field theory formalism defined on colored tensor models. Unitary tensor invariants are simply encoded in a colored graph.

Considered as basic observables and interactions, the same trace invariants were at the basis of the uncovering of the first renormalizable tensor models of rank greater than or equal to 3 [44,45]. These models were investigated quite recently (see the reviews [46–48]) as extensions of the so-called Grosse–Wulkenhaar (GW) model [49], a renormalizable matrix model derived from noncommutative geometry [50]. The fact that a renormalization procedure could be applied to some tensor models is certainly an important step towards better understanding them through known methods in ordinary quantum field theory. We will refer to these models as Tensorial Group Field Theory (TGFT).[1] Why is renormalizability important for tensor models? Renormalizability for any quantum field theory is a very desirable feature because it mainly ensures that the theory will survive after several energy scales. All known interactions of the standard model are renormalizable. This feature gives a sense to a system dealing with several types of infinities (infinitely many degrees of freedom, divergence occurring in their physical constants). Quantum field theory predictions rely on the fact that, from the Wilsonian or Renormalization Group (RG) point of view, these infinities should be not hidden or ignored but should locally (from one scale to the other) reflect a change in the form of the theory [51]. In particular, if tensor models are to describe at low energy any physical reality like our spacetime, and since generically they possess divergent correlation functions, one must explain these divergences. The renormalization program is built for that purpose and the RG offers a natural mechanism to flow from a certain model at some scale to another at another scale while dealing consistently with these infinities.

Before reviewing the main results obtained in TGFTs, let us give now some precisions and basic terminology about tensor models. Consider a model defined via a tensor field of rank d. This field represents a $(d-1)$ simplex. The interaction consists in a d simplex obtained by gluing these fields or $(d-1)$ basic simplexes along their boundary. The path integral of such a model generates d dimensional simplicial complexes from the gluing of the interaction terms along their boundary. Hence, the rank d of the tensor field and the dimension d of the simplicial complexes generated are exactly the same.

[1] The appearance of the name "Group" comes from the fact that the tensors considered in these models are nothing but the Fourier components of some class of functions or fields defined on an abstract group G.

Table 1. List of renormalizable models and their features ($\surd \equiv$ asymptotic freedom proved; $k_{\max}$ is the maximal valence of the vertex)

TGFT (type)	Group	$\Phi^{k_{\max}}$	d	Renormalizability	Asymptotic freedom
	$U(1)$	Φ^6	4	[44] Just-	$\surd$ [58]
	$U(1)$	Φ^4	3	[56] Just-	$\surd$ [56]
gi-	$U(1)$	Φ^{2k}	4	[59] Super-	–
gi-	$U(1)$	Φ^4	6	[60] Just-	$\surd$ [62]
gi-	$U(1)$	Φ^6	5	[60] Just-	$\surd$ [62]
gi-	$U(1)$	Φ^4	5	[60] Super-	–
gi-	$SU(2)^3$	Φ^6	3	[61] Just-	?

The renormalization program for TGFT has achieved many results in the last four years [44,45,52–62]. So far, one identifies two types of renormalizable TGFTs. One of them implements the gauge invariance by Boulatov [21]. Referring to this particular type of TGFT, we shall use the terminology gi-TGFT. Discussing models without gauge invariance we will sometimes use "simple" TGFTs, but most of the time we will simply say TGFTs when the context does not lead to any confusion.

Table 1 collects the different features of both super-renormalizable and just-renormalizable models. It surprisingly happens that most of the just-renormalizable models discovered so far (gauge invariant or not) turn out to be asymptotically free.[2] We are led to the important question: is asymptotic freedom a generic feature in TGFTs ? In general, a model is called UV asymptotically free if it makes sense at arbitrary high energy scales and possesses a trivial UV fixed point defined by the free theory. QCD or the theory of strong interactions is a typical example of this kind. From the UV going in the IR direction, the renormalized coupling constant grows up to some critical value for which one reaches a new phase described in terms of new degrees of freedom (quark confinement in QCD). If tensor models are generically asymptotically free, this could be a nice feature because it would mean that, (1) in the case that these models actually describe a theory of gravity, this theory would be sensible at arbitrary small distances and, (2) in the IR, the models likely experience a phase transition after which, hopefully, the final degrees of freedom may encode more geometrical data than the initial ones (which are totally topological) and may lead to a notion of invariance under coordinate change in the new action.

For the discussion below, it is instructive to provide details on these renormalizable tensor models. The interactions which lead to renormalizable models are of the form of the unitary tensor invariants. Concerning the dynamics, it was an unexpected fact that, starting with a rank 3 gi-TGFT with trivial dynamics in the form of a mass term and expanding the two-point function, one was able to generate diverging corrections of a Laplacian form [55]. Thus, this suggested that one needs to introduce a Laplacian dynamics in order to make sense of a renormalization program in gi-TGFTs. After this stage, introducing a group Laplacian in the kinetic term played a major role in the proof that several models were indeed just-renormalizable [44,60,61]. However, this type of kinetic term is not the only one which might lead to just-renormalizable theories. For instance, the rank $d = 3$ model in [56] has a kinetic term written in momentum space as $(\sum_{s=1}^{3} |p_s| + \mu)$, $p_s \in \mathbb{Z}$ representing the momentum associated with the direct space coordinate θ parametrizing the circle $S^1 \sim U(1)$. There is, at this point, no

[2] The model by Carrozza et al. [61] is presently under analysis.

direct space formulation of this model. A way to think about such a formulation would be to introduce anti-commuting fields ψ[3] and deal with a Dirac field formalism. This leads to another question about the statistics of the tensors and the representation of the Lorentz group associated with it. Nonetheless, at this QG energy scale, there is no reason to enforce that Lorentz invariance should hold and that our fields should be some Dirac spinors. More just-renormalizable classes of tensor models of this kind have been found and several of them are related with classes of matrix models [57]. This urges us to think about some physical selection criteria for tensor models. Since QG is very "special", we should adopt an inclusive attitude and will certainly gain by scrutinizing the space of all possible models with at least some particular features among which is just-renormalizability. According to some minimal physical axioms, the present work establishes that the space of just-renormalizable tensor models is not as huge as one might think and, in fact, several rank $d \geq 3$ models in this space are asymptotically free in the UV.

In this paper, we consider complex and arbitrary rank d TGFT models (without gauge invariance, this is the simplest class of tensor model) written in the momentum space of $G_D = U(1)^D$ or $G_D = SU(2)^D$, and by introducing a free parameter $a \in (0, 1]$ as the power of momenta p^{2a} in the kinetic term, we explore the space of models in order to find renormalizable theories characterized by the maximal valence of the interaction term $k_{\max}$. Any of these models can be written as

$$({}_{\dim G_D}\Phi_d^{k_{\max}}, a),\ a \in (0, 1], \quad D \in \mathbb{N} \setminus \{0\}, \quad k_{\max} \in 2\mathbb{N} \setminus \{0, 2\} \ \text{ and } \ d \in \mathbb{N} \setminus \{0, 1\}. \tag{1}$$

Note that our study includes the case of matrix models recovered for $d = 2$.

This work reports the following new results:

- A multi-scale analysis and power-counting theorem (Theorem 1) for any theory of rank d with kinetic term with at most quadratic momenta and with field background space $SU(2)^D$ and $U(1)^D$. Note that in all previous works discussing renormalization of tensor models except two [56,57], the authors perform their analysis by restricting to a unique group $SU(2)$ and $U(1)$ with exactly Laplacian dynamics. The present analysis allows us to address several other possible renormalizable tensor models in a row.
- The tensor models $({}_1\Phi_3^6, a = \frac{2}{3})$ over $G = U(1)$, $({}_2\Phi_3^4, a = 1)$ over $G = U(1)^2$, $({}_1\Phi_4^4, a = \frac{3}{4})$ over $G = U(1)$, $({}_1\Phi_5^4, a = 1)$ over $G = U(1)$, are all just-renormalizable (Theorem 2). These models, in addition to $({}_1\Phi_4^6, a = 1)$ over $U(1)$ [44] and $({}_1\Phi_3^4, a = \frac{1}{2})$ over $U(1)$ [56], are all asymptotically free in the UV (Sect. 7.2).
- There is a family parametrized by $k \in \mathbb{N}\setminus\{0, 1\}$ of rank 3 tensor models $({}_1\Phi_3^{2k}, a = 1-\frac{1}{k})$ over $G = U(1)$, which are all potentially just-renormalizable. In the following, we refer to such a family of models parametrized by the maximal valence of the interactions as a tower of models. The family described above is clearly missed if one restricts the analysis to models endowed with Laplacian dynamics.
- There are two towers of matrix models $({}_1\Phi_2^{2k}, a = \frac{1}{2}(1 - \frac{1}{k}))$ over $G = U(1)$ and $({}_2\Phi_2^{2k}, a = 1 - \frac{1}{k})$ over $G = U(1)^2$, supplemented by the models $({}_3\Phi_2^6, a = 1)$ over $G = U(1)^3$ or $G = SU(2)$, $({}_3\Phi_2^4, a = \frac{3}{4})$ over $G = U(1)^3$ or $G = SU(2)$, $({}_4\Phi_2^4, a = 1)$ over $G = U(1)^4$ which are just-renormalizable (Theorem 3).

[3] Note that the first color model [26] was defined with anti-commuting Grassmann variables.

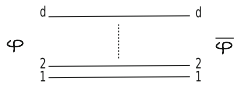

Fig. 1. The propagator or line in a rank d tensor model decomposes in d labeled strands

- The matrix models $({}_1\Phi^4_2, a)$ over their corresponding group all have a vanishing β-function at one-loop (Sect. 7.3). Very likely, they will all be asymptotically safe at all orders like the GW model [49,63]. The models $({}_1\Phi^6_2, a)$ over their corresponding group all have a Landau ghost [51].
- For $k \geq 2$, the towers of matrix models, $({}_1\Phi^{2k}_2, a = \frac{1}{2})$ over $G = U(1)$, and $({}_2\Phi^{2k}_2, a = 1)$ over $G = U(1)^2$, and the tower of rank 3 tensor models $({}_1\Phi^{2k}_3, a = 1)$ over $G = U(1)$, define all super-renormalizable models (Theorem 4).

The plan of this paper is as follows. Section 2 defines the combinatorial ingredients and the topological content of the category of graphs which will support the perturbative expansion of the models discussed in this work. Section 3 is devoted to the construction of models and the ensuing multi-scale analysis leading to the general power counting theorem for a large class of models. We determine specific criteria for seeking super- and just-renormalizable tensor models. Section 4 achieves the proof of the renormalizability of some rank $d \geq 3$ tensor models up to maximal valence of the interaction 6. Section 5 provides a similar analysis and the proof of the renormalizability of several matrix models up to a finite but arbitrary maximal valence of the interaction. Super-renormalizable models are discussed in Sect. 6 whereas Sect. 7 undertakes the computation of the first order of β-functions of all just-renormalizable models found in this work up to maximal valence of the interaction of order 6. Section 8 summarizes our results and discusses some consequences of these. An appendix provides the proof of some claims in the main text together with interesting illustrations and peculiar features of the real matrix model case.

2. Colored and Uncolored Tensor Graphs

Colored tensor models [26,29] expand in perturbation theory as colored Feynman graphs which have a rich stranded structure. From these colored tensor graphs, one builds another type of graph called uncolored [36,41] which will be the useful category of graphs we will be dealing with. In this section, for the sake of this work being self-contained, we quickly review the basic definitions of these combinatorial objects and concepts in the above references.

2.1. Combinatorial and topological structures on colored tensor graphs.

Colored tensor graphs. In a rank d colored tensor model, a graph is a collection of edges or lines and vertices glued together according to quantum field theory rules dictated by the field measure. In such theory, a graph (or tensor graph) has a stranded structure because its main ingredients obey the following properties [64]:

– each edge corresponds to a propagator and is represented by a line with d strands, see Fig. 1 (fields φ are half-lines with the same structure);
– there exists a $(d + 1)$ edge (or line) coloring;

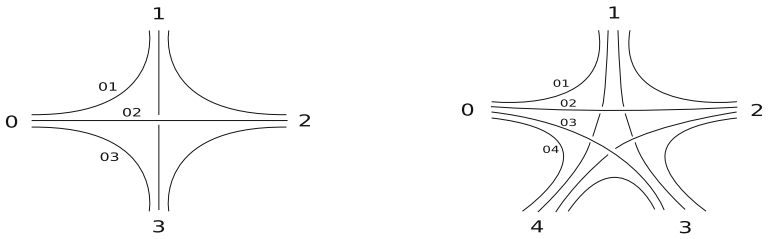

Fig. 2. Two vertices in rank $d = 3$ (*left*) and $d = 4$ (*right*) colored models: they connect like the K_{d+1}-graph. Each leg of the vertex points towards a different colored line providing a bi-coloring on strands

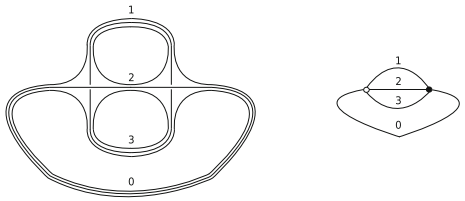

Fig. 3. A rank 3 colored tensor graph (*left*) and its compact colored bi-partite representation (*right*)

- each vertex has coordination or valence $d + 1$ with the complete graph K_{d+1}-type connection between its legs, namely each leg connects all half-lines hooked to the vertex. Due to the stranded structure at the vertex and the existence of an edge coloring, one defines a strand bi-coloring which associates to each strand leaving a leg of color a and joining a leg of color b, $a \neq b$, in the vertex the couple of colors (ab);
- there are two-types of vertices, black and white and one enforces that the graph is bipartite. This also provides an orientation to all the lines, say each line is oriented from a black vertex to a white vertex.

Illustrations of rank $d = 3, 4$ white vertices are provided in Fig. 2. Black vertices have a very similar structure but with labels denoted counterclockwise. The labels of the black vertices possess a bar. An example of a rank 3 colored tensor graph is given in Fig. 3 (left). We will also use simplified diagrams and collapse all the stranded structure into a simple colored graph capturing all the information of the former (see Fig. 3). The result of a collapse procedure is called simplified, compact or collapsed colored graph.

In [28], Gurau proves that rank d colored tensor graphs are dual to simplicial pseudo-manifolds in dimension d. This property might be important if one expects that the type of topological spaces generated by the effective action of the model includes manifolds with a nice topology and smooth geometry like the one of our spacetime. The color prescription drastically reduces the type of simplicial complexes possibly spanned by the partition function.

Open and closed graphs. A graph is said to be open if it contains half-lines incident to a unique vertex otherwise it is called closed. One refers to such half-lines as external legs representing, from the field theory point of view external fields. Examples of open graphs are given in Fig. 4.

***p*-bubbles and faces.** Colored tensor graphs in any rank d have a cellular structure [26]. In rank $d \geq 3$, apart from vertices and edges, there exist several other components in the

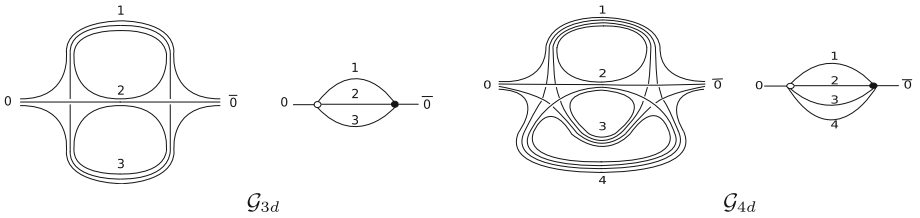

Fig. 4. Rank 3 ($\mathcal{G}_{3d}$) and 4 ($\mathcal{G}_{4d}$) colored open tensor graphs and their compact representation

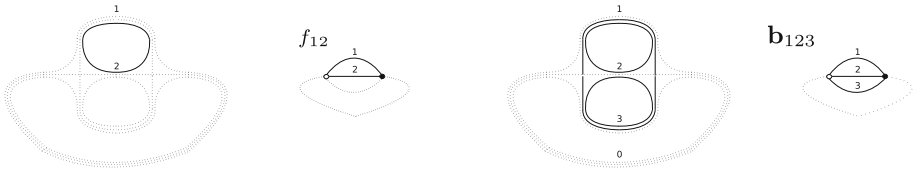

Fig. 5. Shading colors 0 and 3 in the graph of Fig. 3, one gets a bi-colored face f_{12} (*left*). Shading the color 0, one obtains a 3-bubble $\mathbf{b}_{123}$ (*right*)

graphs. Call p-bubble a maximally connected component subgraph[4] of the collapsed colored graph associated with a rank d colored tensor graph, where p is the number of colors of edges used to define that subgraph. Maximally connected because, given a colored graph, the set of p-bubbles can be found by removing $(d + 1 - p)$ colors in the graphs and simply observing the remaining connected components. Thus, 0-bubbles are vertices, 1-bubbles are lines themselves. In a rank $d \geq 3$, there exist other important components called faces which are 2-bubbles. A **face** is a connected component in the graph made with 2 colors. Faces can be viewed in the simplified colored graph as cycles of edges with alternating colors. Next, 3**-bubbles** can be illustrated as connected subgraphs made with 3 colors, etc. Examples are given in Fig. 5.

Some remarks and terminology can be introduced at this level:

- Within this simplified colored picture, a line l may be contained in a $p \geq 1$-bubble $\mathbf{b}$ and we write $l \in \mathbf{b}$. We say that "$\mathbf{b}$ passes through the line l."
- Coming back to the full expansion of the colored graph using strands, a face is nothing but a connected component made with one strand. The color of this strand alternates when passing through the edges which define the face.
- A p-bubble is open if it contains an external half-line otherwise it is closed. For instance, there exists three open 3-bubbles ($\mathbf{b}_{012}$, $\mathbf{b}_{013}$ and $\mathbf{b}_{023}$) and one closed bubble ($\mathbf{b}_{123}$) in the graph $\mathcal{G}_{3d}$ of Fig. 4.

Jackets. Jackets are a ribbon graphs lying within a colored tensor graph. They are proved to be associated with Heegaard splitting surfaces for the triangulation (simplicial complex) dual to the colored tensor graph [65]. Combinatorially [25], a jacket in a rank d colored tensor graph is defined by a permutation of $\{1, \ldots, d\}$ namely $(0, a_1, \ldots, a_d)$, $a_i \in [\![1, d]\!]$, up to orientation. In practice, one splits the $(d + 1)$-valent vertex into cycles of colors using only the strands with color pairs $(0a_1)$, (a_1a_2), $\ldots$, $(a_{d-1}a_d)$. See Fig. 6, for an illustration. The same applies for the edges. Hence, in a jacket, the above collection of pairs defines the face bi-coloring.

[4] A subgraph of a graph $\mathcal{G}$ is defined by a subset of edges of $\mathcal{G}$ together with their incident vertices.

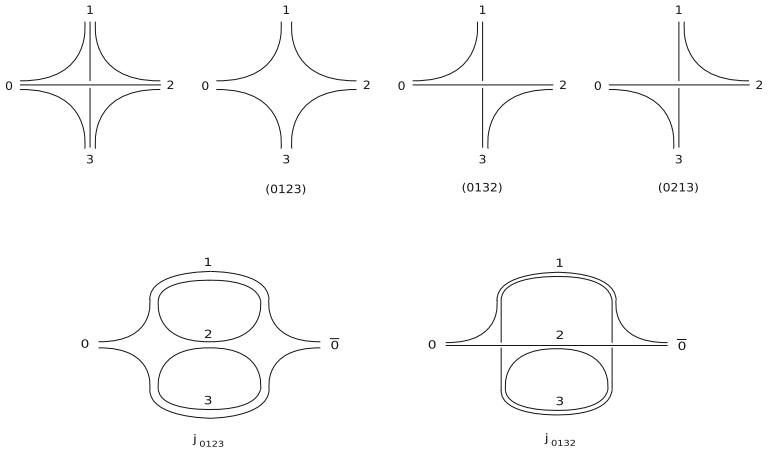

Fig. 6. In the rank 3 colored model, the vertex decomposes in cycles (0123), (0132) and (0213) (*top*). Two open jackets of the rank 3 colored graph $\mathcal{G}_{3d}$ of Fig. 4 and its jackets J_{0123} and J_{0132} associated with the color permutation (0123) and (0132), respectively

A jacket of a colored tensor graph $\mathcal{G}$ is nonlocal in the sense that, given a permutation, it only depends on the overall structure of $\mathcal{G}$. For instance the number of jacket in a rank d colored graph is given by $d!/2$ or simply the number of permutations of $[\![1, d]\!]$ up to orientation, the number of vertices and the number of edges of a jacket equal the number of vertices and the number of edges of its spanning graph, respectively. Meanwhile p-bubbles of $\mathcal{G}$ are local in the sense that they depend on the local structure at each vertex of $\mathcal{G}$.

An open jacket keeps the above sense that it is a jacket touching an external leg (see example in rank 3 in Fig. 6).

Boundary graph. We aim at studying tensor graphs with external legs. From the quantum field theory perspective, external legs or fields probe events which might happen at much higher scale. In the present context, tensor graphs with external legs are viewed as simplicial complexes with boundaries. The latter play the role of the probes that we mentioned before. There is a way to understand this boundary as a simplicial complex itself in the colored case [27]. We can re-translate the boundary complex of a rank d colored graph as a tensor graph with two peculiarities (1) its rank gets lowered to $d-1$ and (2) it possesses an vertex-edge coloring which we will define in a moment [64]. The procedure for achieving this mapping (from boundary to rank $d-1$ colored graphs) is known as "pinching" or closing open tensor graphs [27]. This can be simply illustrated by the insertion of a d-valent vertex at each external leg of a rank d tensor graph. As an effect of this d-valent vertex insertion, we define the boundary $\partial\mathcal{G}$ of a rank d colored tensor graph $\mathcal{G}$ to be the graph

– the vertex set of which is one-to-one with the set of external legs of $\mathcal{G}$;
– the edge set of which is one-to-one with open faces of $\mathcal{G}$.

The boundary graph has a vertex coloring inherited from the edge coloring and has an edge bi-coloring coming from the bi-coloring of the (external) faces of the initial graph. See in Fig. 7 illustrations of some boundary graphs. The boundary $\partial\mathcal{G}$ of a closed rank d colored tensor graph $\mathcal{G}$ is empty. The boundary graph is always closed.

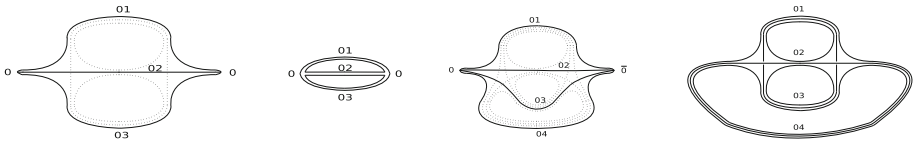

$\partial\mathcal{G}_{3d}$ $\partial\mathcal{G}_{4d}$

Fig. 7. The boundary graph $\partial\mathcal{G}_{3d}$ (and its ribbon structure) of $\mathcal{G}_{3d}$ of Fig. 4 is obtained by inserting a 3-valent vertex at each external leg and shading the closed internal faces. Similarly, $\partial\mathcal{G}_{4d}$ (and its internal rank 3 structure) is the boundary of $\mathcal{G}_{4d}$ of Fig. 4

Note that reducing to rank $d = 3$, the boundary of a rank 3 colored tensor graph is a rank 2 tensor graph. Hence, it forms a ribbon graph coinciding with its unique jacket. For rank $d \geq 4$, the boundary graph has a higher rank internal structure itself. For instance, it has p-bubbles and jackets that we will denote by J_∂.

Degree of a colored tensor graph. By organizing the divergences occurring in the perturbation series of rank d colored tensor graphs, the success of finding a 1/N expansion for amplitudes (here N is some large size of the tensor labels) relies on the introduction of the quantity [25]

$$\omega(\mathcal{G}) = \sum_J g_J, \tag{2}$$

where g_J is the genus of the jacket J and the sum is performed over all jackets in the colored tensor graph $\mathcal{G}$. The quantity $\omega(\mathcal{G})$ is called degree of $\mathcal{G}$ and is useful to re-sum the perturbation series for the present class of models. Such a degree of a colored tensor graph replaces the genus of a ribbon graph in terms of which one organizes the partition function series in matrix models case. After rescaling of the coupling constant by a suitable power of N the typical size of the tensor (cut-off), one finds that the amplitude $A(\mathcal{G})$ of some graph $\mathcal{G}$ scales as $A(\mathcal{G}) \sim N^{d-\frac{2}{(d-1)!}\omega(\mathcal{G})}$ (for a short survey see [39,40]). Gurau proves that the dominant amplitudes in the partition function of colored tensor models of any rank d are of the sphere topology in dimension d. It is direct to see that graphs associated with the most divergent amplitudes are such that $\omega(\mathcal{G}) = 0$. We will call these *melons* or *melonic graphs* [30].

2.2. Uncolored tensor graphs. Consider the partition function Z of some rank d colored tensor model defined by complex tensor fields denoted by φ^a_I, where $a = 0, \ldots, d$ is called color of the tensor and the index I collects the tensor indices. We have

$$Z = \int d\nu_C(\{\varphi^a\}) e^{-S^{\text{color}}[\{\varphi^a\}]}, \tag{3}$$

where $d\nu_C(\{\varphi^a\})$ is the iid Gaussian measure associated with the colored fields and related to a trivial kinetic term of the form

$$S^{\text{kin,color}} = \sum_{a=0}^{d} \sum_I \bar{\varphi}^a_I \varphi^a_I, \tag{4}$$

and where

$$S^{\text{color}} = \sum_I \prod_{a=0}^{d} \varphi^a_{I_a} + \sum_I \prod_{a=0}^{d} \bar{\varphi}^a_{I_a} \tag{5}$$

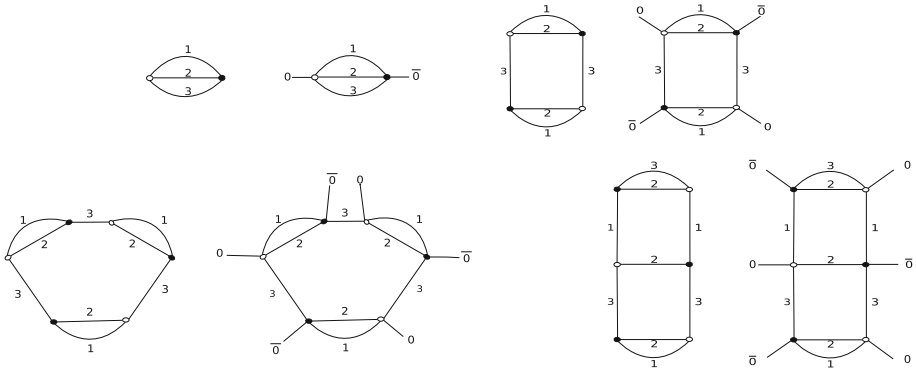

Fig. 8. Some rank 3 colored 3-bubbles and their corresponding tensor invariant

is the colored interaction consisting only in identifications following the pattern of the colored vertex of rank d as discussed in Sect. 2.1.

One could partially integrate Z on all but one field, say φ^0, and gets an effective action in that remaining color:

$$Z = \int d\nu_{\tilde{C}^0}(\{\varphi^0\})\; e^{-S^{\text{uncolor}}[\{\varphi^0\}]}, \tag{6}$$

where S^{uncolor} expresses in terms of the colored field φ^0 and $\bar{\varphi}^0$. The particular form of this action called "uncolored" [37,41] can be found elsewhere,[5] but one can think about it as an action with an infinity of couplings

$$S^{\text{uncolor}}[\{\varphi^0\}] = \sum_{\mathbf{b}\in\mathcal{B}^d} \lambda_{\mathbf{b}}\; \text{tr}_{\mathbf{b}}[\bar{\varphi}^0; \varphi^0]\,, \tag{7}$$

where the sum over $\mathbf{b}$ is performed on the set of (vacuum) d-bubbles $\mathcal{B}^d$ in the remaining colors different from 0 with fixed number of vertices, $\lambda_{\mathbf{b}}$ is some effective coupling constant associated with the tensor operator $\text{tr}_{\mathbf{b}}[\bar{\varphi}^0; \varphi^0]$ which mainly implements the construction of the d-bubble $\mathbf{b}$ from contractions of a set of fields $\bar{\varphi}^0$ and φ^0. The quantity $\text{tr}_{\mathbf{b}}[\bar{\varphi}^0; \varphi^0]$ is called *connected tensor invariant*. In practice, the way that one understands this object is in fact simple. Consider a bubble $\mathbf{b}$, by increasing the valence of its vertices by one, there is a way to compose $\text{tr}_{\mathbf{b}}[\bar{\varphi}; \varphi]$ by adding a color to $\mathbf{b}$. Thus, a connected tensor invariant is labeled by the bubble which defines it. Some connected tensor invariants in rank 3 have been illustrated in Fig. 8.

In the following, we shall consider several tensor models of fixed rank d with action defined with a tensor field associated with the last non integrated color $\varphi = \varphi^0$. This last color would be the one dynamical in the sense that there will be a nontrivial kinetic term associated with φ so that the measure $d\nu(\{\varphi\})$ will no longer be associated with an iid model. The interaction will include all possible tensor invariants in that rank d. An uncolored tensor graph in this setting is made with lines only of the last color and vertices consisting in tensor invariants. The other colored lines are integrated and should be regarded as fictitious. For instance, see Fig. 9. Thus, an uncolored tensor graph $\mathcal{G}$ admits a rank $d+1$ color representation $\mathcal{G}_{\text{color}}$ obtained uniquely by restoring the colors.

[5] The interested reader is referred to one of the above references, see for instance Equation (49) in [37].

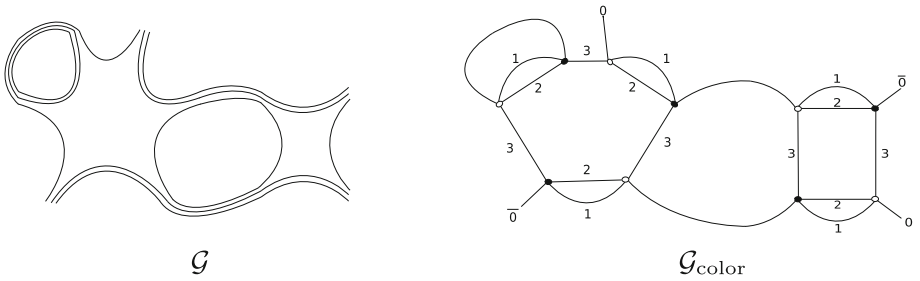

Fig. 9. A rank 3 uncolored graph $\mathcal{G}$ and its associated colored extension $\mathcal{G}_{\text{color}}$

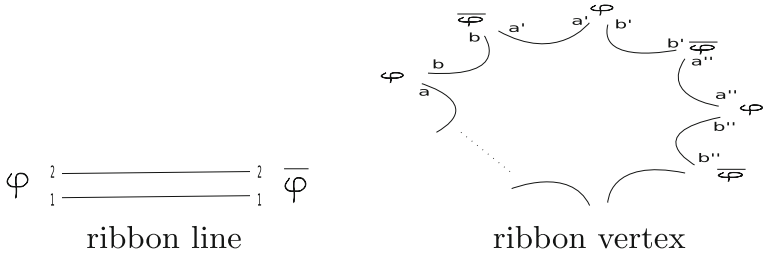

Fig. 10. A ribbon edge and ribbon vertex with arbitrary valence

This procedure called "color extension" of a graph allows the passage from the uncolored to the colored theories. By the renormalization prescription, we aim at truncating the infinite series (7) of interactions and keeping only marginal and relevant coupling in the renormalization group (RG) sense and checking that the model does not generate any other significant coupling. We mention also that a capital point in the proof of the renormalizability is the reintroduction of colors in order to get useful bounds and a clear understanding on the divergence degree of the graph.

2.3. Rank 2, matrix or ribbon graphs. In order to discuss the case of rank 2 graphs, we do not need the above colored graph technology. A ribbon, matrix or rank 2 tensor graph is a graph made with lines which are ribbons and vertices which are cyclic objects with arbitrary valence, see Fig. 10. Note that, so formulated, one may not recognize the vertex as the same ingredient of the so-called ribbon (cyclic) graphs defined by standard combinatorics [66]. In such a context, the vertex is a simple disc. We simply adopt here the quantum field theoretical perspective and put half-lines on this disc.

Regarded as Feynman graphs of some matrix model, ribbon graphs are the gluing of lines corresponding to propagators and vertices corresponding to the model interaction. From the the point of view of topology, ribbon graphs represent triangulations of 2D surfaces or simplicial complexes in 2D. We will consider matrix models defined by complex matrix fields φ_{AB}. The action of such models has the generic form

$$S_{\text{mat}} = \sum_{AB,A'B'} \bar{\varphi}_{AB} K_{AB,A'B'} \varphi_{A'B'} + \sum_{p} \lambda_p \text{tr}[(\bar{\varphi}\varphi)^p], \tag{8}$$

where the kernel $K_{AB,A'B'}$ should have suitable properties so that S_{mat} makes sense, and tr is an ordinary matrix trace. Thus the interaction is defined as a sum of connected

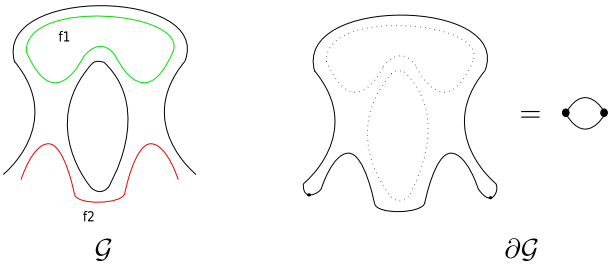

Fig. 11. A open ribbon graph $\mathcal{G}$ with f_1 a closed face and f_2 an open face. The boundary $\partial\mathcal{G}$ of $\mathcal{G}$ after pinching and shading all closed faces of $\mathcal{G}$

unitary matrix invariants represented as in Fig. 10. We will not consider $K_{AB,A'B'}$ as the identity operator and, doing so gives a non trivial dynamics for the fields and will lead us to non iid models. Such models are related to the class of Kontsevich models [67].

The notion of face of a ribbon graph follows from the above description of face (forgetting the colors) or, equivalently, can be defined as the boundary of the ribbon graph when regarded as a geometric ribbon [66]. Ribbon graphs can be closed or open if, in this last case, they have external legs (see Fig. 11). A face can be also open or closed if it passes through an external leg. We can define a pinching procedure for ribbon graphs as well by inserting a 2-valent vertex at each external legs of the graph. The notion of boundary graph $\partial\mathcal{G}$ as the result of the pinching of some ribbon graph naturally restricts to the present situation as well (see Fig. 11).

3. Seeking Renormalizable Models: Generic Multi-Scale Analysis

The goal of this section is to provide a list of potentially just- and super-renormalizable TGFTs models under some specific assumptions. Our main tool for addressing this problem in full generality is the multi-scale analysis [51]. We intend to give a general power-counting theorem and locality principle for a general class of models. The thorough renormalization analysis of some models detected as potentially renormalizable will be deferred to next sections.

Constructing an action for the subsequent analysis, we do have some motivated restrictions:

(i) The fields are defined on a background which is a compact group manifold G. This is assumed for simplicity and any integral on the background position space generates an $O(1)$ factor. After Fourier transform, the fields become tensors with labels in a discrete momentum space and the amplitudes can still entail divergences at large momenta. Typically, we will restrict the study to $G = U(1)$ or $SU(2)$ or several copies of these groups. The case $U(1)^{\times p} \times SU(2)^{\times q}$, for p, q strictly positive integers, could be deduced from this point.

(ii) The propagator is stranded and should involve a sum momenta of the form p^{2a} with $0 < a \leq 1$ associated to each field strand.[6] The upper bound $2a = 2$ might be essential in order to fulfill Osterwalder–Schrader positivity axiom [48,51]. At $a = 1$, one recovers, in direct space, an ordinary Laplacian acting on each field argument.

[6] One may think about a "duality" between the models which will be investigated here and other types of models by performing a symmetry $a \to a^{-1}$. This will deserve a complete understanding.

(iii) The interactions involved are unitary tensor invariant objects as discussed in Sect. 2.2 or unitary matrix invariants (we will generally refer to these as "trace invariants"). These objects belong to the sole class of interactions found so far to generate renormalizable rank $d \geq 2$ tensor theories. They provide a genuinely new notion of locality in TGFTs. Dually, the most dominant ones represent triangulations of simplicial complexes with spherical topology. This property could be of major importance in order to achieve the continuum limit of these models as a spacetime with a large and regular topology and geometry [31,32].

Apart from these restrictions, we shall not exclude any possible model. We must emphasize that, because we are allowing an arbitrary power of the momentum p^{2a} in the kinetic term, a direct space formulation of several models that we shall discuss is still under investigation. For the interaction however, the direct and momentum spaces have the same simple interpretation. In all models discussed below, they are both regarded as a basic simplex. All models are nonlocal: the interactions occur in a region rather than a definite point of the background space and introducing an arbitrary power in momenta in the kinetic terms in these models leads to even more nonlocality. We finally stress that, renormalization is not a goal *per se* [68]. This property will be only useful if associated with the study of phase transition and critical phenomena which hopefully might be associated with Physics. The existence of a class renormalizable tensor models will be useful if we can extract more information on their universal behavior. But at the least, identifying a wide class of models with a controlled (renormalizable) behavior is a step towards the search of "universal" properties and, perhaps from this point, we might have a better comprehension of what is a quantum theory generating topologies and gravity.

3.1. Models. We consider a rank $d \geq 2$ complex tensor field over a compact Lie group G, $\varphi : G^d \to \mathbb{C}$. This field can be decomposed in Fourier modes as

$$\varphi(h_1, h_2, \ldots, h_d) = \sum_{P_{I_l}} \tilde{\varphi}_{P_{I_1}, P_{I_2}, \ldots, P_{I_d}} D^{P_{I_1}}(h_1) D^{P_{I_2}}(h_2) \ldots D^{P_{I_d}}(h_d), \tag{9}$$

where the group elements $h_s \in G$ and the sum is performed on all momenta P_{I_s} labeled by multi-indices $I_s, s = 1, 2, \ldots, d$; I_s defines the representation indices of the group element h_s in the momentum space such that $D^{P_{I_s}}(h_s)$ plays the role of the plane wave in that representation. For the tensor $\tilde{\varphi}$, we will simply use the notation $\varphi_{[I]} := \tilde{\varphi}_{P_{I_1}, P_{I_2}, \ldots, P_{I_d}}$, where the super index $[I]$ collects all momentum labels involved in the sum, i.e. $[I] = \{I_1, I_2, \ldots, I_d\}$. It is important to note that no symmetry under permutation of the arguments is assumed for the tensor $\varphi_{[I]}$. We rewrite (9) in these shorthand notations as

$$\varphi(h_1, h_2, \ldots, h_d) = \sum_{P_{[I]}} \varphi_{[I]} D^{I_1}(h_1) D^{I_2}(h_2) \ldots D^{I_d}(h_d). \tag{10}$$

For $d = 2$, we shall refer to φ_{I_1, I_2} as a matrix.

For any $D \in \mathbb{N}\backslash\{0\}$, consider the group $G = G_D$, $h_k \in G_D$, we are interested in two cases:

(a) $G_D = U(1)^D$: The representation and momentum indices are obtained as

$$\begin{aligned} h_s &= (h_{s,1}, \ldots, h_{s,D}) \in G_D\,, \quad h_{s,l} = e^{i\theta_{s,l}} \in U(1)\,, \\ D^{I_s}(h_s) &= D^{P_{I_s}}(h_s) = \prod_{l=1}^{D} D^{s,l}(\theta_{s,l})\,, \quad D^{s,l}(\theta) = e^{ip_{s,l}\theta}, \\ P_{I_s} &= \{p_{s,1}, \ldots, p_{s,D}\}\,, \quad I_s = \{(s,1), \ldots, (s,D)\}\,, \\ [I] &= \{(1,1), \ldots, (1,D); \ldots; (d,1), \ldots, (d,D)\}. \end{aligned} \tag{11}$$

where $p_{s,l} \in \mathbb{Z}$.

(b) $G_D = SU(2)^D$: In this case, the momentum space is obtained by the transform

$$\begin{aligned} &h_s = (h_{s,1}, \ldots, h_{s,D}) \in G_D\,, \quad h_{s,l} \in SU(2)\,, \\ &D^{I_s}(h_s) = D^{P_{I_s}}(h_s) = \prod_{l=1}^{D} [D^{s,l}]^{j}_{mn}(h_{s,l})\,, \quad [D^{s,l}]^{j}_{mn}(h) := D^{j_{(s,l)}}_{m_{(s,l)}n_{(s,l)}}(h), \\ &D^{j}_{mn}(h) := \langle j, m|h|j, n\rangle, \end{aligned} \tag{12}$$

where, given $j \in \frac{1}{2}\mathbb{N}$, $\{|j,m\rangle\}_{m,n}$ denotes the familiar basis of the spin j representation space of $SU(2)$, $|m| \leq j$, $|n| \leq j$, and $D^j_{mn}(h)$ the Wigner matrix element of h in that space, so that

$$P_{I_s} = \{(j_{s,1}, m_{s,1}, n_{s,1}), \ldots, (j_{s,D}, m_{s,D}, n_{s,D})\}\,, \tag{13}$$

whereas I_s and $[I]$ keep their meaning as in (11).

Remark 1. One notices that, although for $d = 2$ we refer to φ_{I_1,I_2} as a matrix, it can be equally regarded as a tensor itself due to the multi-indices carried by the representation of $G_D = U(1)^D$, $D > 1$ or of $G_D = SU(2)^D$, $D \geq 1$. However, we shall not distinguish these cases from the matrix case because, mainly, the combinatorics and the analysis as performed below follow the ones for matrices in both cases.

Kinetic term. The initial task is to build a general action satisfying the above mentioned restrictions (i)–(iii). Consider the kinetic term given in momentum space as

$$S^{\text{kin}} = \sum_{P_{[I]}} \bar{\varphi}_{P_{[I]}} \Big(\sum_{s=1}^{d} |P_{I_s}|^a + \mu^2 \Big) \varphi_{P_{[I]}}\,, \tag{14}$$

where μ is a mass term, $a \in (0, 1]$, and

- for case (a): $|P_{I_s}|^a := \sum_{l=1}^{D} |p_{s,l}|^{2a}$ and the sum (14) is performed over all the values of the momenta $p_{s,l} \in \mathbb{Z}$;
- for case (b): $|P_{I_s}|^a := \sum_{l=1}^{D} [j_{s,l}(j_{s,l}+1)]^a$ and the sum (14) performed over all triples of momenta $(j_{s,l}, m_{s,l}, n_{s,l}) \in \frac{1}{2}N \times \{-j, \ldots, j\}^2$.

We will need also the following companion sums over momenta:

$$\text{case (a)}: \quad |P_{*I_s}|^a = |P_{I_s}|^a\,; \qquad \text{case (b)}: \quad |P_{*I_s}|^a = \sum_{l=1}^{D} (j_{s,l})^{2a}. \tag{15}$$

Clearly, at $a = 1$, (14) implies a Laplacian dynamics on G_D and on each strand labeled by s. The corresponding Gaussian measure on tensors reads $d\nu_C(\varphi, \bar{\varphi})$ and has a covariance given by

$$C[\{P_{I_s}\}, \{\tilde{P}_{I_s}\}] = \Big[\prod_{s=1}^{d} \delta_{P_{I_s}, \tilde{P}_{I_s}}\Big]\Big(\sum_{s=1}^{d} |P_{I_s}|^a + \mu^2\Big)^{-1}, \tag{16}$$

such that, for (a), $\delta_{P_{I_s}, \tilde{P}_{I_{s'}}} := \prod_{l=1}^{D} \delta_{p_{s,l}, \tilde{p}_{s,I}}$ and, when restricted to (b), $\delta_{P_{I_s}, \tilde{P}_{I_{s'}}} := \prod_{l=1}^{D} [\delta_{j_{s,l}, \tilde{j}_{s,I}} \delta_{m_{s,l}, \tilde{m}_{s,I}} \delta_{n_{s,l}, \tilde{n}_{s,I}}]$. Using the Schwinger parametric integral, it is immediate to get

$$C[\{P_{I_s}\}, \{\tilde{P}_{I_s}\}] = \Big[\prod_{s=1}^{d} \delta_{P_{I_s}, \tilde{P}_{I_s}}\Big] \int_0^\infty d\alpha \, e^{-\alpha(\sum_{s=1}^{d} |P_{I_s}|^a + \mu^2)}. \tag{17}$$

Interactions. The interactions of the model are effective interaction terms obtained after integrating d colors in the rank $d + 1$ colored model as detailed in Sect. 2.2. The above kinetic term is defined over the remaining field $\varphi^0 = \varphi$. The interaction is defined from unsymmetrized tensors as trace invariant objects as discussed in Sect. 2.2 and built from the particular contraction (or convolution) of arguments of some set of tensors $\varphi_{[I]}$ and $\bar{\varphi}_{[I']}$. This contraction is made in such a way that only the s^{th} label of some $\varphi_{[I]}$, i.e. some P_{I_s}, is allowed to be summed with the s^{th} component of some $\bar{\varphi}_{[I']}$. Thus the position of each index is capital in such a theory. We have introduced the trace invariants as connected d colored graphs. In rank $d \geq 3$, a general interaction reads:

$$S^{\text{int}}(\varphi, \bar{\varphi}) = \sum_{\mathbf{b} \in \mathcal{B}} \lambda_{\mathbf{b}} I_{\mathbf{b}}(\varphi, \bar{\varphi}), \tag{18}$$

where the sum is performed over a finite set $\mathcal{B}$ of rank d colored tensor bubble graphs and $\lambda_{\mathbf{b}}$ is a coupling constant. For any $I_{\mathbf{b}}(\varphi, \bar{\varphi})$, we associate a vertex operator of the form of the product of delta functions identifying incoming and outgoing momenta.

In the case of rank $d = 2$ or matrix models, the type of interaction considered is given by

$$S^{\text{int}}(\varphi, \bar{\varphi}) = \sum_{p=2}^{p_{\max}} \lambda_p S_p^{\text{int}}(\varphi, \bar{\varphi}), \qquad S_p^{\text{int}}(\varphi, \bar{\varphi}) = \text{tr}[(\bar{\varphi}\varphi)^p], \tag{19}$$

where λ_p is a coupling constant. Graphically, they are represented by cyclic graphs, see Fig. 10.

Amplitudes. The partition function of a generic model described by (14) and (18) or (19) is of the form

$$Z = \int d\nu_C(\varphi, \bar{\varphi}) \, e^{-S^{\text{int}}(\varphi, \bar{\varphi})}. \tag{20}$$

To any connected graph $\mathcal{G}$ made with set $\mathcal{L}$ of lines and set $\mathcal{V}$ of vertices, we associate the amplitude

$$A_{\mathcal{G}} = \kappa(\lambda) \sum_{P_{I](v)}} \prod_{\ell \in \mathcal{L}} C_\ell[\{P_{I_s(\ell);\, v(\ell)}\}, \{\tilde{P}_{I_s(\ell);\, v'(\ell)}\}] \prod_{v \in \mathcal{V}; s} \delta_{P_{I_s;\, v}; P'_{I_s;\, v}}, \tag{21}$$

where the sum is performed over all the momenta $P_{[I](v)}$ associated with vertices v on which the lines are hooked, and the propagators C_ℓ possess a line label $\ell \in \mathcal{L}$. The function $\kappa(\lambda)$ includes all the coupling constants and the symmetry factors. The specific form of the vertex operator and propagators implies that the amplitude (21) factorizes in terms of connected strand components which are the faces of the graph (in the sense given in Sect. 2.1). There exist two types of faces: open faces the set of which will be denoted $\mathcal{F}_{\text{ext}}$ and closed faces the set of which will be denoted $\mathcal{F}_{\text{int}}$. Using (17), we have from (21):

$$A_{\mathcal{G}} = \kappa(\lambda) \sum_{P_{I_f}} \int \Big[\prod_{\ell\in\mathcal{L}} d\alpha_\ell\Big] \Big\{ \prod_{f\in\mathcal{F}_{\text{ext}}} \Big[e^{-(\sum_{\ell\in f}\alpha_\ell)|P^{\text{ext}}_{I_f}|^a}\Big] \prod_{f\in\mathcal{F}_{\text{int}}} \Big[e^{-(\sum_{\ell\in f}\alpha_\ell)|P_{I_f}|^a}\Big]\Big\}, \tag{22}$$

where $P^{\text{ext}}_{I_f}$ are external momenta and are not summed. One notices that the momenta P_{I_f} depend now only on closed faces. In the specific case of $G_D = SU(2)^D$, since the summand is independent of the momenta $(m_{f,l}, n_{f,l})$, for a closed face f, the sum over P_{I_f} generates a factor $\mathbf{d}^2_{P_{I_f}}$ where

$$\mathbf{d}_{P_{I_f}} := \prod_{l=1}^{D} d_{j_{f,l}}, \qquad d_j := 2j+1. \tag{23}$$

Introducing, in the model $G_D = U(1)^D$, $\mathbf{d}_{P_{I_f}} = 1$ for all I_f, we get in full generality

$$A_{\mathcal{G}} = \kappa(\lambda) \sum_{P_{I_f}} \int \Big[\prod_{\ell\in\mathcal{L}} d\alpha_\ell\Big] \Big\{ \prod_{f\in\mathcal{F}_{\text{ext}}} \Big[e^{-(\sum_{\ell\in f}\alpha_\ell)|P^{\text{ext}}_{I_f}|^a}\Big] \prod_{f\in\mathcal{F}_{\text{int}}} \Big[\mathbf{d}^2_{P_{I_f}} e^{-(\sum_{\ell\in f}\alpha_\ell)|P_{I_f}|^a}\Big]\Big\}, \tag{24}$$

where, though we still keep the notation $\sum_{P_{I_f}}$, this sum is now restricted only to spins $j_{f,l}$ in the case of a model over $G_D = SU(2)^D$.

The amplitude (22) is generally divergent because of the first sum on arbitrarily large momenta. Finding a well defined regularization scheme is the purpose of the renormalization program consisting in three steps [51]: a multi-scale analysis from which results a power counting theorem and the main locality principle of the model. This last point deals with the identification of the main features of the primitively diverging contributions and the reason why they can be recast in term of initial terms in the Lagrangian. Then, one proceeds to the proper subtractions of these divergences yielding a renormalized theory.

3.2. Multi-scale analysis and power counting theorem. We consider the model defined by the partition function (20) introducing arbitrary trace invariant (rank $d \geq 3$) or planar cyclic (rank $d = 2$) polynomial interaction. The multi-scale analysis will be performed at this general level. Only at the end, we will truncate the interaction series to relevant and marginal terms supplemented, if necessary, by anomalous terms (not necessarily included in (18) or (19)), depending on the parameters of our theory, namely the rank d, the group dimension $\dim G_D$, the kinetic term parameter a and the maximal valence of the interaction $k_{\max}$.

The multi-scale analysis starts by a slice decomposition of the theory's propagator. The kernel (17) expresses in the following way:

$$C = \sum_{i=0}^{\infty} \hat{C}_i\,, \qquad \hat{C}_i[\{P_{I_s}\},\{\tilde{P}_{I_s}\}] = \Big[\prod_{s=1}^{d} \delta_{P_{I_s},\tilde{P}_{I_s}}\Big] C_i[\{P_{I_s}\}],$$
$$C_i[\{P_{I_s}\}] = \int_{M^{-2i}}^{M^{-2(i-1)}} d\alpha\, e^{-\alpha(\sum_{s=1}^{d}|P_{I_s}|^a+\mu^2)}\,,\ \ \forall i \geq 0\,,$$
$$\hat{C}_0[\{P_{I_s}\},\{\tilde{P}_{I_s}\}] = \Big[\prod_{s=1}^{d} \delta_{P_{I_s},\tilde{P}_{I_s}}\Big] C_0[\{P_{I_s}\}],\ C_0[\{P_{I_s}\}] = \int_{1}^{\infty} d\alpha\, e^{-\alpha(\sum_{s=1}^{d}|P_{I_s}|^a+\mu^2)}\,, \tag{25}$$

for some constant $M > 1$. The regularization scheme requires to introduce a ultraviolet (UV) cut-off Λ on the sum over i. The cut-offed propagator reads as $C^{\Lambda} = \sum_{i=0}^{\Lambda} C_i$. The following bounds hold

$$\begin{aligned}\forall i \geq 1,\, C_i[\{P_{I_s}\}] &\leq K_1 M^{-2i} e^{-M^{-2i}(\sum_{s=1}^{d}|P_{I_s}|^a+\mu^2)} \leq K M^{-2i} e^{-\delta M^{-2i}(\sum_{s=1}^{d}|P_{*I_s}|^a+\mu^2)} \\ &\leq K M^{-2i} e^{-\delta M^{-i}(\sum_{s=1}^{d}|P_{*I_s}|^{\frac{a}{2}}+\mu^2)}, \\ C_0[\{P_{I_s}\}] &\leq K e^{-(\sum_{s=1}^{d}|P_{*I_s}|^{\frac{a}{2}}+\mu^2)} \leq K,\end{aligned} \tag{26}$$

for some constant K_1, K, δ. Hence, for all $a \in (0,1]$, high i probes high momenta $p_{s,l}$ or $j_{s,l}$ of order $M^{\frac{i}{a}}$ (or short distance on the group manifold) and therefore, the slice 0 refers to the infrared (IR) and the slice Λ to the UV.

The next stage is to find an optimal bound on the amplitude $A_{\mathcal{G}}$ for any graph $\mathcal{G}$. From (21), the following amplitude is found

$$\begin{aligned}A_{\mathcal{G}} &= \sum_{\boldsymbol{\mu}} \kappa_{\boldsymbol{\mu}}(\lambda) A_{\mathcal{G};\boldsymbol{\mu}}, \\ A_{\mathcal{G};\boldsymbol{\mu}} &= \sum_{P_{[I](v)}} \prod_{\ell\in\mathcal{L}} C_{i_\ell}[\{P_{I_s(\ell);\,v(\ell)}\},\{\tilde{P}_{I_s(\ell);\,v'(\ell)}\}] \prod_{v\in\mathcal{V};s} \delta_{P_{I_s;\,v};P_{I_s;\,v}},\end{aligned} \tag{27}$$

where $\boldsymbol{\mu} = (i_\ell)_{\ell\in\mathcal{L}}$ is a multi-index called momentum assignment which collects the momentum scales $i_\ell \in [0,\Lambda]$ from each propagator. From the point of view of the effective expansion, the constant $\kappa_{\boldsymbol{\mu}}$ collects effective couplings corresponding to $\boldsymbol{\mu}$. The important quantity which needs to be analyzed is $A_{\mathcal{G};\boldsymbol{\mu}}$. The sum over assignments $\boldsymbol{\mu}$ will be only performed after renormalization according to a standard procedure [51].

Optimal bounds on amplitudes very similar to (27) have been analyzed recently, in several contexts and using different bases (direct or momentum space) of TGFTs [44,56,59–61]. The first optimal bounds have been sorted out in the simpler TGFT framework [44] and [56] were restricted to $\dim G_D = 1$ and $d = 3,4$ and $a = 1, \frac{1}{2}$, respectively. Then, these amplitudes have been studied in Abelian [59,60] and non Abelian [61] gi-TGFTs. Today, the state of the art is given in [61], the analysis has been carried out in direct space for any $\dim G_D$ and any rank $d \geq 3$. All of these works except [56,57], consider only Laplacian dynamics and so are defined at the point $a = 1$. The purpose of the following is to gather all these results and to establish in the momentum

space and for general dim G_D, d and a, a power counting theorem for the present class of simple TGFTs. At the end, one must obtain a degree of divergence for graphs which overlaps with the result of [61] but also which includes the new parameter a. Thus, a will allow us to explore the theory space without restricting to models with Laplacian dynamics.

Consider a graph $\mathcal{G}$, with set of lines $\mathcal{L}$ with cardinal $L = |\mathcal{L}|$, set of internal faces $\mathcal{F}_{\text{int}}$ with cardinality $|\mathcal{F}_{\text{int}}| = F_{\text{int}}$ and set of external faces $\mathcal{F}_{\text{ext}}$ with cardinality $|\mathcal{F}_{\text{ext}}| = F_{\text{ext}}$. Let $A_{\mathcal{G};\boldsymbol{\mu}}$ be the associated amplitude as given in (27). The divergence degree of this amplitude will be expressed in terms of specific subgraphs of $\mathcal{G}$ which make transparent the notion of locality. These subgraphs are called quasi-local (or dangerous) and are defined by a subset of lines of $\mathcal{G}$ with internal scale much higher than any external scale. Let i be a fixed slice index and consider $\mathcal{G}^i$ the subgraph of $\mathcal{G}$ defined by the set of lines such that $\forall \ell \in \mathcal{L}(\mathcal{G}^i) \cap \mathcal{L}(\mathcal{G}), i_\ell \geq i$. $\mathcal{G}^i$ may have several connected components, we denote each component by G^i_k. The set $\{G^i_k\}_{i,k}$ defines the quasi-local subgraphs. Seeking if a subgraph g is quasi-local there is the following specific criterion: define $\mathcal{L}(g)$ and $\mathcal{L}_e(g)$ the set of internal and set external lines of g, respectively, given a momentum assignment $\boldsymbol{\mu}$ in $\mathcal{G}$, $i_g(\boldsymbol{\mu}) = \inf_{\ell \in \mathcal{L}(g)} i_\ell$ and $e_g(\boldsymbol{\mu}) = \sup_{\ell \in \mathcal{L}_e(g)}$, then g is quasi-local if and only if $i_g(\boldsymbol{\mu}) > e_g(\boldsymbol{\mu})$.

The set $\{G^i_k\}_{i,k}$ is partially ordered by inclusion and forms a tree if $\mathcal{G}$ is connected. In this situation, the tree has a root, namely the graph itself $\mathcal{G} = \mathcal{G}^0$. This tree is called the Gallavotti-Nicolò tree [69]. Figure 12 gives an example of such a tree for a graph. The optimal bound on the amplitude of a connected graph will be found by integrating internal momenta along a tree T (in the graph) in a specific way to be compatible with the abstract Gallavotti-Nicolò tree.

Using the bounds (26), (27) can be evaluated in a similar way to (24) as

$$|A_{\mathcal{G};\boldsymbol{\mu}}| \leq K^L K_1^{F_{\text{ext}}} \Big[\prod_{\ell \in \mathcal{L}} M^{-2i_\ell} \Big] \sum_{P_{I_f}} \Big\{ \prod_{f \in \mathcal{F}_{\text{int}}} \Big[\mathbf{d}^2_{P_{I_f}} e^{-\delta(\sum_{\ell \in f} M^{-i_\ell})|P_{*I_f}|^{\frac{a}{2}}} \Big] \Big\}. \tag{28}$$

Each sum over an internal P_{I_f} used in an exponential yields (see Appendix A for details pertaining to the following identities):

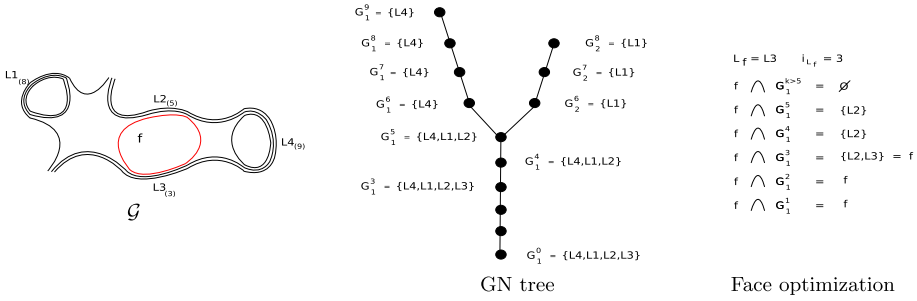

Fig. 12. A rank 3 graph $\mathcal{G}$ with lines $L1$, $L2$, $L3$ and $L4$ at a given momentum attribution (8, 5, 3, 9), respectively, and a face composed by lines $L2$ and $L3$. The corresponding Gallavotti-Nicolò (GN) tree and the face optimization procedure

– for case (a) $U(1)^D$:

$$\sum_{P_{I_f}} e^{-\delta' M^{-i}|P_{*I_f}|^{\frac{a}{2}}} = \sum_{p_{f,1},\ldots,p_{f,D}} e^{-\delta' M^{-i}(\sum_{l=1}^{D}|p_{f,l}|^a)}$$
$$= \left[\sum_{p\in\mathbb{Z}} e^{-\delta' M^{-i}|p|^a}\right]^D = cM^{\frac{D}{a}i}(1+O(M^{-\frac{i}{a}})), \quad (29)$$

for some constants c, δ' and some scale i;

– for case (b) $SU(2)^D$:

$$\sum_{P_{I_f}} \mathbf{d}^2_{P_{I_f}} e^{-\delta' M^{-i}|P_{*I_f}|^{\frac{a}{2}}} = \sum_{j_{f,1},\ldots,j_{f,D}} \left[\prod_{l=1}^{D}(2j_{f,l}+1)^2 e^{-\delta' M^{-i}|j_{f,l}|^a}\right]$$
$$= \left[\sum_{p\in\frac{1}{2}\mathbb{N}} (2p+1)^2 e^{-\delta' M^{-i}|p|^a}\right]^D$$
$$= cM^{\frac{3D}{a}i}(1+O(M^{-\frac{i}{a}})), \quad (30)$$

for some constants c, δ' and scale i.

Finding an optimal bound on $A_{\mathcal{G};\boldsymbol{\mu}}$ requires to sum over P_{I_f} such that each integral of an exponential will bring a minimal divergence. In order to satisfy this, we must choose in the face evaluation (29) and (30) the scale i such that it corresponds to $i_f = \min_{\ell\in f} i_\ell$. Call ℓ_f the line such that $i_{\ell_f} = i_f$. We must show that the end result after all optimal integrations of this kind is compatible with the Gallavotti-Nicolò tree in the sense that result formulates in terms of the set $\{G^i_k\}$.

Let us remark that a face f becomes closed in some G^i_k only if all its lines belong to that quasi-local subgraph. This means that f is closed in some G^i_k if $i \le i_{l_f}$ which further implies that the set of lines contributing to f close exactly in the $G_k^{i_{\ell_f}}$ and for all $i_\ell, 0 \le i \le i_{\ell_f}$, $f \in \mathcal{F}_{\text{int}}(G^i_k)$ (this is illustrated in Fig. 12). Using this remark, introducing $\rho_{D,a} = \dim G_D/a$ and integrating (28) in a optimal way using i_f, we expand the result using the set of quasi-local graphs (in the way of [51]) as

$$|A_{\mathcal{G};\boldsymbol{\mu}}| \le K^L K_1^{F_{\text{ext}}} K_2^{F_{\text{int}}} \left[\prod_{\ell\in\mathcal{L}} M^{-2i_\ell}\right] \prod_{f\in\mathcal{F}_{\text{int}}} \left[M^{\rho_{D,a} i_f}\right]$$
$$\le K^L K_1^{F_{\text{ext}}} K_2^{F_{\text{int}}} \left[\prod_{\ell\in\mathcal{L}} \prod_{(i,k)/\ell\in\mathcal{L}(G^i_k)} M^{-2}\right] \prod_{f\in\mathcal{F}_{\text{int}}} \prod_{(i,k)/\ell_f\in\mathcal{L}(G^i_k)} \left[M^{\rho_{D,a}}\right]$$
$$\le K^L K_1^{F_{\text{ext}}} K_2^{F_{\text{int}}} \left[\prod_{(i,k)} \prod_{\ell\in\mathcal{L}(G^i_k)} M^{-2}\right] \prod_{(i,k)} \prod_{f\in\mathcal{F}_{\text{int}}(G^i_k)} \left[M^{\rho_{D,a}}\right]$$
$$\le K^L K_1^{F_{\text{ext}}} K_2^{F_{\text{int}}} \left[\prod_{(i,k)} M^{-2L(G^i_k)+\rho_{D,a}F_{\text{int}}(G^i_k)}\right]. \quad (31)$$

Changing M for M^a in (31) leads to following statement.

Theorem 1 (Power counting theorem). *Let $\mathcal{G}$ be a connected graph of the model (20), there exist some large constants K, K_1 and K_2, such that*

$$|A_{\mathcal{G},\boldsymbol{\mu}}| \leq K^L K_1^{F_{\text{ext}}} K_2^{F_{\text{int}}} \prod_{(i,k)\in\mathbb{N}^2} M^{\omega_{\text{d}}(G_k^i)}, \qquad \omega_{\text{d}}(G_k^i) = -2aL(G_k^i) + \dim G_D \, F_{\text{int}}(G_k^i). \tag{32}$$

The quantity $\omega_{\text{d}}(\mathcal{G})$ is called the divergence degree of the graph $\mathcal{G}$. Setting $a = 1$, we get from (32), as expected, the degree of divergence as established in the gi-TGFT [61] after putting to zero an additional term associated with the so-called gauge invariance constraint on tensors (the interested reader will find details in this reference). Setting $\dim G_D = 1, a = 1$, we obtain the power counting of [44], and $a = 1/2$ yields the power counting of [56]. We also understand that, introducing a dynamics depending on a has the same effect as dilating the group dimension $\dim G_D$ by the factor a^{-1}. If we introduced $a > 1$, then the effect would be naturally to decrease the group dimension or enhancing the damping effect that the propagator has on the amplitude. Note also that the above power counting is valid for matrix models. We must then emphasize that the introduction of a non integer power a in propagator momenta might lead to a non integer divergence degree. We will see however that, seeking renormalizable models, the possible values of a are limited to rational numbers.

A remark on $G_D = U(1)^p \times SU(2)^q$, $\dim G_D = p + 3q$. Considering G_D now as a product of $U(1)^p$ and $SU(2)^q$ is straightforward: the kinetic term builds as sums of kinetic terms of the form (14) in each sector. The slice decomposition can be performed as in (26) and, after the multi-scale analysis, the final degree of divergence (32) splits as

$$\omega_{\text{d}}(G_k^i) = -2aL(G_k^i) + p\, F_{\text{int}}^1(G_k^i) + 3q\, F_{\text{int}}^2(G_k^i), \tag{33}$$

where two types of faces have to be introduced according to the fact that these can be generated in the $U(1)$ sector (F_{int}^1) or in the $SU(2)$ sector (F_{int}^2). This study will be postponed to a subsequent work.

3.3. Divergence degree and list of potentially renormalizable models.

Divergence degree. In form (32), the divergence degree ω_{d} is not very insightful for the determination of all primitively divergent graphs. To fully understand this quantity, we must introduce further details on the graph which are related to the underlying color structure corresponding to the trace invariants.

Consider a connected graph $\mathcal{G}$ and its colored extension $\mathcal{G}_{\text{color}}$ as introduced in Sect. 2.2. The following result has been established for a reduced case $d = 4$ [44] and then extended to any rank in [60].

Proposition 1 (Number of internal faces in a rank $d \geq 3$ model). *Let $\mathcal{G}$ be a rank d connected graph, $\mathcal{G}_{\text{color}}$ its colored extension, $\partial\mathcal{G}$ its boundary with number $C_{\partial\mathcal{G}}$ of connected components, V_k its number of vertices of coordination k, $V = \sum_k V_k$ its total number of vertices, $n \cdot V = \sum_k kV_k$ its number of half lines exiting from vertices, N_{ext} its number of external legs.*

The number of internal faces of $\mathcal{G}$ is given by

$$F_{\text{int}}(\mathcal{G}) = -\frac{2}{(d-1)!}(\omega(\mathcal{G}_{\text{color}}) - \omega(\partial\mathcal{G})) - (C_{\partial\mathcal{G}} - 1) - \frac{d-1}{2} N_{\text{ext}} + d - 1 - \frac{d-1}{4}(4 - 2n) \cdot V, \tag{34}$$

where $\omega(\mathcal{G}_{\text{color}}) = \sum_J g_{\tilde{J}}$ is the degree of $\mathcal{G}_{\text{color}}$, $\tilde{J}$ is the pinched jacket associated with J a jacket of $\mathcal{G}_{\text{color}}$, $\omega(\partial\mathcal{G}) = \sum_{J_\partial} g_{J_\partial}$ is the degree of $\partial\mathcal{G}$.

Proof. See Proposition 3.7 in [60]. □

Note that the number of internal faces does not depend on the dimension of the group or the gauge invariance of the theory but only on the combinatorics of the graph itself. From this proposition, we are in position to reformulate the divergence degree of a graph.

Proposition 2 (Divergence degree). *The divergence degree of a graph $\mathcal{G}$ is given by*

$$\begin{aligned}\omega_{\text{d}}(\mathcal{G}) = &-\frac{2\dim G_D}{(d-1)!}(\omega(\mathcal{G}_{\text{color}}) - \omega(\partial\mathcal{G})) - \dim G_D(C_{\partial\mathcal{G}} - 1)\\ &-\frac{1}{2}\Big[(\dim G_D(d-1) - 2a)N_{\text{ext}} - 2\dim G_D(d-1)\Big]\\ &-\frac{1}{2}\Big[2\dim G_D(d-1) + (2a - \dim G_D(d-1))n\Big]\cdot V. \end{aligned} \tag{35}$$

Proof. This formula $\omega_{\text{d}}(\mathcal{G})$ can be easily obtained after substituting the combinatorial relation (we omit the dependence in the graph $\mathcal{G}$)

$$-2L = -(n\cdot V - N_{\text{ext}}) \tag{36}$$

and (34) in the divergence degree (32). □

Since we will be also interested in matrix models, it is relevant to understand the above power counting in the rank 2 case. In that situation, the following proposition holds (in the same notations).

Proposition 3 (Divergence degree of matrix models). *The divergence degree of a graph $\mathcal{G}$ is given by*

$$\begin{aligned}\omega_{\text{d}}(\mathcal{G}) = &-2\dim G_D g_{\tilde{\mathcal{G}}} - \dim G_D(C_{\partial\mathcal{G}} - 1) - \frac{1}{2}\Big[(\dim G_D - 2a)N_{\text{ext}} - 2\dim G_D\Big]\\ &-\frac{1}{2}\Big[2\dim G_D + (2a - \dim G_D)n\Big]\cdot V, \end{aligned} \tag{37}$$

where $\tilde{\mathcal{G}}$ is the closed (pinched) graph associated with $\mathcal{G}$.

Proof. Introducing the closed graph $\tilde{\mathcal{G}}$ (closing all external faces by inserting a two-leg vertex at each external half-line, see Fig. 11), one gets from the Euler characteristic of $\tilde{\mathcal{G}}$

$$F_{\text{int}} = 2 - 2g_{\tilde{\mathcal{G}}} - (V - L + C_{\partial\mathcal{G}}). \tag{38}$$

Substituting the last result and (36) in (32) yields the desired relation. □

Criteria for potentially renormalizable models. There is a proof that, for any graph in this category of models ([44] and its addendum [45])

$$\omega(\mathcal{G}_{\text{color}}) - \omega(\partial\mathcal{G}) \geq 0. \tag{39}$$

Also, for any graph with external legs (as those of interest in the renormalization procedure are), $C_{\partial\mathcal{G}} \geq 1$. Therefore, for any connected graph with $N_{\text{ext}} \geq 2$, the following is valid (introducing $d^- = d - 1$)

$$\omega_{\text{d}}(\mathcal{G}) \leq \frac{1}{2}\Big[2\dim G_D d^- + (2a - \dim G_D d^-)N_{\text{ext}}\Big] - \frac{1}{2}\Big[2\dim G_D d^- + (2a - \dim G_D d^-)n\Big] \cdot V. \tag{40}$$

Furthermore, in any theory rank $d \geq 3$, melonic graphs (recalling that these are defined such that $\omega(\mathcal{G}_{\text{color}}) = 0$) with melonic boundary (such that $\omega(\partial\mathcal{G}) = 0$) with a unique connected component on the boundary saturate this bound. Thus (40) is optimal. The particular rank $d = 2$ situation is similar. The class of dominant graphs in power counting are planar graphs $g_{\tilde{\mathcal{G}}} = 0$ with $C_{\partial\mathcal{G}} = 1$ for which (40) is saturated as well. Given the above bound, we can now investigate which parameters $(\dim G_D, a, d)$ will lead to potentially super- and just-renormalizable models.

Consider $D \geq 1, d \geq 2, a \in (0, 1]$, and $k_{\max} \geq 4$ the maximal coordination among all interactions of a graph $\mathcal{G}$ ($k_{\max} = 2$ leads to a quadratic trivial interactions; $k_{\max}$ odd is possible for matrix models but not when using complex matrices; $k_{\max} = 3$ is also impossible in the tensor case because there is no trace invariant built from contractions of an odd number of tensors [37]).

From (40), we shall call a model

(i) nonrenormalizable if $\exists k$, such that $2\dim G_D d^- + (2a - \dim G_D d^-)k < 0$;
(ii) renormalizable if $\forall k$, $2\dim G_D d^- + (2a - \dim G_D d^-)k \geq 0$.

Referring to the first condition, one can show that, in such a model, there exists an infinite number of graphs with arbitrary large degree of divergence depending on their number of vertices.[7] Meanwhile, the second condition will be further specified in order to establish which models will be super- and just-renormalizable. Note that the class of super-renormalizable models includes models with all convergent amplitudes. In the rest of this section, we shall not exclude from the discussion convergent models (however, from the next section onwards, such convergent models will not be discussed because our main interest lies in the renormalization of divergent models).

Now, we seek a finer criterion in order to distinguish super- from just-renormalizable models. Two cases might occur:

(A) Assume $2a - \dim G_D d^- \geq 0$, then for all $k \geq 0$, we have $2\dim G_D d^- + (2a - \dim G_D d^-)k > 0$. Hence, one agrees that

$$\omega_{\text{d}}(\mathcal{G}) \leq -\dim G_D d^-(V - 1) - \frac{1}{2}(2a - \dim G_D d^-)(n \cdot V - N_{\text{ext}}). \tag{41}$$

For any graph, we know that $V \geq 1$ and $n \cdot V \geq N_{\text{ext}}$. Then the above bound of the divergence degree leads to either convergent amplitudes or to logarithmically divergent (log-divergent) graphs characterized by $\omega_{\text{d}}(\mathcal{G}) = 0$. The case $n \cdot V = N_{\text{ext}}$ corresponds to a graph without propagator which is not of interest. Thus we can

[7] First, one must recall that the divergence degree is optimal, i.e. there are always some graphs which saturate the bound (40). Consider some vertex valence k_0 satisfying $2\dim G_D d^- + (2a - \dim G_D d^-)k_0 < 0$. Remark that one must have $(2a - \dim G_D d^-) < 0$, otherwise the previous condition can never be satisfied. Consider then the class of graphs made specifically with V_{k_0} vertices and no other type of vertices. We can certainly focus on the graphs such that $N_{\text{ext}} < k_0$, for which ω_{d} admits an upper bound which depends on V_{k_0} and thus ω_{d} for these graphs can be arbitrarily large.

assume $n \cdot V > N_{\text{ext}}$. If $2a - \dim G_D d^- > 0$, all amplitudes are convergent: the model is super-renormalizable. Thus the only possible situation leading to divergences is given by

$$V = 1 \quad \text{and} \quad 2a - \dim G_D d^- = 0. \tag{42}$$

Note that the condition $2a - \dim G_D d^- = 0$ depends only on the model parameters and can be implemented from the beginning. We write

$$\omega_{\text{d}}(\mathcal{G}) \leq \dim G_D d^{-1}(1 - V). \tag{43}$$

Then, in these theories, only graphs $\mathcal{G}$ such that $\omega(\mathcal{G}_{\text{color}}) = 0 = \omega(\partial\mathcal{G})$ (or $g_{\tilde{\mathcal{G}}} = 0$ for $d = 2$, resp.) and $C_{\partial\mathcal{G}} = 1$ made with 1 vertex with an arbitrary number of external legs are diverging. In other words, only melonic (planar, resp.) tadpoles with arbitrary number of legs are possibly logarithmically divergent (log–divergent) in this theory. If one performs a truncation in the interaction (18), choosing all trace invariants from valence 2 up to order $k_{\max}$, then contracting any of these interactions (of coordination larger than 4) in order to form melonic (planar, resp.) tadpoles, might give another graph the boundary of which is again a trace invariant of lower order or a disjoint union of such trace invariants. The latter case has been called anomalous terms in anterior studies [44,60,61]. Thus, at a maximal order $k_{\max}$, including all lower order trace invariants (the set of which should be finite) and their possible anomalous terms by successive contractions (the set of which should be finite too), yields a possible class of stable (does not generate any other vertex than the one included) and super-renormalizable theories. At the end, the number of diverging tadpole graphs in such a theory is always determined by the number of vertices which is finite. Hence, $2a - \dim G_D d^{-1} \geq 0$ defines super-renormalizable models (similarly to the so-called $P(\phi^2)$ model).
Inspecting when $2a - \dim G_D d^{-1} = 0$ vanishes, we get the following solutions:

$$\begin{aligned} &0 < \dim G_D(d-1) \leq 2\,, \\ &\dim G_D(d-1) = 1, \qquad \dim G_D = 1\,, \quad G_D = U(1)\,, \quad d = 2, \qquad a = \frac{1}{2}\,; \\ &\dim G_D(d-1) = 2, \qquad \dim G_D = 2\,, \quad G_D = U(1)^2\,, \quad d = 2, \qquad a = 1, \\ &\qquad\qquad\qquad\quad \dim G_D = 1\,, \quad G_D = U(1)\,, \quad d = 3, \qquad a = 1. \end{aligned} \tag{44}$$

(B) Let us assume now that $2a - \dim G_D d^{-1} < 0$. Interested in the case when, $\forall k$, $2\dim G_D d^- + (2a - \dim G_D d^-)k \geq 0$, this leads to

$$k_{\max} \leq \frac{2\dim G_D d^-}{\dim G_D d^- - 2a}. \tag{45}$$

Then, if $k_{\max}$ is exactly the upper bound, the model is just-renormalizable. If $k_{\max}$ is strictly smaller than the upper bound then, the model is super-renormalizable. In general, the number of external legs improves as well the power counting (recalling that $(2a - \dim G_D d^{-1})N_{\text{ext}} < 0$). We comment that, by specifying $k_{\max}$ for a just-renormalizable model, we can immediately infer a tower of super-renormalizable models labelled by all $k'_{\max} \in [\![4, k_{\max})$, where $k'_{\max}$ is the new maximal valence of the vertices in these models. We will address such models implicitly encoded in the class of just-renormalizable models only in Sect. 6.

Potentially just-renormalizable models. Just-renormalizable models require that $\dim G_D d^- - 2a > 0$ and

$$k_{\max} = \frac{2 \dim G_D d^-}{\dim G_D d^- - 2a} = 2 + \gamma_{a,D}, \qquad \gamma_{a,D} = \frac{4a}{\dim G_D (d-1) - 2a}. \tag{46}$$

We immediately see that this class of simple TGFT models radically differs from the class of gauge invariant ones [61] for which a similar condition is obtained using $d^- = d - 2$ and $a = 1$. Focusing on the term involving V in (40), one has

$$\begin{aligned} &\Big[2 \dim G_D d^- + (2a - \dim G_D d^-)\tilde{n}\Big] \cdot \tilde{V} \\ &:= - \sum_{k < k_{\max}} \Big[(\dim G_D d^- - 2a)k - 2 \dim G_D d^-\Big] V_k < 0. \end{aligned} \tag{47}$$

Thus, any graph having $N_{\text{ext}} = k_{\max}$, $V_{k_{\max}} > 0$ and $V_{k<k_{\max}} > 0$ is converging. This gives us the interesting property that *a graph with $N_{\text{ext}} = k_{\max}$ is log-divergent if and only if it is built with vertices of maximal valence $k_{\max}$*.

We compile this in order to have a first et of condition for obtaining just-renormalizable models and it reads

$$\{\dim G_D (d-1) > 2a\}\,; \quad \Big\{k_{\max} = 2 + \gamma_{a,D} > 2 \quad \Leftrightarrow \quad \dim G_D (d-1) \leq 6a\Big\}$$

$$\text{so that} \qquad 2a < \dim G_D (d-1) \leq 6a. \tag{48}$$

Assuming $d = 2$, the above condition translates as

$$\begin{aligned} &\dim G_D > 2a, \\ &a = 1, \qquad \dim G_D > 2a \geq 2\,, \quad \dim G_D > 2, \\ &1 > a \geq 1/2, \qquad \dim G_D > 2a \geq 1, \quad \dim G_D \geq 2, \\ &a < 1/2, \qquad \dim G_D \geq 1 > 2a, \quad \dim G_D \geq 1. \end{aligned} \tag{49}$$

Assume now that $d \geq 3$, then we have

$$\begin{aligned} &\dim G_D > a, \\ &a = 1, \qquad \dim G_D > 1 = a, \quad \dim G_D \geq 2, \\ &a < 1, \qquad \dim G_D \geq 1 > a, \quad \dim G_D \geq 1. \end{aligned} \tag{50}$$

For an arbitrary N_{ext}, (40) translates now as

$$\begin{aligned} \omega_{\text{d}}(\mathcal{G}) \leq &- \frac{1}{2}(\dim G_D d^- - 2a)(N_{\text{ext}} - k_{\max}) \\ &- \frac{1}{2}\Big[2 \dim G_D d^- + (2a - \dim G_D d^-)\tilde{n}\Big] \cdot \tilde{V}. \end{aligned} \tag{51}$$

Assuming then that $N_{\text{ext}} > k_{\max}$ gives a convergent amplitude provided the fact that $\dim G_D d^- > 2a$. For the situation, such that $N_{\text{ext}} < k_{\max}$, the amplitude may or may not diverge.

We are now in position to determine models which are potentially just-renormalizable. Let us focus on $d = 2$ (49), then one realizes from (48) that

$$a=1, \qquad 2<\dim G_D\leq 6$$

$$\begin{aligned}
&\dim G_D=3, \quad k_{\max}=6,\\
&\dim G_D=4, \quad k_{\max}=4,\\
&\dim G_D=5, \quad k_{\max}=\frac{10}{3}\notin\mathbb{N},\\
&\dim G_D=6\,, \quad k_{\max}=3.
\end{aligned} \tag{52}$$

The last case $\dim G_D=6$ would not be retained because $k_{\max}\geq 4$ for complex matrix models. However, this case could still induce a potentially renormalizable real matrix model.

Recalling that

$$k_{\max}=2+\gamma_{a,D}, \quad \gamma_{a,D}=\gamma=\frac{4a}{\dim G_D-2a}\in\mathbb{N}\backslash\{0\}, \quad a(4+2\gamma)=\dim G_D\gamma, \tag{53}$$

in the second sector, the following is satisfied:

$$\begin{aligned}
&1>a\geq 1/2, \qquad 2\leq\dim G_D<6, \qquad \frac{4}{\dim G_D-2}>\gamma\geq\frac{2}{\dim G_D-1}\,,\\
&\quad \dim G_D=2, \qquad \forall\gamma\geq 2 \text{ and } \gamma\in\mathbb{N}\,, \quad a=\frac{\gamma}{2+\gamma}\,, \qquad k_{\max}=2+\gamma>2\,;\\
&\quad \dim G_D=3, \qquad 4>\gamma\geq 1 \text{ and } \gamma\in\mathbb{N}\,, \quad a=\frac{3\gamma}{4+2\gamma}\,, \qquad k_{\max}=2+\gamma>2\,;\\
&\quad \dim G_D=4,5, \qquad \gamma=1, \quad a=\frac{\dim G_D}{6}\,, \qquad k_{\max}=3>2.
\end{aligned} \tag{54}$$

In the last sector, we have

$$\begin{aligned}
&0<a<1/2, \qquad 1\leq\dim G_D<3, \quad 0<\gamma<\frac{2}{\dim G_D-1}\,,\\
&\quad \dim G_D=1, \quad \forall\gamma\geq 1 \text{ and } \gamma\in\mathbb{N}\,, \quad a=\frac{\gamma}{4+2\gamma}\,, \qquad k_{\max}=2+\gamma>2\,;\\
&\quad \dim G_D=2, \qquad \gamma=1\,, \quad a=\frac{1}{3}\,, \qquad k_{\max}=3>2.
\end{aligned} \tag{55}$$

This exhausts potentially just-renormalizable models in the rank $d=2$ case. We point out that several of the above models in (54) and (55) defined with $k_{\max}$ an odd positive integer are potentially interesting only in the case of real matrix models. Table 2 gives a summary of the previous analysis.

Next, we study the rank $d\geq 3$ situation. It is important to keep in mind the following feature: for any $d\geq 3$, $k_{\max}$ cannot be an odd integer as it turns out to be impossible to built a trace invariant out off a odd number of tensors in any theory rank $d\geq 3$. One has:

$$\dim G_D>a\,,$$

$$\begin{aligned}
&a=1, \qquad \dim G_D>1=a, \quad \dim G_D\geq 2,\\
&a<1, \qquad \dim G_D\geq 1>a, \quad \dim G_D\geq 1.
\end{aligned} \tag{56}$$

Table 2. List of all potentially just-renormalizable matrix models $_{\dim G_D}\Phi^k_2$

$\dim G_D$	$a = 1$	$a \in (0, 1/2)$	$a \in [1/2, 1)$	
1	$\times$	$\Phi^{2k>2}$	$\times$	
2	$\times$	$\times$	$\Phi^{2k\geq 4}$	
3	Φ^6	$\times$	$\Phi^4, a = \frac{3}{4}$	
4	Φ^4	$\times$	$\times$	
1	$\times$	$\Phi^{2k+1>2}$	$\times$	
2	$\times$	$\Phi^3, a = \frac{1}{3}$	$\Phi^{2k+1\geq 4}$	
3	$\times$	$\times$	$\Phi^{k=3,5}, a = \frac{1}{2}, \frac{9}{10}$	(resp.)
4	$\times$	$\times$	$\Phi^3, a = \frac{2}{3}$	
5	$\times$	$\times$	$\Phi^3, a = \frac{5}{6}$	
6	Φ^3	$\times$	$\times$	

All interactions of the Φ^{2k+1} type may only be considered in a real model

Table 3. List of rank $d \geq 3$ tensor models potentially just-renormalizable

$\dim G_D d^-$	$a = 1$	$a \in (0, 1)$
2	$\times$	$\Phi^{2k>2}$
3	Φ^6	$\Phi^4, a = \frac{3}{4}$
4	Φ^4	$\times$

We define

$$\gamma = \frac{4a}{\dim G_D d^- - 2a} \in \mathbb{N}\backslash\{0\}\,, \qquad a(4+2\gamma) = \dim G_D d^- \gamma\,, \tag{57}$$

such that $a = 1$ yields

$$\begin{aligned} &2 < \dim G_D d^- \leq 6, \qquad (4+2\gamma) = \dim G_D d^- \gamma\,, \\ &\dim G_D d^- = 3, \qquad \gamma = 4, \quad k_{\max} = 6, \\ &\dim G_D d^- = 4, \qquad \gamma = 2, \quad k_{\max} = 4, \\ &\dim G_D d^- = 5, \qquad 3\gamma = 4, \quad k_{\max} \notin \mathbb{N}, \\ &\dim G_D d^- = 6, \qquad \gamma = 1, \quad k_{\max} = 3. \end{aligned} \tag{58}$$

The last case should be excluded because of the same above reason. Next, one focuses on $0 < a < 1$, for which the sole relevant situations are obtained as

$$\begin{aligned} &\dim G_D d^- \geq 2, \qquad 0 \leq (\dim G_D d^- - 2)\gamma < 4, \\ &\dim G_D d^- = 2, \qquad \forall \gamma \geq 2 \text{ and } \gamma \in 2\mathbb{N}, \quad a = \frac{\gamma}{2+\gamma}, \qquad k_{\max} = 2 + \gamma > 2, \\ &\dim G_D d^- = 3, \qquad \gamma = 2, \quad a = \frac{3}{4}, \qquad k_{\max} = 4, \end{aligned} \tag{59}$$

where in the above cases, the cases of odd γ giving an odd $k_{\max}$ have been precluded (same above remark). Let us summarize at this point the data in Table 3.

Compiling Tables 2 and 3 and considering the group dimension $\dim G_D$ and theory rank d yield Table 4 (each model depends also on a) giving a summary of all potentially renormalizable models (including real in the matrix case).

Table 4. List of rank $d \geq 2$ tensor models which are potentially just-renormalizable

$\dim G_D \downarrow$	$d-1 \rightarrow$					
	1	2	3	4	5	6
1	${}_1\Phi_2^{k>2}$	${}_1\Phi_3^{2k>2}$	${}_1\Phi_4^{6,4}$	${}_1\Phi_5^4$	×	×
2	${}_2\Phi_2^{k>2}$	${}_2\Phi_3^4$	×	×	×	×
3	${}_3\Phi_2^{3,4,5,6}$	×	×	×	×	×
4	${}_4\Phi_2^{3,4}$	×	×	×	×	×
5	${}_5\Phi_2^3$	×	×	×	×	×
6	${}_6\Phi_2^3$	×	×	×	×	×

Some comments are in order:

(a) First, one notices that there is no model over $SU(2)$ which could be just-renormalizable when $d \geq 3$. $G_1 = SU(2)$ can only be the background group manifold for the ${}_3\Phi_2^{3,4,5,6}$ models and $G_2 = SU(2)^2$ for ${}_6\Phi_2^3$.

(b) The tensor models ${}_1\Phi_4^6$ and ${}_1\Phi_3^4$ (in first row) have been already proved to be renormalizable in [44] and [56], respectively.

(c) The matrix models ${}_1\Phi_2^{k_1>2}$ and ${}_2\Phi_2^{k_2\geq 4}$ may be in fact very similar when both k_1 and k_2 coincide after mapping $a \to 2a$, if $2a \in (1/2, 1)$, that is if $a \in (1/4, 1/2)$. Otherwise these models are actually different and, in the following, we will treat them as such unless otherwise explicitly stated.

(d) Another strong fact is that there are, a priori, three towers of potentially interesting models: any $\Phi^{2k\geq 4}$ over $G = U(1)$ in rank $d = 3$, and $\Phi^{k\geq 3,4}$ over $G \in \{U(1), U(1)^2\}$ in rank $d = 2$.

(e) Interestingly, one notices that the Φ^4 interaction appears several times in that list up to the group dimension $\dim G_D = 4$. It is a kind of "privileged" interaction for the tensor and matrix field models.

(f) The complex Grosse–Wulkenhaar (GW) model in 4 dimensions written in the matrix basis and at its self-dual point [49] is a matrix model which can be written in terms of rank two tensors $\bar{\varphi}_{\vec{m},\vec{n}}$ and $\varphi_{\vec{m},\vec{n}}$, $\vec{n} = (n_1, n_2) \in \mathbb{N}^2$, as

$$S_{GW} = \frac{1}{2} \sum_{\vec{p},\vec{q}\in\mathbb{N}^2} \bar{\varphi}_{\vec{p},\vec{q}} \Big[|p| + |q| + \mu \Big] \varphi_{\vec{q},\vec{p}} + \frac{\lambda}{4} \sum_{\vec{m},\vec{n},\vec{p},\vec{q}\in\mathbb{N}^2} \bar{\varphi}_{\vec{m},\vec{n}}\, \varphi_{\vec{n},\vec{p}}\, \bar{\varphi}_{\vec{p},\vec{q}}\, \varphi_{\vec{q},\vec{m}}, \tag{60}$$

where we introduce the notation, for any $\vec{n} \in \mathbb{N}^2$, $|n| = n_1 + n_2$.

One should pay attention to the fact that, although the GW model can be naively considered as defined with rank 4 tensors $\varphi_{\vec{p},\vec{q}} = \varphi_{p_1,p_2,q_1,q_2}$ then, according to the previous developments, it is not the ${}_1\Phi_4^4$ tensor model with $a = \frac{1}{2}$ (according to Table 4, only the ${}_1\Phi_4^4$ tensor model with $a = \frac{3}{4}$ is potentially just-renormalizable). The reason why this is not the case comes from the particular form of the GW interaction. In the above analysis, we strongly use the fact that the divergence degree (40) is saturated for melonic graphs. However, in the GW model viewed as a rank 4 tensor

I_{GW} I'_{GW} I''

Fig. 13. The interaction of GW model in 4D viewed as a matrix model is I_{GW} and, viewed as a rank 4 model, the interaction reads I'_{GW}. Both have to be distinguished with the melonic rank 4 interaction I''

Table 5. List of potentially just-renormalizable rank $d \geq 2$ complex tensor models

$\dim G_D \downarrow$	$d-1 \rightarrow$					
	1	2	3	4	5	6
1	${}_1\Phi_2^{2k>2}$	${}_1\Phi_3^{2k>2}$	${}_1\Phi_4^{6,4}$	${}_1\Phi_5^4$	×	×
2	${}_2\Phi_2^{2k>2}$	${}_2\Phi_3^4$	×	×	×	×
3	${}_3\Phi_2^{4,6}$	×	×	×	×	×
4	${}_4\Phi_2^4$	×	×	×	×	×

model, the vertex is of the form I'_{GW} of Fig. 13, and cannot generate such category of melonic graphs (see $I''$of Fig. 13 representing a rank 4 melonic Φ^4 interaction). Thus, the GW model should be strictly considered as a matrix model and its power counting theorem should follow from Proposition 3 and not from Proposition 2. The way to embed the 4D GW in the above formalism comes from the fact that the tensor indices in that model are one to one with representation indices of $U(1)^2$. Hence, the GW model as a matrix model might read ${}_2\Phi_2^4$ for $a = 1/2$. This model is included in Table 4. Using the projection mapping introduced in [57], which allows to reduce the rank of the tensor and still to preserve the power counting, we can map $\varphi_{\vec{n},\vec{m}} \rightarrow \varphi_{n,m}, n, m \in \mathbb{N}$, so that we might fully represent the GW model over $U(1)$ as ${}_1\Phi_2^4$ with $a = 1/4$ again a matrix model included in the table.

Concentrating on rank $d \geq 2$ complex tensors, Table 5 provides the list of models that we will discuss in the following.

4. Just Renormalizable Rank $d \geq 3$ Tensor Models

The previous section determines the maximal valence $k_{\max}$ of the vertices which may actuate the model renormalizability. In this section, we intend to build models which are indeed renormalizable given the above data. The models are constructed in a standard way: we include all vertices of lower valence up to $k_{\max}$ and, due to some specific higher rank structure, we also should pay attention to the appearance of peculiar anomalous terms which should be included as well. Afterwards, given a model ${}_{\dim G_D}\Phi_d^k$, we provide a list of all divergent amplitudes and their associated graphs which must be renormalized in the subsequent section.

One proceeds according to the general recipe: Consider any model susceptible to be renormalizable as given by Table 5. This will determine a, the kinetic term and covariance, $k_{\max}$ and from this, use all trace invariants of lower order up to 4. In the rank $d \geq 3$ case, among the trace invariants, use only melonic ones as the interaction terms.

4.1. Tensor models and their renormalizability.

Truncating the rank $d = 3$ tower. The tower $({}_1\Phi_3^{k_{\max}}, a = 1 - \frac{2}{k_{\max}})$, $k_{\max} \in 2\mathbb{N}\backslash\{0, 2\}$, is worth discussing in more details. At a given order $k_{\max}$, the problem of finding specific criteria for listing $k_{\max}$ connected unitary tensor invariants is not known to the best of our knowledge. In fact, this problem is very subtle because we do not need to list all 3-bubbles, but only specific 3-bubbles of the melonic kind. Melonic bubbles, in general, will govern the locality principle of tensor models. Returning to the above tower dealing with models of rank $d = 3$, we did not successfully identify an algorithm for generating all possible connected melonic 3-bubbles made with $k_{\max}$ vertices up to a line-coloring. It is known [30] that melonic two-point functions made with q vertices map to rooted colored trees with q unlabeled vertices. The number of such combinatorial species is given by a generalized $(d+1)-$Catalan number. The problem addressed now is to identify all possible melonic $k_{\max}$-point function made with $k_{\max}$ vertices. This is more intricate because of the equivalence of several configurations if there is not a unique root. Certainly the number of these objects is bounded by the generalized Catalan number because a $k_{\max}$-point function can be obtained by cutting more lines (of color 0 for instance) in the 2-point function. Also, even knowing the number of different configurations does not necessarily gives a way to list them according to some criteria. Certainly, the recently developed counting techniques built on permutation groups might be useful to list those invariants in an appropriate way [70]. This delicate study will require more combinatorial tools. For this reason, we will address only the renormalizability of models such that $k_{\max} = 4, 6$ in this tower.

At a given $k_{\max} = 4, 6$, we aim at studying all rank $d \geq 3$ tensor models ${}_{\dim G_D}\Phi_d^{k_{\max}}$. Note that the ${}_1\Phi_4^6$ and ${}_1\Phi_3^4$ have been already proved renormalizable [44,56]. We provide in the following here a unifying perspective towards the study of renormalizability of TGFTs. Hence, in addition to the aforementioned models, we will address the renormalizability proof of the following models

$$ {}_1\Phi_3^6, \qquad {}_2\Phi_3^4, \qquad {}_1\Phi_4^4, \qquad {}_1\Phi_5^4. \tag{61} $$

Block index notations. Dealing with an arbitrary rank $d = 3, 4, 5$ and a group $G_D = U(1)^D$ with $D = 1, 2$, we must find adequate notations for representing the different types of interactions. We have already introduced $\varphi_{[I]}$ the rank d tensor field where $[I] = \{I_1, \ldots, I_d\}$ collects all momentum labels. The interactions are built from particular contractions of the indices I_s between tensor fields. This is done in such a way that we can further decompose $[I]$ in sub-blocks fully contracted with other sub-blocks in other tensor fields. We write

$$ \varphi_{[I]} = \varphi_{[1][2]\ldots[q]}\,, \quad [s] = (I_{s,1}, \ldots, I_{s,l})\,, \quad s = 1, \ldots, q\,, \tag{62} $$

where q may vary according to the contraction we are interested in. For any rank d tensor field $\varphi_{[I]} = \varphi_{12\ldots d}$, there are two particular decompositions of the tensor labels of interest in the following. The first can be called the identical decomposition and is given by

$$ \varphi_{12\ldots d} = \varphi_{[1][2]\ldots[d]}, \quad [s] = s\,, \tag{63} $$

and the second is the so-called matrix type decomposition of the tensor entries which can be written as

$$ \varphi_{123\ldots d} = \varphi_{[a]\{\check{a}\}}\,, \quad [a] = a\,, \quad \{\check{a}\} = (1, 2, \ldots, \check{a}, \ldots d)\,, \tag{64} $$

where, at least, one block uses brace brackets. Note that, in this latter decomposition, one block contains a single element and, though not explicit, the brace bracket depends on the tensor rank. On matrix models, only the identical decomposition will be significant. Furthermore, the matrix decomposition is "canonical" in the sense that, even though its seems that we have changed the place of the index a in the tensor as $\varphi_{\dots a \dots} = \varphi_{[a]\dots}$, the previous position of that index is still encoded in $\{\check{a}\}$. Thus, this prescription preserves the (colored-like) gluing rule for graphs depending on the position of labels in the tensor.

For all models ${}_{(\cdot)}\Phi^4_{d\geq 3}$, a matrix type decomposition will be used. For the model ${}_1\Phi^6_3$, we will use a matrix and an identical decomposition to describe the model. Last, for the ${}_1\Phi^6_4$ model, we introduce the non trivial decomposition characterized by

$$\varphi_{1234} = \varphi_{[1][2][3]}, \quad [1] = 1\,, \quad [2] = (2,3)\,, \quad [3] = 4. \tag{65}$$

One should pay attention to the fact that, in the above notations, discussing either ${}_1\Phi^6_3$ or ${}_1\Phi^6_4$, the tensor field will be denoted as $\varphi_{[1][2][3]}$. However, according to the model context, these block notations of tensor do not refer to the same quantities. The point for introducing such notations comes from the fact that the model properties and its renormalization analysis only depend on these decompositions of the tensor indices.

Propagators. Propagators has been already discussed. They are given by (16) and are represented by stranded lines as in Fig. 1.

Melonic interactions. The interactions of the models must be chosen according to the truncation of the series of all possible interactions from relevant to marginal terms. Here, the interactions are generated by the series $S^{\text{int}}(\varphi, \bar{\varphi})$ (18) of all connected melonic contractions for a certain rank d theory. From the power-counting theorem, Proposition 2, and subsequent analysis of the divergence degree, for a given ${}_{(\cdot)}\Phi^{k_{\max}}_d$ model, we have a specific criterion to truncate the series $S^{\text{int}}(\varphi, \bar{\varphi})$. We will only consider melonic interactions with at most $k_{\max} = N_{\text{ext}}$ external legs. It may happen that terms called anomalies [44] appear because generated by the RG flow without being initially present in (18). In such instance, one must add these terms in the initial action and check that the resulting action does not generate any further term.

– For $k_{\max} = 6$ ($d = 3, 4$ and $\dim G_D = 1$), two types of interactions $S^{\text{int}}_{6;1}$ and $S^{\text{int}}_{6;2}$ of the Φ^6-form can be constructed. These are given by

$$S^{\text{int}}_{6;1} = \sum_{P_{[I]}} \varphi_{[1]\{\check{1}\}} \bar{\varphi}_{[1']\{\check{1}\}} \varphi_{[1']\{\check{1}'\}} \bar{\varphi}_{[1'']\{\check{1}'\}} \varphi_{[1'']\{\check{1}''\}} \bar{\varphi}_{[1]\{\check{1}''\}} + \text{permutations}, \tag{66}$$

$$S^{\text{int}}_{6;2} = \sum_{P_{[I]}} \varphi_{[1][2][3]} \bar{\varphi}_{[1]'[2]'[3]} \varphi_{[1]'[2]'[3]'} \bar{\varphi}_{[1]''[2][3]'} \varphi_{[1]''[2]''[3]''} \bar{\varphi}_{[1][2]''[3]''} + \text{permutations}, \tag{67}$$

where the sum of "permutations" is performed on colors. For the ${}_1\Phi^6_{d=3,4}$ model, (66) contains exactly d terms, meanwhile (67) contains $d(d-1)/2$ terms. Using the colored extension of these vertex (as discussed in Sect. 2.2), one may check that the resulting colored graphs satisfy the condition that their degree are vanishing. A drawing of these interactions is given in Fig. 14 where bold lines may encapsulate several strands depending on the model. Within a model, from $V_{6;1}$ to $V_{6;2}$, these bold lines may not contain the same number of strands. As one realize, the block index notation is a handy way for writing vertices (and not always Feynman graphs, because in the gluing the propagator may not follows the block index) and to perform the subsequent calculations.

In addition to these interactions, we must introduce a Φ^4 interaction as

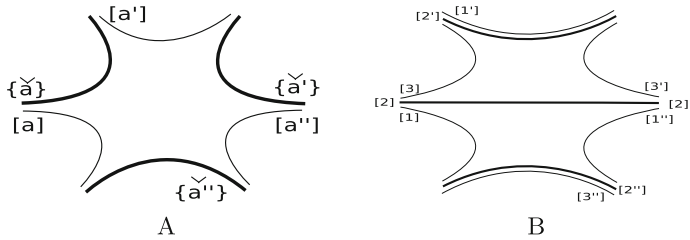

Fig. 14. The vertices of the types $V_{6;1}$ (A) and $V_{6;2}$ (B)

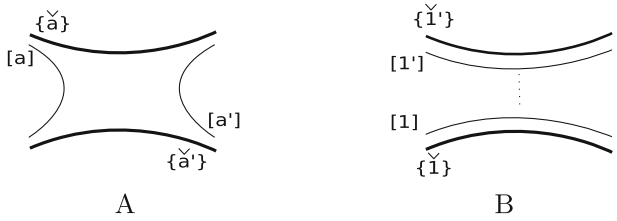

Fig. 15. Vertices Φ^4 of the V_4 (A) and $V_{4;\mathrm{a}}$ (B) types

$$S_4^{\mathrm{int}} = \sum_{P_{[I]}} \varphi_{[1]\{\check{1}\}} \bar{\varphi}_{[1']\{\check{1}\}} \varphi_{[1']\{\check{1}'\}} \bar{\varphi}_{[1]\{\check{1}'\}} + \text{permutations} \tag{68}$$

which contains d terms (Fig. 15 A shows a general term in this interaction). It turns out that the ${}_1\Phi_4^6$ model generate an anomalous term of the $(\Phi^2)^2$ type given by

$$S_{4;\mathrm{a}}^{\mathrm{int}} = \sum_{P_{[I]}} (\varphi_{[1]\{\check{1}\}} \bar{\varphi}_{[1]\{\check{1}\}})(\varphi_{[1']\{\check{1}'\}} \bar{\varphi}_{[1']\{\check{1}'\}}). \tag{69}$$

The graphical representation of the vertex associated with this interaction is given by Fig. 15 B.

– Turning our attention to the ${}_{\dim G_D}\Phi_d^4$ models ($(d, \dim G_D) \in \{(3,1),(3,2),(4,1),(5,1)\}$), there is a unique type of interaction of the same form given by S_4^{int} (68) hence possesses the same graphic as given by Fig. 15 A. We will use the same notation S_4^{int} for this interaction because no confusion will occur discussing one model or the other. No anomalous can be generated here.
  Introducing a UV cut-off in the propagator C becomes C^Λ, we must consider bare and renormalized couplings and their difference known as coupling constant counter-terms CT. In particular, we must introduce mass and wave function counter-terms for each model as

$$S_{2;1} = \sum_{P_{[I]}} \bar{\varphi}_{[I]} \varphi_{[I]}\ , \qquad S_{2;2} = \sum_{P_{[I]}} \bar{\varphi}_{[I]} \Big(\sum_{s=1}^{d} |P_{I_s}|^a \Big) \varphi_{[I]}\ . \tag{70}$$

  The action that we will consider are given by
– For $k_{\max} = 6$, $d = 3, 4$,

$$S^\Lambda = \frac{\lambda_{6;1}^\Lambda}{3} S_{6;1}^{\mathrm{int}} + \lambda_{6;2}^\Lambda S_{6;2}^{\mathrm{int}} + \frac{\lambda_{4;1}^\Lambda}{2} S_4^{\mathrm{int}} + \frac{\lambda_{4;2}^\Lambda}{2} \delta_{d,4}\, S_{4;\mathrm{a}}^{\mathrm{int}} + CT_{2;2}^\Lambda S_{2;2} + CT_{2;1}^\Lambda S_{2;1}, \tag{71}$$

  where $\delta_{d,4}$ is a Kronecker symbol.

– For $k_{\max} = 4$, $(d, \dim G_D) \in \{(3,1),(3,2),(4,1),(5,1)\}$,

$$S^{\Lambda} = \frac{\lambda^{\Lambda}_{4;1}}{2} S^{\text{int}}_4 + CT^{\Lambda}_{2;2} S_{2;2} + CT^{\Lambda}_{2;1} S_{2;1}. \tag{72}$$

The following statement holds

Theorem 2 (Renormalizable tensor models). *The models* $({}_{\dim G_D}\Phi^{k_{\max}}_d, a)$ *such that*

$$\begin{aligned} &({}_1\Phi^6_4, a = 1) \text{ over } U(1), \quad ({}_1\Phi^6_3, a = \frac{2}{3}) \text{ over } U(1), \\ &({}_1\Phi^4_4, a = \frac{3}{4}) \text{ over } U(1), \quad ({}_1\Phi^4_3, a = \frac{1}{2}) \text{ over } U(1), \\ &({}_1\Phi^4_5, a = 1) \text{ over } U(1), \quad ({}_2\Phi^4_4, a = 1) \text{ over } U(1)^2, \end{aligned} \tag{73}$$

with action defined by (71) *or* (72) *are all just-renormalizable at all orders of perturbation.*

The proof of this theorem has been nearly achieved through the multi-scale analysis and analysis of the divergence degree in the generic situation of Sect. 3.2 and Sect. 3.3. Our remaining task is to introduce wave function counter-terms in the divergence degree, list all possible divergent amplitudes for each case and perform the renormalization of these divergences.

Introducing in a graph, a number of $V_{2;2}$ wave function counter-term vertices (70) each of which bringing a factor of $|P_{I_s}|^a \sim M^{2i}$ in a slice i, it is simple to find from the previous multi-scale analysis the degree of divergence a connected graph $\mathcal{G}$ as

$$\omega_{\text{d}}(\mathcal{G}) = -2aL(\mathcal{G}) + \dim G_D \, F_{\text{int}}(\mathcal{G}) + 2aV_{2;2}. \tag{74}$$

If one includes the anomalous term $S^{\text{int}}_{2;\text{a}}$ then, from the point of view of the external legs, the anomalous vertex is disconnected. We will consider only half of the anomalous vertex when discussing connected graphs.

The formula of number of internal faces $F_{\text{int}}(\mathcal{G})$ given by Proposition 1 remains barely of the same form but in the definition of $V = \sum_k V_k$ and $n \cdot V = \sum_k k V_k$, one should incorporate the number $V_{2;2}$ of wave function vertices, the number $V_{2;1}$ of mass vertices and number $\delta_{d,4} V_{2;\text{a}}$ of half-anomalous vertices. It is direct to realize from (34) that $F_{\text{int}}(\mathcal{G})$ does not depend on 2-valent vertices, in particular on $V_{2;2}$. We can finally express the degree of divergence $\omega_{\text{d}}(\mathcal{G})$ of a connected graph again as (35) with a number of vertices V which does not include the wave function counter-term vertices but still includes mass and anomalous vertices. Thus, as expected, the degree of divergence does not depends on wave function counter-terms.

List of primitively divergent graphs. We consider graphs with an even number of external legs such that $\partial\mathcal{G} \neq \emptyset$ and $C_{\partial\mathcal{G}} \geq 1$. There are some important features satisfied the difference $\omega(\mathcal{G}_{\text{color}}) - \omega(\partial\mathcal{G})$. In particular in [44], it has been proved that either this quantity is vanishing or it obeys

$$\frac{2}{(d-1)!}\big(\omega(\mathcal{G}_{\text{color}}) - \omega(\partial\mathcal{G})\big) \geq d - 2 \geq 0. \tag{75}$$

Table 6. List of primitively divergent graphs of the ${}_1\Phi^6_{d=3}$

$N_{\rm ext}$	$V_2 + V_2''$	V_4	$\omega(\partial\mathcal{G})$	$C_{\partial\mathcal{G}} - 1$	$\omega(\mathcal{G}_{\rm color})$	$\omega_{\rm d}(\mathcal{G})$
6	0	0	0	0	0	0
4	0	0	0	0	0	a
4	0	1	0	0	0	0
2	0	0	0	0	0	$2a$
2	0	1	0	0	0	a
2	0	2	0	0	0	0
2	1	0	0	0	0	0

We can now fully address the list of divergent amplitudes for the different models by introducing

$$\omega_{\rm d}(\mathcal{G}) = -\frac{2\dim G_D}{(d-1)!}(\omega(\mathcal{G}_{\rm color}) - \omega(\partial\mathcal{G})) - P_a(\mathcal{G})\,, \tag{76}$$

$$P_a(\mathcal{G}) = \dim G_D(C_{\partial\mathcal{G}} - 1) + \frac{1}{2}\Big[(\dim G_D(d-1) - 2a)N_{\rm ext} - 2\dim G_D(d-1)\Big] + \frac{1}{2}\Big[2\dim G_D(d-1) + (2a - \dim G_D(d-1))n\Big]\cdot V \tag{77}$$

and then by seeking conditions under which $\omega_{\rm d}(\mathcal{G}) \geq 0$.

• For $k_{\max} = 6$, $\dim G_D = 1$, $(d, a) \in \{(3, \frac{2}{3}), (4, 1)\}$, respectively, then $(d - 1 - 2a) \geq 0$ and, given a connected graph $\mathcal{G}$ with V_4 number of vertices of the Φ^4 type, $\delta_{d,4}V_{2;\rm a}$ number of half anomalous vertices and $V_{2;1}$ number of mass vertices, the upshot of the analysis of divergent graphs of the model ${}_1\Phi^6_3$ is given in the Table 6 (the list of divergent graph for the model ${}_1\Phi^6_4$ can be found in [44]).

Note that the list of graphs with divergent amplitudes of the ${}_1\Phi^6_4$ contains those of ${}_1\Phi^6_3$ plus two more lines defined by (a2) and (e1). From (e1), one notices the fact that only the model ${}_1\Phi^6_4$ generates sub-leading divergent non-melonic contributions.

We prove now that the data of Table 6 hold.

– if $N_{\rm ext} > 6$,

$$\begin{aligned} &((d-1) - 2a)N_{\rm ext} - 2(d-1) > ((d-1) - 2a)6 - 2(d-1) = 0,\\ &\forall 2 \leq k \leq 4\,, \qquad 2(d-1) + (2a - (d-1))k = (2-k)(d-1) + 2ak \geq 0 \end{aligned} \tag{78}$$

so that

$$P_a(\mathcal{G}) = (C_{\partial\mathcal{G}} - 1) + \frac{1}{2}\Big[((d-1) - 2a)N_{\rm ext} - 2(d-1)\Big] + \Big[(d-1) + 2(2a - (d-1))\Big]V_4 + 2a(V_{2;1} + \delta_{d,4}V_{2;\rm a}) > 0 \tag{79}$$

which proves that $\omega_{\rm d}(\mathcal{G}) < 0$ and hence the graph amplitude converges;

– if $N_{\rm ext} = 6$, the graph amplitude is at most log–divergent, i.e. $\omega_{\rm d}(\mathcal{G}) \leq 0$. Focusing on $\omega_{\rm d}(\mathcal{G}) = 0$, this can be satisfied if and only if $\omega(\mathcal{G}_{\rm color}) = 0 = \omega(\partial\mathcal{G})$ and $P_a(\mathcal{G}) = 0$ that is $C_{\partial\mathcal{G}} = 1$, $V_4 = 0 = V_{2;1} = V_{2;\rm a}$;

– if $N_{\rm ext} = 4$, we have

$$P_a(\mathcal{G}) = (C_{\partial\mathcal{G}} - 1) + \Big[(d-1) - 4a\Big] + \Big[(d-1) + 2(2a - (d-1))\Big] V_4 + 2a(V_{2;1} + \delta_{d,4} V_{2;\mathrm{a}}) = (C_{\partial\mathcal{G}} - 1) + a\Big(-1 + V_4 + 2(V_{2;1} + \delta_{d,4} V_{2;\mathrm{a}})\Big). \tag{80}$$

Then the divergence degree is at most a.

(a) We can have $P_a(\mathcal{G}) = 0$, and in this case the graph amplitude is at most log–divergent. Then, $\omega_{\mathrm{d}}(\mathcal{G}) = 0$, if
  (a1) $V_4 = 1, C_{\partial\mathcal{G}} = 1, V_{2;1} = 0 = V_{2;\mathrm{a}}$, and $\omega(\mathcal{G}_{\mathrm{color}}) = 0 = \omega(\partial\mathcal{G})$;
  (a2) $V_4 = 0, C_{\partial\mathcal{G}} = 1 + a, V_{2;1} = 0 = V_{2;\mathrm{a}}$, and $\omega(\mathcal{G}_{\mathrm{color}}) = 0 = \omega(\partial\mathcal{G})$. However $C_{\partial\mathcal{G}} = 1 + a$ must be an integer, then only the situation for which $(d, a) = (4, 1)$ is consistent. This case incorporates indeed the anomaly discovered in [44].

(b) One may also have $P_a(\mathcal{G}) = -a$ entailed by $C_{\partial\mathcal{G}} = 1$, $V_4 = 0$ and $V_{2;1} = 0 = V_{2;\mathrm{a}}$. In this case, the graph amplitude is at most a. We seek for cases such that $0 \leq \omega_{\mathrm{d}}(\mathcal{G}) \leq a$,
  (b1) $\omega_{\mathrm{d}}(\mathcal{G}) = a$, if $\omega(\mathcal{G}_{\mathrm{color}}) = 0 = \omega(\partial\mathcal{G})$.
  (b2) Let us assume now that $\omega(\partial\mathcal{G}) > 0$, then Proposition 1 in [45] ensures that $\frac{2}{(d-1)!}(\omega(\mathcal{G}_{\mathrm{color}}) - d\omega(\partial\mathcal{G})) \geq d - 2$ then, from (75), we have $\omega_{\mathrm{d}}(\mathcal{G}) \leq a - (d-2) < 0$.
  (b3) Let us assume now that $\omega(\partial\mathcal{G}) = 0$ and $\omega(\mathcal{G}_{\mathrm{color}}) > 0$, then we use (75) in order to have $\frac{2}{(d-1)!}\omega(\mathcal{G}_{\mathrm{color}}) \geq d - 2$, then $\omega_{\mathrm{d}}(\mathcal{G}) \leq a - (d-2)) < 0$. Thus, both (b2) and (b3) gives convergent amplitudes;

– $N_{\mathrm{ext}} = 2$ necessarily leads to $C_{\partial\mathcal{G}} = 1$ and $\omega(\partial\mathcal{G}) = 0$ (there is a unique configuration of the boundary of a graph with two external legs such that this equality holds: for $d = 4$, all boundary jackets are planar; in $d = 3$ the boundary graph is itself a planar graph), and

$$P_a(\mathcal{G}) = a\Big(-2 + V_4 + 2(V_{2;1} + \delta_{d,4} V_{2;\mathrm{a}})\Big). \tag{81}$$

The divergence degree is at most $2a$.

(c) We can set $P_a(\mathcal{G}) = 0$, once again the graph amplitude is at most log–divergent. Finding configurations for which $\omega_{\mathrm{d}}(\mathcal{G}) = 0$ leads to
  (c1) $V_4 = 2, V_{2;1} = 0 = V_{2;\mathrm{a}}$, and $\omega(\mathcal{G}_{\mathrm{color}}) = 0 = \omega(\partial\mathcal{G})$;
  (c2) $V_4 = 0, V_{2;1} + \delta_{d,4} V_{2;\mathrm{a}} = 1$, and $\omega(\mathcal{G}_{\mathrm{color}}) = 0 = \omega(\partial\mathcal{G})$;

(d) Setting $P_a(\mathcal{G}) = -a$, the graph divergence degree is $\omega_{\mathrm{d}}(\mathcal{G}) \leq a$, and
  (d1) $V_4 = 1, V_{2;1} = 0 = V_{2;\mathrm{a}}$, and $\omega(\mathcal{G}_{\mathrm{color}}) = 0 = \omega(\partial\mathcal{G})$, for which $\omega_{\mathrm{d}}(\mathcal{G}) = a$.
  (d2) $V_4 = 1, V_{2;1} = 0 = V_{2;\mathrm{a}}$, and $\omega(\partial\mathcal{G}) \geq 0$, then using similar arguments as in (b2) and (b3), one proves that $\omega_{\mathrm{d}}(\mathcal{G}) < 0$.

(e) Choosing $P_a(\mathcal{G}) = -2a$, the amplitude is such that $\omega_{\mathrm{d}}(\mathcal{G}) \leq 2a$. We have
  (e1) $V_4 = 0, V_{2;1} = 0 = V_{2;\mathrm{a}}$, let us assume that $\omega(\mathcal{G}_{\mathrm{color}}) > 0$, according to (75) $\frac{2}{(d-1)!}\omega(\mathcal{G}_{\mathrm{color}}) \geq 2$ so that $\omega_{\mathrm{d}}(\mathcal{G}) \leq -2(1-a)$. Then $\omega_{\mathrm{d}}(\mathcal{G}) < 0$ if $(d, a) = (3, \frac{2}{3})$. We can only have $\omega_{\mathrm{d}}(\mathcal{G}) = 0$ for $(d, a) = (4, 1)$ if $\omega(\mathcal{G}_{\mathrm{color}}) = (d-1)! = 6$.
  (e2) $V_4 = 0, V_{2;1} = 0 = V_{2;\mathrm{a}}$, considering $\omega(\mathcal{G}_{\mathrm{color}}) = 0$, then we obtain $\omega_{\mathrm{d}}(\mathcal{G}) = 2a$.

Table 7. List of primitively divergent graphs of the $_{\dim G_D}\Phi^4_d$

N_{ext}	$V_{2;1}$	$\omega(\partial\mathcal{G})$	$C_{\partial\mathcal{G}}-1$	$\omega(\mathcal{G}_{\text{color}})$	$\omega_{\text{d}}(\mathcal{G})$
4	0	0	0	0	0
2	0	0	0	0	$2a$
2	1	0	0	0	0
2	0	0	0	$\frac{1}{2}(d-1)!(d-2)$	0

The last line with $N_{\text{ext}}=2$ only concerns the cases $(d, \dim G_D, a) \in \{(3,1,\frac{1}{2}), (3,2,1), (4,1,1)\}$

• For $k_{\max}=4$, $(d, \dim G_D, a) \in \{(3,1,\frac{1}{2}), (3,2,1), (4,1,\frac{3}{4}), (4,1,1), (5,1,1)\}$, consider a connected graph $\mathcal{G}$ with $V_{2;1}$ number of mass terms. Then Table 7 gives the list of divergent graphs for any of these models.

In order to prove this, we start by noting that (76) still holds with

$$P_a(\mathcal{G}) = \dim G_D(C_{\partial\mathcal{G}}-1)+\frac{1}{2}\Big[(\dim G_D(d-1)-2a)N_{\text{ext}}-2\dim G_D(d-1)\Big]+2aV_{2;1}. \tag{82}$$

We then consider the following cases:

– If $N_{\text{ext}} > 4$, noting that $(\dim G_D(d-1)-2a) \geq 0$, one has

$$\begin{aligned}&(\dim G_D(d-1)-2a)N_{\text{ext}} - 2\dim G_D(d-1)\\ &> (\dim G_D(d-1)-2a)4 - 2\dim G_D(d-1) = 0\,,\end{aligned} \tag{83}$$

so that $P_a(\mathcal{G}) > 0$ and $\omega_{\text{d}}(\mathcal{G}) < 0$. Thus all graphs of this kind have a convergent amplitude;

– if $N_{\text{ext}} = 4$, the amplitude of $\mathcal{G}$ is at most log–divergent and so $\omega_{\text{d}}(\mathcal{G}) = 0$, if $V_{2;1}=0$, $C_{\partial\mathcal{G}}=1$, and $\omega(\mathcal{G}_{\text{color}})=0=\omega(\partial\mathcal{G})$;

– $N_{\text{ext}} = 2$ necessarily gives $C_{\partial\mathcal{G}}=1$ and $\omega(\partial\mathcal{G})=0$ as the boundary graph here becomes the standard one. We get

$$P_a(\mathcal{G}) = 2a(-1+V_{2;1})\,, \tag{84}$$

and the divergence degree is at most $2a$. The following relevant cases can be read off:

(f) $P_a(\mathcal{G})=0$, if this case the amplitude is at best $\omega_{\text{d}}(\mathcal{G})=0$ occurring if $V_{2;1}=1$ and $\omega(\mathcal{G}_{\text{color}})=0$.

(g) $P_a(\mathcal{G})=-2a$, that means $V_{2;1}=0$, and in this situation

(g1) $\omega(\mathcal{G}_{\text{color}})=0$ yields $\omega_{\text{d}}(\mathcal{G})=2a$.

(g2) $\omega(\mathcal{G}_{\text{color}})>0$, by (75), we have $\frac{2\dim G_D}{(d-1)!}\omega(\mathcal{G}_{\text{color}}) \geq \dim G_D(d-2)$, so that

$$\omega_{\text{d}}(\mathcal{G}) \leq -\dim G_D(d-2)+2a \tag{85}$$

and this leads to only log–divergent amplitude, namely $\omega_{\text{d}}(\mathcal{G})=0$, if $\omega(\mathcal{G}_{\text{color}}) = \frac{1}{2}(d-1)!(d-2)$, which only occurs for $(d, \dim G_D, a) \in \{(3,1,\frac{1}{2}), (3,2,1), (4,1,1)\}$. This completes Table 7.

4.2. Renormalization in tensor models. The subsequent part of the renormalization program consists in the proof that the divergent and local part of all amplitudes can be recast in terms present in the Lagrangian of the models studied so far. This is the purpose of this section where we perform the Taylor expansion of the amplitudes of graphs listed in Tables 6 and 7. We will not study separately the renormalization of the N-point functions for each model but rather perform the renormalization in more general notations valid for any model.

Renormalization of marginal 4- and 6-point functions. 6-point functions are at most marginal and encountered only in the ${}_1\Phi^6_{d=3,4}$ models. Marginal 4-point functions occur in both Φ^6 and Φ^4 models.

The significant 6-point functions must be characterized by the first line of Table 6 (which is identical in both models ${}_1\Phi^6_{d=3,4}$). The external momenta data of such graphs follows necessarily the pattern of vertices $V_{6;1}$ or $V_{6;2}$ (see Fig. 14). This is the locality principle in such models. On the other hand, marginal 4-point functions are given by the third line of Table 6 for ${}_1\Phi^6_{d=3,4}$ models, and the first line of Table 7 for all Φ^4 models. The pattern of their external momenta should follow from V_4 vertices (see Fig. 15).

In the following, since the analysis can be carried out for any other external momentum configurations of the form given by vertices given by $V_{6;1}$, $V_{6;2}$, V_4 and $V_{4;\mathrm{a}}$ and will yield a similar result, we will treat in a row

- a 6-point graph with external data of the same form of one vertex of the $V_{6;1}$ type, namely the one given in Fig. 14 A.
- a 4-point graph the external momenta of which is given by the particular vertex V_4 given in Fig. 15 A.

To be precise, consider a 6-point graph (respectively, a 4-point graph) with 6 external propagator lines (respectively, 4 propagators) attached to it with momenta dictated by the pattern of the $V_{6;1}$ (respectively, V_4) vertex. For any rank d model, each external field $\varphi_{[1]\{\check{1}\}}$ is written in the block matrix index notation as introduced in the beginning of Sect. 4.1. The notation $f = f_{\{\check{1}\}}$ refers to $d-1$ external faces whereas $f = f_{[1]}$ always refers to a unique external face in all models. We denote $\{P_f^{\mathrm{ext}}\}$ the set of external face momenta associated with $f \in \mathcal{F}_{\mathrm{ext}} = \{f_{[1]}, f_{\{\check{1}\}}, f_{[1']}, f_{\{\check{1}'\}}, f_{[1'']}, f_{\{\check{1}''\}}\}$ (respectively, $f \in \mathcal{F}_{\mathrm{ext}} = \{f_{[1]}, f_{\{\check{1}\}}, f_{[1']}, f_{\{\check{1}'\}}\}$).

In a compact notation, consider $A_{6/4}(\{P_f^{\mathrm{ext}}\})$ the amplitude of a G_k^i graph of the form described above. There are two types of scale indices to be considered in this amplitude: external scales j_l associated to each external field corresponding to an external propagator line denoted l and the internal scale i related to all internal propagator lines. G_k^i being quasi-local, this means that $j_l \ll i$.

The amplitude of G_k^i is given by (in simplified notations)

$$A_{6/4}(\{P_f^{\mathrm{ext}}\}) = \sum_{P_f} \int [\prod_{\ell} d\alpha_\ell e^{-\alpha_\ell \mu^2}] \prod_{f\in\mathcal{F}_{\mathrm{ext}}} \left[e^{-(\sum_{\ell\in f}\alpha_\ell)|P_f^{\mathrm{ext}}|^a}\right] \prod_{f\in\mathcal{F}_{\mathrm{int}}} \left[\mathbf{d}^2_{P_f} e^{-(\sum_{\ell\in f}\alpha_\ell)|P_f|^a}\right], \tag{86}$$

where $\alpha_\ell \in [M^{-2ai_\ell}, M^{-2a(i_\ell-1)}]$ if ℓ is internal, and if ℓ is external, we denote it by l, such that $\alpha_l \in [M^{-2aj_l}, M^{-2a(j_l-1)}]$. We have $j_l \ll i \leq i_\ell$.

The next stage is to perform a Taylor expansion of an external face amplitude using the fact that $\sum_{\ell\in f;\ell\neq l}\alpha_\ell$ is small such that

$$e^{-(\sum_{\ell\in f}\alpha_\ell)|P_f^{\rm ext}|^a} = e^{-(\alpha_l+\alpha_{l'})|P_f^{\rm ext}|^a}[1-R_f]$$
$$R_f = \Big(\sum_{\ell\in f;\ell\neq l}\alpha_\ell\Big)|P_f^{\rm ext}|^a\int_0^1 e^{-t(\sum_{\ell\in f;\ell\neq l}\alpha_\ell)|P_f^{\rm ext}|^a}dt. \tag{87}$$

We substitute this external face expansion in the amplitude and get

$$A_{6/4}(\{P_f^{\rm ext}\}) = \sum_{P_f}\int[\prod_\ell d\alpha_\ell e^{-\alpha_\ell\mu^2}]\Big[\prod_{f\in\mathcal{F}_{\rm ext}} e^{-(\alpha_l+\alpha_{l'})|P_f^{\rm ext}|^a}\Big]$$
$$\times\Big[1-\sum_{f\in\mathcal{F}_{\rm ext}}R_f+\sum_{f,f'\in\mathcal{F}_{\rm ext}}R_fR_{f'}+\dots\Big]$$
$$\times\prod_{f\in\mathcal{F}_{\rm int}}\Big[\mathbf{d}^2_{P_f}e^{-(\sum_{\ell\in f}\alpha_\ell)|P_f|^a}\Big], \tag{88}$$

where the ellipses invoke terms involving higher order products of the Taylor remainders R_f.

The divergence of $A_6(\{P_f^{\rm ext}\})$ come from the 0th order term of this expansion which is given by

$$A_{6/4}(\{P_f^{\rm ext}\};0) = \sum_{P_f}\int[\prod_\ell d\alpha_\ell e^{-\alpha_\ell\mu^2}]\prod_{f\in\mathcal{F}_{\rm ext}}\Big[e^{-(\alpha_l+\alpha_{l'})|P_f^{\rm ext}|^a}\Big]\prod_{f\in\mathcal{F}_{\rm int}}\Big[\mathbf{d}^2_{P_f}e^{-(\sum_{\ell\in f}\alpha_\ell)|P_f|^a}\Big] \tag{89}$$

and which factors as

$$A_{6/4}(\{P_f^{\rm ext}\};0) = \Big[\int[\prod_l d\alpha_l e^{-\alpha_l\mu^2}]\prod_{f\in\mathcal{F}_{\rm ext}}e^{-(\alpha_l+\alpha_{l'})|P_f^{\rm ext}|^a}\Big]\sum_{P_f}\int\Big[\prod_{\ell\neq l}d\alpha_\ell e^{-\alpha_\ell\mu^2}\Big]$$
$$\times\prod_{f\in\mathcal{F}_{\rm int}}\Big[\mathbf{d}^2_{P_f}e^{-(\sum_{\ell\in f}\alpha_\ell)|P_f|^a}\Big]. \tag{90}$$

In this expression, the first factor of $A_6(\{P_f^{\rm ext}\};0)$ can be fully expanded as

$$\int[\prod_l d\alpha_l e^{-\alpha_l\mu^2}]\prod_{f\in\mathcal{F}_{\rm ext}}e^{-(\alpha_l+\alpha_{l'})|P_f^{\rm ext}|^a}$$
$$=\int[\prod_l d\alpha_l e^{-\alpha_l\mu^2}]e^{-(\alpha_{l_{[1]}}+\alpha_{l'_{[1]}})|P^{\rm ext}_{f_{[1]}}|^a}e^{-(\alpha_{l_{\{\check{1}\}}}+\alpha_{l'_{\{\check{1}\}}})|P^{\rm ext}_{f_{\{\check{1}\}}}|^a}$$
$$\times e^{-(\alpha_{l_{[1']}}+\alpha_{l'_{[1']}})|P^{\rm ext}_{f_{[1']}}|^a}e^{-(\alpha_{l_{\{\check{1}'\}}}+\alpha_{l'_{\{\check{1}'\}}})|P^{\rm ext}_{f_{\{\check{1}'\}}}|^a}e^{-(\alpha_{l_{[1'']}}+\alpha_{l'_{[1'']}})|P^{\rm ext}_{f_{[1'']}}|^a}e^{-(\alpha_{l_{\{\check{1}''\}}}+\alpha_{l'_{\{\check{1}''\}}})|P^{\rm ext}_{f_{\{\check{1}''\}}}|^a}. \tag{91}$$

Now using the pattern of the $V_{6;1}$ for each external momenta, we have

$$\alpha_{l_{[1]}}=\alpha_{l_{\{\check{1}\}}}=\alpha_{l_1},\quad \alpha_{l_{[1']}}=\alpha_{l'_{\{\check{1}\}}}=\alpha_{l_2},\quad \alpha_{l'_{[1']}}=\alpha_{l_{\{\check{1}'\}}}=\alpha_{l_3},$$
$$\alpha_{l_{[1'']}}=\alpha_{l'_{\{\check{1}'\}}}=\alpha_{l_4},\quad \alpha_{l'_{[1'']}}=\alpha_{l_{\{\check{1}''\}}}=\alpha_{l_5},\quad \alpha_{l'_{[1]}}=\alpha_{l'_{\{\check{1}''\}}}=\alpha_{l_6} \tag{92}$$

from which we identify that the first factor of (90) determines nothing but a product of 6 propagators glued together in the pattern of a $V_{6;1}$ interaction. Using a similar kind of expansion, such that

$$\alpha_{l_{[1]}} = \alpha_{l_{\{\check{1}\}}} = \alpha_{l_1}, \quad \alpha_{l_{[1']}} = \alpha_{l'_{\{\check{1}\}}} = \alpha_{l_2}, \quad \alpha_{l'_{[1']}} = \alpha_{l_{\{\check{1}'\}}} = \alpha_{l_3}, \quad \alpha_{l'_{[1]}} = \alpha_{l'_{\{\check{1}'\}}} = \alpha_{l_4}, \tag{93}$$

we can identify in the amplitude $A_4(\{P_f^{\text{ext}}\}; 0)$ that the first factor is a product of 4 propagators glued together as a V_4 vertex. The second factor in (90) is a log–divergent term. In all cases, this term should contribute to the renormalization of the coupling constant associated with either a $V_{6;1}$ or a V_4 interaction for the corresponding situation.

Next we must prove that the remainders appearing in $A_{6/4}$ (88) improve in a significant way the power counting. We have the first order remainder:

$$\begin{aligned} R_{6/4} &= \sum_{P_f} \int [\prod_{\ell} d\alpha_\ell e^{-\alpha_\ell \mu^2}] \Big[\prod_{f \in \mathcal{F}_{\text{ext}}} e^{-(\alpha_l + \alpha_{l'})|P_f^{\text{ext}}|^a} \Big] \Big[- \sum_{f \in \mathcal{F}_{\text{ext}}} R_f \Big] \\ &\quad \times \prod_{f \in \mathcal{F}_{\text{int}}} \Big[\mathbf{d}^2_{P_f} e^{-(\sum_{\ell \in f} \alpha_\ell)|P_f|^a} \Big] \\ &= \sum_{P_f} \int [\prod_{\ell} d\alpha_\ell e^{-\alpha_\ell \mu^2}] \Big[\prod_{f \in \mathcal{F}_{\text{ext}}} e^{-(\alpha_l + \alpha_{l'})|P_f^{\text{ext}}|^a} \Big] \\ &\quad \times \Big[- \sum_{f \in \mathcal{F}_{\text{ext}}} \Big(\sum_{\ell \in f; \ell \neq l} \alpha_\ell \Big) |P_f^{\text{ext}}|^a \int_0^1 e^{-t(\sum_{\ell \in f; \ell \neq l} \alpha_\ell)|P_f^{\text{ext}}|^a} dt \Big] \\ &\quad \times \prod_{f \in \mathcal{F}_{\text{int}}} \Big[\mathbf{d}^2_{P_f} e^{-(\sum_{\ell \in f} \alpha_\ell)|P_f|^a} \Big]. \end{aligned} \tag{94}$$

Using $i(G_k^i) = \inf_{\ell \in G_k^i} i_\ell$ and $e(G_k^i) = \sup_{l \in G_k^i} j_l$, the last quantity can be optimally bounded as

$$|R_{6/4}| \leq K M^{-2a(i(G_k^i) - e(G_k^i))} \sum_{P_f} \int [\prod_{\ell \neq l} d\alpha_\ell e^{-\alpha_\ell \mu^2}] \prod_{f \in \mathcal{F}_{\text{int}}} \Big[\mathbf{d}^2_{P_f} e^{-(\sum_{\ell \in f} \alpha_\ell)|P_f|^a} \Big], \tag{95}$$

for some constant K and where the integral in t brings simply a $O(1)$ factor. The factor $M^{-2a(i(G_k^i) - e(G_k^i))}$ improves the power counting and will bring enough decay in such way that the last sum on momentum scale attributions can be performed [51]. One can prove in a similar way that higher order remainders in (88) will be even more convergent.

Renormalization of a-divergent 2- and 4-point functions. This type of 4-point and 2-point functions appears in the ${}_1\Phi^6_{3,4}$ models. We call them a-divergent for their property $\omega_{\text{d}}(\mathcal{G}) = a$. Such 4-point graphs should be characterized by the second row of Table 6 and of the external form given again by one of the V_4 vertex. Concerning 2-point functions, these are determined by the fifth row of the same table. These should appear in both models ${}_1\Phi^6_{3,4}$.

In the following, dealing with the 4-point function, we will concentrate on the situation of Fig. 15 A again. The following developments can be easily reported accordingly for other types of configurations. Meanwhile for the 2-point function, there is a unique set of data encoding the external face configuration for a graph with 2-external legs:

$\mathcal{F}_{\rm ext} = \{f_{[1]}, f_{[2]}, f_{[3]}\}$, where [1] and [3] are 1-index, and where [2] is either a block containing two indices for ${}_1\Phi^6_4$, or a 1-index for ${}_1\Phi^6_3$.

In a similar way as in the previous case, we perform a Taylor expansion of the face amplitude as given in (87) and write the amplitude expansion $A_{4/2}(\{P_f^{\rm ext}\})$ for a G_k^i graph with 4 and 2 external legs the external data of which follow the pattern of a V_4 and V_2 vertex configuration, respectively. One should obtain the expression (88).

The 0th order term $A_4(\{P_f^{\rm ext}\}; 0)$ factorizes in the same way given in (90) and, using still (93), provides a divergent term of degree a contributing to the renormalization of the coupling constant associated with the V_4 interaction in all models. The 0th order term $A_2(\{P_f^{\rm ext}\}; 0)$ factorizes as well as (90) with its first factor recast as

$$\begin{aligned}&\int [\prod_{l=1,2} d\alpha_l e^{-\alpha_l \mu^2}]\Big[\prod_{f\in\mathcal{F}_{\rm ext}} e^{-(\alpha_l+\alpha_{l'})|P_f^{\rm ext}|^a}\Big]\\ &\quad = \int [\prod_{l=1,2} d\alpha_l] e^{-\alpha_1(\sum_s |P_s^{\rm ext}|^a+\mu^2)} e^{-\alpha_2(\sum_s |P_s^{\rm ext}|^a+\mu^2)}\Big]\end{aligned} \tag{96}$$

corresponding to the gluing of two propagators. Thus, $A_2(\{P_f^{\rm ext}\}; 0)$ is associated with a mass renormalization term.

Concerning the remainders that we denote $R_{4/2}$, noting their similarity with (94), they are bounded as

$$|R_{4/2}| \leq K M^{-2a(i(G_k^i)-e(G_k^i))} \sum_{P_f} \int [\prod_{\ell\neq l} d\alpha_\ell e^{-\alpha_\ell \mu^2}] \prod_{f\in\mathcal{F}_{\rm int}} \Big[\mathbf{d}^2_{P_f} e^{-(\sum_{\ell\in f}\alpha_\ell)|P_f|^a}\Big]. \tag{97}$$

Now since the last integral provides a divergence degree of a, it is direct to get

$$|R_{4/2}| \leq K M^{-2a(i(G_k^i)-e(G_k^i))} M^{\omega_{\rm d}(G_k^i)=a} \tag{98}$$

ensuring already the convergence of all of the remainders and the summability over the attributions.

Renormalization of $2a$-divergent 2-point functions. Such 2-point functions occur in all model and they satisfy $\omega_{\rm d}(\mathcal{G}) = 2a$.

A second order Taylor expansion of the face amplitude is performed as

$$\begin{aligned}e^{-(\sum_{\ell\in f}\alpha_\ell)|P_f^{\rm ext}|^a} &= e^{-(\alpha_l+\alpha_{l'})|P_f^{\rm ext}|^a}[1+R_f+Q_f],\\ R_f &= -\Big(\sum_{\ell\in f;\ell\neq l}\alpha_\ell\Big)|P_f^{\rm ext}|^a,\\ Q_f &= [\Big(\sum_{\ell\in f;\ell\neq l}\alpha_\ell\Big)|P_f^{\rm ext}|^a]^2 \int_0^1 (1-t) e^{-t(\sum_{\ell\in f;\ell\neq l}\alpha_\ell)|P_f^{\rm ext}|^a} dt\,,\end{aligned} \tag{99}$$

and the amplitude expansion for a G_k^i graph satisfies

$$\begin{aligned}A_2(\{P_f^{\rm ext}\}) = \sum_{P_f} \int [\prod_{\ell} d\alpha_\ell e^{-\alpha_\ell\mu^2}]\Big[\prod_{f\in\mathcal{F}_{\rm ext}} e^{-(\alpha_l+\alpha_{l'})|P_f^{\rm ext}|^a}\Big]\\ \times\Big[1+\sum_{f\in\mathcal{F}_{\rm ext}}(R_f+Q_f)+\sum_{f,f'\in\mathcal{F}_{\rm ext}}(R_f+Q_f)(R_{f'}+Q_{f'})+\dots\Big]\\ \times\prod_{f\in\mathcal{F}_{\rm int}}\Big[\mathbf{d}^2_{P_f} e^{-(\sum_{\ell\in f}\alpha_\ell)|P_f|^a}\Big].\end{aligned} \tag{100}$$

The 0th order term $A_2(\{P_f^{\text{ext}}\}; 0)$ factorizes in the way of (90) and, using (96), provides a $2a$ divergent term contributing to the renormalization of the mass coupling.

The remainders are now treated. The first order remainder involving the sum $\sum_f R_f$ factorizes as

$$\begin{aligned} A_2'(\{P_f^{\text{ext}}\}; 0) = -\Big[\int [\prod_l d\alpha_l e^{-\alpha_l \mu^2}] \prod_{f \in \mathcal{F}_{\text{ext}}} e^{-(\alpha_l + \alpha_{l'})|P_f^{\text{ext}}|^a} \Big] \\ \times \sum_{f \in \mathcal{F}_{\text{ext}}} |P_f^{\text{ext}}|^a \int [\prod_{\ell \neq l} d\alpha_\ell e^{-\alpha_\ell \mu^2}] \Big[\Big(\sum_{\ell \in f; \ell \neq l} \alpha_\ell \Big) \\ \times \sum_{P_f} \prod_{f \in \mathcal{F}_{\text{int}}} \Big[\mathbf{d}^2_{P_f} e^{-(\sum_{\ell \in f} \alpha_\ell)|P_f|^a} \Big]. \end{aligned} \tag{101}$$

One notices that the first factor is again the product of two propagators using (96). Hence, this term should correspond to a wave function renormalization if and only if the last integral over α_ℓ, $\ell \neq l$, should give the same result for all $|P_{f_{[1]}}^{\text{ext}}|^a$, $|P_{f_{[2]}}^{\text{ext}}|^a$, and $|P_{f_{[3]}}^{\text{ext}}|^a$. It may happen that for a given graph G_k^i, the integral is not the same at fixed $f \in \mathcal{F}_{\text{ext}}$. Because the model is symmetric in all colors, it is simple to define in this case another graph $\tilde{G}_k^i$ so that the sum of contributions of G_k^i and $\tilde{G}_k^i$ appears now to be symmetric for all P_f^{ext}. A unique factor or wave function renormalization A' can be defined from that colored symmetric quantity and yields $\Big(\sum_s |P_s^{\text{ext}}|^a\Big) A'$. The sum $\sum_{\ell \in f; \ell \neq l} \alpha_\ell \leq c M^{-2ai(G_k^i)}$ and the last integrals give $M^{\omega(G_k^i)=2a}$ so that the overall contribution to the wave function renormalization is $A' \sim \log M$.

Focusing on the sum $\sum_f Q_f$, we can work out a bound as

$$\begin{aligned} |R_2| &\leq K \Big[\int [\prod_l d\alpha_l e^{-\alpha_l \mu^2}] \prod_{f \in \mathcal{F}_{\text{ext}}} e^{-(\alpha_l + \alpha_{l'})|P_f^{\text{ext}}|^a} \Big] \sum_{f, f' \in \mathcal{F}_{\text{ext}}} |P_f^{\text{ext}}|^a |P_{f'}^{\text{ext}}|^a \\ &\quad \times \int [\prod_{\ell \neq l} d\alpha_\ell e^{-\alpha_\ell \mu^2}] \Big[\Big(\sum_{\ell \in f; \ell \neq l} \alpha_\ell \Big) \Big(\sum_{\ell \in f'; \ell \neq l} \alpha_\ell \Big) \sum_{P_f} \prod_{f \in \mathcal{F}_{\text{int}}} \Big[\mathbf{d}^2_{P_f} e^{-(\sum_{\ell \in f} \alpha_\ell)|P_f|^a} \Big] \\ &\leq K' M^{-4a(i(G_k^i) - e(G_k^i))} M^{\omega_{\text{d}}(G_k^i)=2a}, \end{aligned} \tag{102}$$

for some constants K and K'. This last expression manifests the fact that the remainder is convergent and will bring enough decay for the summability over the momentum assignment. One can show that, in the same vein, higher order remainders are convergent as well.

In conclusion,

- the expansion of marginal 6- and 4-point functions around their local part gives a log–divergent term which renormalize the coupling constant associated with the 6- and 4-valent vertices, respectively.
- the expansion of a-divergent 4- and 2-point amplitudes around their local part gives a a-divergent term which renormalize the coupling of 4-valent and mass vertices, respectively;
- the expansion of a $2a$-divergent 2-point graph around its local part yields a $2a$-divergent term renormalizing the mass and a log–divergent term which contributes to the wave function renormalization;

– all remainders are convergent and will bring enough decay for ensuring the final summability over scale attributions. From this point, the procedure for performing this last sum over attributions is standard and will secure the renormalization at all orders of perturbation theory according to techniques developed in [51]. Thus, Theorem 2 holds.

5. Just Renormalizable Matrix Models

5.1. Matrix models and their renormalizability. Table 2 provides a list of matrix model interactions and kinetic terms susceptible to generate renormalizable actions. These are defined by

$$({}_1\Phi_2^{2+\gamma}, a=\frac{\gamma}{2(2+\gamma)}\leq\frac{1}{2}),\ ({}_2\Phi_2^{2+\gamma}, a=\frac{\gamma}{2+\gamma}\geq\frac{1}{2}),\ ({}_3\Phi_2^{4,6}, a=\frac{3}{4}, 1),\ ({}_4\Phi_2^4, a=1), \tag{103}$$

where γ is an even integer.

Propagators. The propagator keeps its form (16) and can be pictured like a ribbon line as found in Fig. 10.

Planar (and cyclic) interactions. The interactions that we will introduce in the following will govern the locality principle of the matrix models designed simply by a planarity condition. These are matrix trace invariants represented by planar graphs with p legs.

For any ${}_{\dim G_D}\Phi_2^{k_{\max}}$ model, consider the interactions giving by, for all $k = 4, 6, \ldots, k_{\max}$,

$$S_k^{\rm int} = \sum_{P_{[I]}} {\rm tr}\Big[(\bar\varphi_{[I]}\varphi_{[I]})^k\Big] = \sum_{P_{[I]}} \bar\varphi_{12}\,\varphi_{1'2}\,\bar\varphi_{1'2'}\,\varphi_{1''2'}\ldots\bar\varphi_{1'''2'''}\,\varphi_{12'''}. \tag{104}$$

Figure 10 illustrates $S_k^{\rm int}$ as a cyclic and planar ribbon diagram with k external fields.

We introduce a cut-off Λ on large momenta, so that the propagator in the UV reads C^Λ. Counter-term couplings CT define as usually as the difference between bare and renormalized couplings. Mass and wave function counter-terms keeps their form $S_{2;1}$ and $S_{2;2}$ (70), where $\varphi_{[I]}$ may be simply written as a matrix φ_{12}.

Given a matrix model ${}_{\dim G_D}\Phi_2^{k_{\max}}$, we introduce the action defined by

$$S^\Lambda = \sum_{k=2}^{k_{\max}/2} \frac{\lambda_k^\Lambda}{k} S_k^{\rm int} + CT_{2;1}^\Lambda S_{2;1} + CT_{2;2}^\Lambda S_{2;2}\,, \tag{105}$$

and the following statement is valid.

Theorem 3 (Renormalizable matrix models). *The models* $({}_{\dim G_D}\Phi_2^{k_{\max}}, a)$ *defined by*

$$\begin{aligned}\forall k\geq 2,\quad & ({}_1\Phi_2^{2k}, a=\frac{1}{2}(1-\frac{1}{k})) \text{ over } G=U(1)\,,\quad ({}_2\Phi_2^{2k}, a=1-\frac{1}{k}) \text{ over } G=U(1)^2,\\ & ({}_3\Phi_2^6, a=1) \text{ over } G=U(1)^3 \text{ or } G=SU(2)\,,\\ & ({}_3\Phi_2^4, a=\frac{3}{4}) \text{ over } G=U(1)^3 \text{ or } G=SU(2)\,,\\ & ({}_4\Phi_2^4, a=1) \text{ over } G=U(1)^4,\end{aligned} \tag{106}$$

with actions defined by (105) *are renormalizable at all orders of perturbation.*

The multi-scale analysis has been already performed and gives a power counting theorem stated in Theorem 1. This provides in return a divergence degree as described by Proposition 3. In the same way proved earlier, adding mass and wave function counter-terms in the action and brings $V_{2;1}$ and $V_{2;2}$ vertices, respectively, but does not affect the divergence degree (37). One pays attention that this divergence degree includes now $V_{2;1}$ mass counter-term vertices.

List of divergent graphs. We consider a connected graph $\mathcal{G}$ with external legs such that we always have $C_{\partial\mathcal{G}} \geq 1$. We consider also V_k the number of vertices of coordination k and, in particular, $V_2 = V_{2;1}$ the number of mass vertices. Using the same strategy developed in the previous section, the divergence degree is recast in the form

$$\begin{aligned}\omega_{\mathrm{d}}(\mathcal{G}) &= -2\dim G_D g_{\tilde{\mathcal{G}}} - P_a(\mathcal{G}),\\ P_a(\mathcal{G}) &= \dim G_D(C_{\partial\mathcal{G}} - 1) + \frac{1}{2}\Big[(\dim G_D - 2a)N_{\mathrm{ext}} - 2\dim G_D\Big]\\ &\quad + \frac{1}{2}\sum_{k=2}^{k_{\max}-2}\Big[2\dim G_D + (2a - \dim G_D)k\Big]V_k,\end{aligned} \tag{107}$$

where the sum $\sum_{k=2}^{k_{\max}-2}$ is performed over even integers. Given the fact that $\dim G_D - 2a > 0$, one keeps in mind that, for $2 \leq k < k' \leq k_{\max}$,

$$2\dim G_D + (2a - \dim G_D)k > 2\dim G_D + (2a - \dim G_D)k' \geq 0. \tag{108}$$

In the last inequality, the upper bound is only saturated at $k' = k_{\max}$. Another useful relation is provided by the following: if $C_{\partial\mathcal{G}} > 1$, then, for all $2 \leq k < k_{\max}$,

$$\dim G_D(C_{\partial\mathcal{G}} - 1) - \frac{1}{2}\Big[2\dim G_D + (2a - \dim G_D)k\Big] \geq \frac{1}{2}(\dim G_D - 2a)k > 0. \tag{109}$$

We are now in position to analyze the divergent contributions.

- If $N_{\mathrm{ext}} > k_{\max}$, then

$$(\dim G_D - 2a)N_{\mathrm{ext}} - 2\dim G_D > (\dim G_D - 2a)k_{\max} - 2\dim G_D = 0 \tag{110}$$

  so that $P_a(\mathcal{G}) > 0$ and the amplitude converges;
- if $N_{\mathrm{ext}} = k_{\max}$, then the amplitude is at most log–divergent and $\omega_{\mathrm{d}}(\mathcal{G}) = 0$ holds if $g_{\tilde{\mathcal{G}}} = 0$ and $P_a(\mathcal{G}) = 0$. This latter condition occurs if $C_{\partial\mathcal{G}} = 1, V_k = 0$, for $2 \leq k < k_{\max}$;
- if $N_{\mathrm{ext}} < k_{\max}$, we are interested in the divergent amplitudes with $N_{\mathrm{ext}} = k_{\max} - q$, $2 \leq q \leq k_{\max} - 2$, q even. The quantity (107) can be recast in the following way

$$\begin{aligned}P_a(\mathcal{G}) &= \dim G_D(C_{\partial\mathcal{G}} - 1) + \frac{1}{2}\Big[2\dim G_D + (2a - \dim G_D)(k_{\max} - q)\Big](V_{k_{\max}-q} - 1)\\ &\quad + \frac{1}{2}\sum_{k\in S_{k_{\max},q}}\Big[2\dim G_D + (2a - \dim G_D)k\Big]V_k,\end{aligned} \tag{111}$$

  where $S_{k_{\max},q} = \{2, \ldots, k_{\max} - 2\} \setminus \{k_{\max} - q\}$ is a set of even integers. Note that $S_{4,2} = \emptyset$ for all Φ^4 models.

(h) Let us assume that $P_a(\mathcal{G}) = 0$, then the amplitude is at most log-divergent. We have $\omega_{\rm d}(\mathcal{G}) = 0$ in the following cases:

(hq) For $2 \leq q \leq k_{\max} - 2$, $V_{k_{\max}-q} = 1$, $V_k = 0$, $k \in S_{k_{\max},q}$, and $C_{\partial\mathcal{G}} = 1$;

($\bar{\rm h}q$) For $2 \leq q \leq k_{\max} - 2$, the cases $V_{k_{\max}-q} > 1$ or $C_{\partial\mathcal{G}} > 1$, from (111) and (109), yield a convergent amplitude. Hence, we must have $V_{k_{\max}-q} = 0$ and $C_{\partial\mathcal{G}} = 1$. The second equality entails that there is no anomalous term in the above matrix models. Then, necessarily, one has

$$P_a(\mathcal{G}) = -\frac{1}{2}\Big[2\dim G_D + (2a - \dim G_D)(k_{\max} - q)\Big] + \frac{1}{2}\sum_{k\in S_{k_{\max},q}} \Big[2\dim G_D + (2a - \dim G_D)k\Big]V_k. \tag{112}$$

For $2 \leq k \leq k_{\max} - q < k_{\max}$, by (108), we know that if there is some $V_k > 0$ with $2 \leq k \leq k_{\max} - q$ then $P_a(\mathcal{G}) > 0$ and thus leads to a convergent amplitude. We therefore focus on $V_k = 0$ for $2 \leq k \leq k_{\max} - q$ giving

$$P_a(\mathcal{G}) = -\frac{1}{2}\Big[2\dim G_D + (2a - \dim G_D)(k_{\max} - q)\Big] + \frac{1}{2}\sum_{k\in S'_{k_{\max},q}} \Big[2\dim G_D + (2a - \dim G_D)k\Big]V_k, \tag{113}$$

where $S'_{k_{\max},q} = \{k_{\max} - q + 2, \ldots, k_{\max} - 2\}$ including only even integer elements and is non empty only for $q \geq 4$. Note that for $k_{\max} = 4$, $S'_{4,2} = \emptyset$ and, considering $k_{\max} = 6$, $S'_{6,2} = \emptyset$ and $S'_{6,4} = \{4\}$.

Whenever $S'_{k_{\max},q} = \emptyset$, then $P_a(\mathcal{G}) < 0$ should be treated in the sequel point. Thus, looking for conditions such that $P_a(\mathcal{G}) = 0$ for graphs with $N_{\rm ext} = k_{\max} - 2 = 2$ models reduces to solutions (h2) for ${}_{\dim G_D}\Phi_2^4$ models. Note also that the solutions of $P_a(\mathcal{G}) = 0$ in both models ${}_1\Phi_2^{2+\gamma}$ or ${}_2\Phi_2^{2+\gamma}$ should coincide since the quantities $P_a(\mathcal{G})$ in these models turn out to be proportional.

Expanding further (113) and using a change of variable $k \to k - (k_{\max} - q)$, it can be found

$$\begin{aligned} 0 = 2P_a(\mathcal{G}) &= (2a - \dim G_D)q + \sum_{k\in S'_{k_{\max},q}} \Big[2\dim G_D + (2a - \dim G_D)k\Big]V_k \\ 0 &= (2a - \dim G_D)q + \sum_{k\in S_q} (2a - \dim G_D)(k - q)V_{k+(k_{\max}-q)} \\ &= (2a - \dim G_D)\Big(q - \sum_{k\in S_q}(q - k)V_{k+(k_{\max}-q)}\Big), \end{aligned} \tag{114}$$

where $S_q = \{2, \ldots, q-2\}$ still includes only even integers. Since $2a - \dim G_D < 0$, we understand now that solving $P_a(\mathcal{G}) = 0$ turns out to find non trivial partitions of $q/2 \geq 0$ (i.e. excluding $q/2 = q/2 + 0$). Indeed, changing variables $q \to q' = q/2$, $k \to k' = k/2$, we then rename k' in k and get from (114)

$$0 = q' - \sum_{k=1}^{q'-1}(q' - k)V_{k_{\max}-2(q'-k)} \Leftrightarrow q' = \sum_{k=1}^{q'-1} kV'_k, \quad V'_k := V_{k_{\max}-2k}. \tag{115}$$

It is clearly difficult to work out for an arbitrary q' the possible set of solutions but certainly these solutions are in finite number and order by order in q' can be read off. [8]

(i) Let us consider the case $P_a(\mathcal{G}) = \frac{1}{2}(2a - \dim G_D)q_1 < 0$, where q_1 even and $2 \leq q_1 \leq q$. (Note that we must have once again $C_{\partial\mathcal{G}} = 1$ otherwise (i.e. $C_{\partial\mathcal{G}} > 1$), by (109), $P_a(\mathcal{G}) > 0$.) One has

$$\begin{aligned} P_a(\mathcal{G}) &= \frac{1}{2}(2a - \dim G_D)(q - q_1 + q_1) + \frac{1}{2}\sum_{k\in S_q}(2a - \dim G_D)(k-q)V_{k+(k_{\max}-q)} \\ &= \frac{1}{2}(2a - \dim G_D)q_1 + \frac{1}{2}(2a - \dim G_D)(q - q_1 - \sum_{k\in S_q}(q-k)V_{k+(k_{\max}-q)}). \end{aligned} \tag{119}$$

Hence the hypothesis $P_a(\mathcal{G}) = \frac{1}{2}(2a - \dim G_D)q_1 < 0$ would require

$$0 = q - q_1 - \sum_{k\in S_{q_1}}(q-k)V_{k+(k_{\max}-q)} - \sum_{k\in S'_{q_1,q}}(q-k)V_{k+(k_{\max}-q)}, \tag{120}$$

where $S_{q_1} = \{2, \ldots, q_1 - 2\}$ contains only even integers and $S'_{q_1,q} = \{q_1, q_1 + 2, \ldots, q - 2\} = S_q \setminus S_{q_1}$.

If for any $2 \leq k \leq q_1 - 2$, $V_{k+(k_{\max}-q)} > 0$ then $q - q_1 - (q-k)V_{k+(k_{\max}-q)} < 0$, then $P_a(\mathcal{G}) \neq \frac{1}{2}(2a - \dim G_D)q_1$. Then necessarily, for any $2 \leq k < q_1$, $V_{k+(k_{\max}-q)} = 0$. We obtain, changing the variable such that $k \to k - q_1$,

$$0 = q - q_1 - \sum_{k\in S'_{0,q-q_1}}((q-q_1)-k)V_{k+(k_{\max}-(q-q_1))}, \tag{121}$$

with $S'_{0,q-q_1} = \{0, 2, \ldots, q - q_1 - 2\}$ including only even integers, with $q - q_1 \geq 2$. Thus this case again reduces again to the search of partitions of $(q - q_1)/2$ including trivial ones. If $q - q_1 = 0$, there is a unique possibility given by $V_k = 0$, for all $k \in S_q$.

[8] For an illustration, we apply the formalism to the order $k_{\max} = 6$, such that $q = 2, 4 \leq 6 - 2$. We concentrate on the possibility $q = 4 \geq 4$, providing $q' = 2$. A non trivial partition of $q' = 2$ is given by $2 = 1 + 1$. Then, from (115), we have

$$0 = 2 - (2-1)V_{6-2(2-1)} = 2 - V_4 \quad \Leftrightarrow \quad V_4 = 2. \tag{116}$$

$V_4 = 2$ gives the number of times that 1 appears the above partition of 2. Requiring $V_{2;1} = 0$ and $g_{\tilde{\mathcal{G}}} = 0$ leads to a log–divergent amplitude. We can apply also the formalism to $k_{\max} = 8$, for which are relevant $q = 4, 6$. For $q = 6$, one gets $q' = 3$, and (115) gives

$$0 = 3 - \sum_{k=1}^{2}(3-k)V_{8-2(3-k)} = 3 - 2V_4 - V_6 \quad \Leftrightarrow \quad (V_4, V_6) \in \{(1,1), (0,3)\} \tag{117}$$

expressing the fact that V_4 and V_6 are the number of times that 2 and 1, respectively, should appear in the partitions of 3=2+1=1+1+1. Imposing in addition $V_{2;1} = 0$ and $g_{\tilde{\mathcal{G}}} = 0$, this configuration will be log–divergent.

For $q = 4$, $q' = 2$, (115) becomes

$$0 = 2 - (2-1)V_{8-2(2-1)} = 2 - V_6 \quad \Leftrightarrow \quad V_6 = 2. \tag{118}$$

with the same interpretation in terms of the partition of 2. Now putting $V_4 = 0 = V_{2;1}$ will lead to a log–divergent amplitude.

Assuming now that $P_a(\mathcal{G}) = \frac{1}{2}(2a - \dim G_D)q_1 < 0$, where q_1 is odd and $2 \leq q_1 < q$, one has

$$P_a(\mathcal{G}) = \frac{1}{2}(2a-\dim G_D)q_1+\frac{1}{2}(2a-\dim G_D)(q-q_1-\sum_{k\in S_q}(q-k)V_{k+(k_{\max}-q)}), \quad (122)$$

and thus the hypothesis requires

$$0 = q - q_1 - \sum_{k\in S_q}(q-k)V_{k+(k_{\max}-q)}. \quad (123)$$

Noting that $q - q_1 > 0$ is odd and that the summation k runs on even indices so that $q - k$ is even, this contradicts the fact that the above expression vanishes. In conclusion, writing $P_a(\mathcal{G}) = \frac{1}{2}(2a - \dim G_D)q_1 < 0$, q_1 should be always even.

The divergence degree in the present situation is bounded by $\omega_{\rm d}(\mathcal{G}) \leq \frac{1}{2}(\dim G_D - 2a)q_1, 2 \leq q_1 \leq q < k_{\max}$. Consider $g_{\tilde{\mathcal{G}}} > 0$, one infers

$$\begin{aligned}\omega_{\rm d}(\mathcal{G}) &= -2\dim G_D g_{\tilde{\mathcal{G}}} + \frac{1}{2}(\dim G_D - 2a)q_1 \leq -2\dim G_D + \frac{1}{2}(\dim G_D - 2a)q_1 \\ &\leq -2\dim G_D + \frac{1}{2}(\dim G_D - 2a)q < -2\dim G_D + (\dim G_D - 2a)k_{\max} = 0.\end{aligned} \quad (124)$$

Thus whenever $g_{\tilde{\mathcal{G}}} > 0$, the amplitude is convergent. We only have a divergent amplitude for $g_{\tilde{\mathcal{G}}} = 0$ such that $\omega_{\rm d}(\mathcal{G}) = \frac{1}{2}(\dim G_D - 2a)q_1$.[9]

This achieves the study of divergent contributions in matrix models presented in (103). Appendix C illustrates the formalism by discussing a nontrivial example of the list of divergent amplitudes for the model $({}_{\dim G_D}\Phi^8_2, a)$.

5.2. Renormalization in matrix models. We address, in this section, the renormalization analysis of the diverging N-point functions in the matrix models studied in previous section.

Renormalization of marginal $k_{\max}$-point functions. Consider a marginal $k_{\max}$-point function with $k_{\max}$ propagators hooked to it such that the graph G^i_k associated with that amplitude obeys $g_{\tilde{G}^i_k} = 0$, $C_{\partial G^i_k} = 1$, $V_k = 0$ for $2 \leq k < k_{\max}$, and with external data following a cyclic matrix trace invariant pattern. The associated amplitude is given by

[9] As an illustration, we study $k_{\max} = 8, q = 6$ such that $S_6 = \{2, 4\}$. If $q_1 = 2$, $S'_{0,4} = \{0, 2\}$

$$P_a(\mathcal{G}) = \frac{1}{2}(2a - \dim G_D)2 + \frac{1}{2}(2a - \dim G_D)\big(4 - 4V_4 - 2V_6\big). \quad (125)$$

Requiring $P_a(\mathcal{G}) = \frac{1}{2}(2a - \dim G_D)2$, leads to the solutions of $2 - 2V_4 - V_6 = 0$, which are $(V_4, V_6) = \{(1, 0), (0, 2)\}$ related to the partitions of $2 = 2 + 0 = 1 + 1$. It is simple to fix the rest of parameters to zero in order to get $\omega_{\rm d}(\mathcal{G}) = -P_a(\mathcal{G})/a > 0$.

If $q_1 = 4$, $S'_{0,2} = \{0\}$, we have $P_a(\mathcal{G}) = \frac{1}{2}(2a - \dim G_D)4$, if $2 - 2V_6 = 0$ corresponding to the partition of $1 = 1 + 0$. We have a divergence degree $\omega_{\rm d}(\mathcal{G}) = -P_a(\mathcal{G}) > 0$ in this case too after setting the other parameters to zero. If $q_1 = 6$, then $S'_{0,2} = \emptyset$ and $\omega_{\rm d}(\mathcal{G}) = -P_a(\mathcal{G}) > 0$ for all parameters V_k and $g_{\tilde{\mathcal{G}}}$ set to 0.

$$A_{k_{\max}}(\{P_f^{\text{ext}}\}) = \sum_{P_f} \int [\prod_{\ell} d\alpha_\ell e^{-\alpha_\ell \mu^2}] \prod_{f \in \mathcal{F}_{\text{ext}}} \left[e^{-(\sum_{\ell \in f} \alpha_\ell)|P_f^{\text{ext}}|^a} \right] \prod_{f \in \mathcal{F}_{\text{int}}} \left[\mathbf{d}^2_{P_f} e^{-(\sum_{\ell \in f} \alpha_\ell)|P_f|^a} \right]. \tag{126}$$

Next we perform a Taylor expansion in each external face amplitude as done in (87) and insert the result in (126). The 0th order term in the expansion factorizes in a similar way as found in (90) as

$$A_{k_{\max}}(\{P_f^{\text{ext}}\}; 0) = \Big[\int [\prod_{l} d\alpha_l e^{-\alpha_l \mu^2}] \prod_{f \in \mathcal{F}_{\text{ext}}} e^{-(\alpha_l + \alpha_{l'})|P_f^{\text{ext}}|^a} \Big] \sum_{P_f} \int [\prod_{\ell \neq l} d\alpha_\ell e^{-\alpha_\ell \mu^2}] \times \prod_{f \in \mathcal{F}_{\text{int}}} \left[\mathbf{d}^2_{P_f} e^{-(\sum_{\ell \in f} \alpha_\ell)|P_f|^a} \right]. \tag{127}$$

We write $\mathcal{F}_{\text{ext}} = \{f_1, \ldots, f_{k_{\max}}\}$ such that the first factor of $A_{k_{\max}}(\{P_f^{\text{ext}}\}; 0)$ expands as

$$\int [\prod_{l=1}^{k_{\max}} d\alpha_l e^{-\alpha_l \mu^2}] \prod_{j=1}^{k_{\max}} e^{-(\alpha_{l_j} + \alpha_{l'_j})|P_{f_j}^{\text{ext}}|^a} = \int [\prod_{l=1}^{k_{\max}} d\alpha_l] \prod_{l=1}^{k_{\max}} e^{-\alpha_l (\sum_{s=1}^{2} |P_{l,s}^{\text{ext}}|^a + \mu^2)}, \tag{128}$$

where one identifies the pattern of the cyclic matrix interaction $V_{k_{\max}}$ for external momenta,

$$j = 1, \ldots, k_{\max}, \quad P_{j,1}^{\text{ext}} = P_{f_j}^{\text{ext}}, \quad P_{j,2}^{\text{ext}} = P_{f_{j+1}}^{\text{ext}} \quad \text{and} \quad \alpha_{l'_j} = \alpha_{l_{j+1}} = \alpha_j. \tag{129}$$

The first factor of (127) represents the gluing of $k_{\max}$ propagators in the pattern of the $V_{k_{\max}}$ interaction. By the power counting theorem this term is log–divergent.

Studying the remainders, in same anterior notations, the first order can be bounded up to some constant K as

$$|R_{k_{\max}}| \leq K M^{-2a(i(G_k^i) - e(G_k^i))} M^{\omega_{\text{d}}(G_k^i) = 0}. \tag{130}$$

This shows that the remainder converges and will bring additional convergence during the final assignment summation.

Renormalization of $(k_{\max} - q)$-point functions. We treat now the case of an amplitude associated with a graph G_k^i with $N = k_{\max} - q$ external propagators, $2 \leq q \leq k_{\max} - 2$. According to the previous dissection of the type of divergent graphs, this case splits in several situations. The positive degree of divergence may vary as $0 \leq \omega_{\text{d}}(G_k^i) \leq -P_a(G_k^i) = \frac{q_1}{2}(\dim G_D - 2a)$, where $0 \leq q_1 \leq q$ and q_1 is even.

$\star$ If $q_1 = 0$, then the amplitude is log–divergent and can be handled in the same way as in the marginal $N = k_{\max}$-point functions. The quasi local part of the amplitude renormalizes the $(k_{\max} - q)$-valent vertex if the initial external data configuration of the graph follow the cyclic pattern of a $V_{k_{\max} - q}$ vertex. All remainders are convergent.

$\star$ Let us assume now that $q_1 \geq 2$. We choose a graph G_k^i such that $g_{\tilde{G}_k^i} = 0$, $C_{\partial G_k^i} = 1$, $V_{p + (k_{\max} - q)} = 0$, for $2 \leq p \leq q_1$ and a partition of $(q - q_1)/2$ as

$$\text{if } q - q_1 > 0\,, \qquad 0 = q - q_1 - \sum_{p=0;\, p \text{ even}}^{q - q_1 - 2} (q - q_1 - p) V_{p + k_{\max} - (q - q_1)}, \tag{131}$$

and if $q = q_1$ set $V_p = 0$ for all $2 \leq p \leq q-2$. The amplitude of such a graph G^i_k is given by

$$A_{k_{\max}-q}(\{P_f^{\rm ext}\}) = \Big[\int [\prod_l d\alpha_l e^{-\alpha_l \mu^2}] \prod_{f\in\mathcal{F}_{\rm ext}} e^{-(\alpha_l+\alpha_{l'})|P_f^{\rm ext}|^a}\Big] \sum_{P_f} \int [\prod_{\ell\neq l} d\alpha_\ell e^{-\alpha_\ell \mu^2}] \times \prod_{f\in\mathcal{F}_{\rm int}} \Big[\mathbf{d}^2_{P_f} e^{-(\sum_{\ell\in f}\alpha_\ell)|P_f|^a}\Big]. \tag{132}$$

Two main cases occur:

(A) Assuming $2 \leq q < k_{\max}-2$, we perform a Taylor expansion of the face amplitude at first order as given by (87). Using the same previous techniques, it is direct to show that the 0th order term $A_{k_{\max}-q}(\{P_f^{\rm ext}\})$ factors and reproduces the gluing of $k_{\max}-q$ propagator according the pattern of a vertex with $k_{\max}-q$ number of legs. Let us discuss the remainder and concentrate on the first term involving $\sum_f R_f$. This term can be bounded as

$$|R_{q_1}| \leq K M^{-2a(i(G^i_k)-e(G^i_k))} \sum_{P_f} \int [\prod_\ell d\alpha_\ell e^{-\alpha_\ell \mu^2}] \Big[\prod_{f\in\mathcal{F}_{\rm ext}} e^{-(\alpha_l+\alpha_{l'})|P_f^{\rm ext}|^a}\Big] \times \prod_{f\in\mathcal{F}_{\rm int}} \Big[\mathbf{d}^2_{P_f} e^{-(\sum_{\ell\in f}\alpha_\ell)|P_f|^a}\Big]. \tag{133}$$

The integration over $\alpha_{\ell\neq l}$ and summation over P_f yield the overall divergence degree of the G^i_k. We have

$$|R_{q_1}| \leq K M^{-2a(i(G^i_k)-e(G^i_k))} M^{\omega_{\rm d}(G^i_k)}. \tag{134}$$

We need the following result (in the same previous notations).

Lemma 1. *$\forall q_1$ such that $2 \leq q_1 \leq q \leq k_{\max}-2$,*

$$\begin{aligned} &\text{if} \quad q_1 < k_{\max}-2, \qquad -2a + \frac{q_1}{2}(\dim G_D - 2a) < 0\,, \\ &\text{if} \quad q_1 = k_{\max}-2, \qquad -2a + \frac{q_1}{2}(\dim G_D - 2a) = 0. \end{aligned} \tag{135}$$

Proof. We have

$$\begin{aligned} \frac{1}{2}\big(-4a + q_1(\dim G_D - 2a)\big) &\leq \frac{1}{2}\big(-4a + (k_{\max}-2)(\dim G_D - 2a)\big) \\ &\leq \frac{1}{2}\big(-4a + (\frac{2\dim G_D}{\dim G_D - 2a} - 2)(\dim G_D - 2a)\big) = 0 \end{aligned} \tag{136}$$

The inequation is saturated only if $q_1 = k_{\max}-2$. □

Using Lemma 1, one shows that the remainder R_{q_1} converges since $-2a+\omega_{\rm d}(G^i_k) < 0$ because $q_1 \leq q < k_{\max}-2$. This means that having a $(k_{\max}-q)$-point function, where $q < k_{\max}-2$ diverging like $\omega_{\rm d}(G^i_k) = \frac{q_1}{2}(\dim G_D - 2a)$, for all $2 \leq q_1 \leq q$, with all graph properties required for being renormalizable, then expanding this function gives a unique contribution renormalizing the coupling constant of a vertex $V_{k_{\max}-q}$ and all remainders are convergent.

(B) Let us assume that $q = k_{\max} - 2$, we are dealing necessarily with a $N_{\text{ext}} = 2$-point function. The graph G_k^i has a divergence degree of the form $\omega_{\text{d}}(G_k^i) = \frac{q_1}{2}(\dim G_D - 2a)$, for all $2 \leq q_1 \leq k_{\max} - 2$.

- If $q_1 < k_{\max} - 2$, we perform a Taylor expansion on external faces as (87) and, just as in the above situation, it is simple to check that the 0th order of the graph amplitude yields a vertex coupling renormalization for $V_{k_{\max}-q}$ whereas all remainders are convergent (by Lemma 1) and obey a bound like (134).
- If $q_1 = k_{\max} - 2$, we use in this case a Taylor expansion of the form (99) for each external face. The procedure is similar to tensor situation: the Taylor expansion at 0th order of the graph amplitude yields a mass renormalization for $V_{2;1}$ the first order remainder containing $\sum_f R_f$ provides the log–divergent term embodying the wave function renormalization term. This again holds by invoking symmetry arguments on graphs. All other remaining terms are simply convergent and will bring additional decay useful for the summation over momentum assignments.

In conclusion of this part, we realize that all expansions of diverging graphs respecting precise renormalizability criteria yield diverging local terms which can be recast as term present in the matrix model action (103). The remainders give enough decay allowing the summation over scale attributions in the last stage and proof of the finiteness of the Schwinger functions when removing the cut-off [51]. Thus, Theorem 3 holds.

6. Super-Renormalizable Models

There are two conditions, namely $\dim G_D(d-1) = 2a$ and $[\dim G_D(d-1) > 2a;\ k_{\max} < 2\dim G_D(d-1)/(\dim G_D(d-1) - 2a)]$ which both lead to potentially super-renormalizable models (without being convergent). We review these in this section.

Super-renormalizable models of type I. Let us consider models such that $\dim G_D(d-1) = 2a$. We have identified some situations for which this occurs. For $d = 3$, the divergence degree of a graph $\mathcal{G}$ in the model $({}_1\Phi_3^k, a = 1)$ assumes the form

$$\omega_{\text{d}}(\mathcal{G}) = -(\omega(\mathcal{G}_{\text{color}}) - \omega(\partial\mathcal{G})) - (C_{\partial\mathcal{G}} - 1) + 2(1 - V). \tag{137}$$

On the other hand, for $d = 2$, the divergence degree of a graph in the models $({}_{\dim G_D}\Phi_2^k, a)$, with $(\dim G_D, a) \in \{(1, \frac{1}{2}), (2, 1)\}$, is given by

$$\omega_{\text{d}}(\mathcal{G}) = -4g_{\tilde{\mathcal{G}}} - 2(C_{\partial\mathcal{G}} - 1) + 2(1 - V). \tag{138}$$

For any rank, (137) and (138) tell us that only graphs with $V = 1$ vertex may diverge. Graphs with $V = 1$ are called tadpoles. This situation is typical of super-renormalizable models.

Given a maximal valence of vertices $k_{\max}$, the number of melonic or planar interactions which can be built with maximal valence $k_{\max}$ is certainly a finite number. Consider an action including all these vertices up to order $k_{\max}$. We do not need to consider any anomalous term here ($C_{\partial\mathcal{G}} > 1$ leads to convergence).

For the $({}_1\Phi_3^{k_{\max}}, a = 1)$ model, introducing a UV cut-off Λ, in a similar way as in (71), it can be inferred that

$$S^\Lambda = \sum_{k=4}^{k_{\max}} \sum_i \frac{\lambda_{k;i}^\Lambda}{\sigma_{k;i}} S_{k;i}^{\text{int}} + CT_{2;1}^\Lambda S_{2;1}, \tag{139}$$

where $\sigma_{k;i}$ is a symmetry factor of the interaction $S^{\rm int}_{k;i}$ including all interactions of the melonic form of valence k up to some color permutation. The index i is at this point totally formal and parameterize the types of melonic interactions which differ up to a color permutation.

Concerning matrix models $({}_{\dim G_D}\Phi_2^{k_{\max}}, a)$, we introduce an interaction

$$S^{\Lambda} = \sum_{k=4}^{k_{\max}} \frac{\lambda_k^{\Lambda}}{\sigma_k} S_k^{\rm int} + C T^{\Lambda}_{2;1} S_{2;1}, \tag{140}$$

where $S_k^{\rm int}$ is the familiar trace invariant of order k for matrices. Note that we did not introduce a wave-function renormalization counter-term but only a mass counter-term vertex in both (139) and (140).

The following statement holds.

Theorem 4 (Super-renormalizable tensor models I.) *The models* $({}_{\dim G_D}\Phi_d^{k_{\max}}, a)$ *defined by*

$$\forall k \geq 2\,, \qquad ({}_1\Phi_2^{2k}, a = \frac{1}{2}) \text{ over } G = U(1)\,, \qquad ({}_2\Phi_2^{2k}, a = 1) \text{ over } G = U(1)^2,$$
$$({}_1\Phi_3^{2k}, a = 1) \text{ over } G = U(1)\,, \tag{141}$$

with action defined by (139) *and* (140) *are super-renormalizable.*

Proof. The multi-scale analysis of a connected graph as performed in anterior sections will lead to power counting governed by (137) or (138). We can investigate the type of divergences which occur in the model and prove that they appear in finite number. Their expansion and subtraction scheme can be done as in Sect. 4.2 and will lead to finiteness after summing over scale attribution. Since this last part is completely standard, it will be not addressed here.

We already know that all possible diverging connected graphs are generated by one vertex.

- Considering $N_{\rm ext} \geq k_{\max}$ implies that one uses more than 1 vertex, then it is immediate that the amplitude will be convergent. Having a graph such that $N_{\rm ext} = k_{\max}$ defined by a unique vertex necessarily means that the graph (which should be connected) is defined to be the open vertex itself. This also leads to the convergence of the amplitude.
- Consider now graphs such that $N_{\rm ext} < k_{\max}$. Given any vertex with valence $k \leq k_{\max}$, we can only built a finite number of tadpoles out of it. Hence tadpole graphs are certainly of finite number. The number of divergent graphs which should be chosen among these tadpoles is therefore finite.
  Associated with a tadpole with have a divergence degree

$$\omega_{\rm d}(\mathcal{G}) = -(\omega(\mathcal{G}_{\rm color}) - \omega(\partial\mathcal{G})) - (C_{\partial\mathcal{G}} - 1) \tag{142}$$

  which leads at most to a log–divergent amplitude. Thus $\omega_{\rm d}(\mathcal{G}) = 0$ if and only if $\omega(\mathcal{G}_{\rm color}) = 0 = \omega(\partial\mathcal{G})$ and $C_{\partial\mathcal{G}} = 1$.

Performing a Taylor expansion around the local part of a N_{ext} -point amplitude graph such that $\omega(\mathcal{G}_{\text{color}}) = 0 = \omega(\partial\mathcal{G})$ and $C_{\partial\mathcal{G}} = 1$ and such that the external momentum data of this graph follows the pattern of a vertex of the theory with valence N_{ext} can be done in exact conformity with the previous developments. We can show that the 0th order term is log–divergent should renormalize a vertex of valence equals N_{ext} . The remainders are convergent and there is no need to introduce a wave function renormalization.

Using the techniques of [51], we can sum over momentum assignments using the additional decay of the remainders appearing in the Taylor expansion of tadpoles. This achieves the proof of Theorem 4. □

Super-renormalizable models of type II. This class of super-renormalizable models is directly inferred from the existence of just-renormalizable models. Precisely, each model $({}_{\dim G_D}\Phi_d^{k'_{\max}}, a)$ of this second type is obtained from a just-renormalizable $({}_{\dim G_D}\Phi_d^{k_{\max}}, a)$ by simply restricting $k'_{\max} < k_{\max}$, provided $k_{\max} \geq 6$. The reason why this restriction leads to super-renormalizable models is quite direct: the presence of some vertices of lower valence $V_k < V_{k_{\max}}$ in a just-renormalizable model always tends to improve the power counting hence to more convergence.

We must prove here the following theorem:

Theorem 5 (Super-renormalizable models II). *The models* $({}_{\dim G_D}\Phi_d^{k_{\max}}, a)$ *such that*

$$({}_1\Phi_4^4, a = 1) \text{ over } U(1)\,, \quad ({}_1\Phi_3^4, a = \frac{2}{3}) \text{ over } U(1)\,, \tag{143}$$

with an action defined by (72) *are super-renormalizable at all orders of perturbation.*

The models $({}_{\dim G_D}\Phi_2^{k_{\max}}, a)$ *defined by*

$$\begin{aligned} \forall k \geq 3 \ \text{ and } \ \forall q, \ \ k - q \geq 2\,, \quad ({}_1\Phi_2^{2(k-q)}, a = \frac{1}{2}(1 - \frac{1}{k})) \text{ over } G = U(1)\,, \\ ({}_2\Phi_2^{2(k-q)}, a = 1 - \frac{1}{k}) \text{ over } G = U(1)^2\,, \\ ({}_3\Phi_2^4, a = 1) \text{ over } G = U(1)^3 \text{ or } G = SU(2)\,, \end{aligned} \tag{144}$$

with actions defined by (105) *are renormalizable at all orders of perturbation.*

Proof. We only give the main arguments for completing the proof of the above statement which is already contained in anterior proofs.

- Consider the rank $d \geq 3$ tensor models given by (143). Consider now, in the proof of Theorem 2 as given in Sect. 4.1, the list of primitively divergent graphs of the models Φ^6. The analysis of primitively divergent graphs for the present Φ^4 models follows the same logic. Now, one directly realizes that a graph with $N_{\text{ext}} \geq 6$ must be convergent. The only dangerous case $\omega_{\text{d}}(\mathcal{G}) = 0$ at $N_{\text{ext}} = 6$ can no longer appear in the present models because a nontrivial graph must have $V_4 \neq 0$ (note also that the case of a graph made only with mass vertices is not considered). Following step by step the remaining analysis, we see that diverging graphs must have $V_4 = 1$ or 2. The only sub-cases valid in the present models are given by (c1), (d) (note that we must exclude (a1) because $N_{\text{ext}} = 4$ and $V_4 = 1$ is a vertex graph). The number of graphs that one can build with $V_4 = 1, 2$ is certainly finite.

- Rank $d = 2$ matrix models (144) are now considered. The main idea is again the same as above: using the proof of Theorem 3 in Sect. 5.1, we must prove that all diverging graphs must have a specific number of vertices with valence up to $2(k-q)$. This will make this class of diverging graphs of finite cardinal (even though this cardinal can be large). Consider a model $\Phi_2^{k_{\max}-q}$ given above, where both $k_{\max}$ and q are even and fulfill the corresponding conditions. The case of a graph with $N_{\text{ext}} \geq k_{\max}$ is simply convergent because V_k cannot vanish all at the same time. From now, consider $N_{\text{ext}} = k_{\max} - p$, $p > 0$ and even. Two cases occur (A) $p < q$ or (B) $p \geq q$. In the same notation of the proof of Theorem 3, we have:

(A) $p < q$, then any term in $\sum_{k=2}^{k_{\max}-q}(2\dim G_D+(2a-\dim G_D)k)V_k$, such that $V_k > 0$, is larger than $(2\dim G_D+(2a-\dim G_D)N_{\text{ext}}$. Note that these terms cannot vanish all at the same time ($\exists k_0$ such that $V_{k_0} > 0$). All amplitudes converge in this case.

(B) $p \geq q$, then $2 \leq k_{\max}-p \leq k_{\max}-q$, and the rest of the proof is now exactly similar to that of Theorem 3. There may be some divergent configurations. For log-divergent situations, namely case (h), either one has $V_{k_{\max}-p} = 1$ and all the rest of numbers of vertices cancel (but this case is immediately rule out, one cannot construct a divergent graph with a unique vertex $V_{k_{\max}-p} = 1$ with exactly $N_{\text{ext}} = k_{\max} - p$ external legs; because of this, one must exclude $p = q$ as well), or one has to express the contribution of $N_{\text{ext}} = k_{\max} - p$ as a finite set of number of vertices V_k indexed by a partition of $p/2$. For $\frac{1}{2}(\dim G_D - 2a)p_1$-divergent graphs, $p_1 \leq p$, we refer to case (i) with another type of partition which must be considered. All the possible cases reduce to graphs with a fixed number of vertices determined by these partitions. The number of these graphs is finite.
The renormalization procedure can be reproduced along the lines of Sect. 4.2 for the rank $d = 3$, and Sect. 5.2 for $d = 2$.

  - We consider the Φ^4 models in rank $d \geq 3$. All diverging amplitudes are of the form of 2-point functions. Marginal and a-divergent amplitudes renormalize the mass and there is no wave function counterterms. All remainders are convergent.
  - Second, let us focus on the matrix models, $\Phi^{k_{\max}-q}$, $q > 0$ and even. Consider log-divergent amplitudes made with a $N_{\text{ext}} = k_{\max} - p$ of external legs, $p > q$. We can expand such amplitudes on their local part and they renormalize the cyclic vertex made with $k_{\max} - p$ external legs. Higher order divergences $\omega_{\text{d}}(\mathcal{G}) = \frac{1}{2}(\dim G_D - 2a)p_1$, $2 \leq p_1 \leq p$ and even, can be also handled along the study of just-renormalizable matrix models. The analysis turns out to exclude certain situations only but it is straightforward. □

7. First Order β-Functions

The renormalizability of the above models leads to another important question related to the UV asymptotic behavior of these models. This section undertakes the computation of the β-functions of the $_{\dim G_D}\Phi^{4,6}_{d=2,3,4,5}$ models at enough number of loops so that we may conclude about their UV behavior. The generic situation $\Phi^{k\geq 8}$ is intricate and will have numerous perturbative corrections. We will not address the study of these couplings here.

7.1. Method. Consider a bare coupling constant λ_k associated with some interaction S_k^{int} itself associated with a vertex V_{2k} of valence $2k \geq 4$, and its renormalized coupling constant λ_k^{ren}. The first order β-functions and renormalized coupling constant equations of the models are encoded in the ratio

$$\lambda_k^{\text{ren}} = -\frac{\Gamma_{2k}(\{0\})}{Z^k}, \tag{145}$$

where $\Gamma_{2k}(\{b^{\text{ext}}\})$ is the sum of all amputated one-particle irreducible (1PI) $2k$-point functions satisfying the renormalization criteria in order to be associated with the coupling λ_k and evaluated at first loops. In particular among these criteria, the external momentum data $\{b^{\text{ext}}\}$ of any graph contributing to this this quantity should reproduce the pattern of the V_{2k} vertex and should be planar or melonic. The quantity Z is the so-called wave function renormalization which evaluates from

$$Z = 1 - \partial_{(b^{\text{ext}})^{2a}} \Sigma\big|_{b^{\text{ext}}=0}, \tag{146}$$

where Σ is the self-energy or sum of all amputated 1PI two-point functions evaluated at the first loop orders. Note that, according to the maximal valence $k_{\max}$ of the interactions, the number of loops may vary from one model to another. The function $\Sigma(b_1^{\text{ext}}, \ldots, b_d^{\text{ext}})$ is symmetric in its variables b_s^{ext} where s refers again to strand momentum variables.

In order to make clear the following developments, let us consider a simple coupling formulation of some renormalizable theory. In such case, the wave function renormalization Z and Γ_{2k} function generally express at first loop expansion in the simple form as

$$Z = 1 - \mathrm{a}\lambda + O(\lambda^2), \qquad \Gamma_{2k} = -\lambda + \mathrm{b}\lambda^2 + O(\lambda^3), \tag{147}$$

where $\mathrm{a} \geq 0$ and $\mathrm{b} \geq 0$ are real numbers involving the different graph contributions and their combinatorics. Computing now the ratio (145), one finds

$$\lambda^{\text{ren}} = \lambda + (k\mathrm{a} - \mathrm{b})\lambda^2 + O(\lambda^3). \tag{148}$$

Then the quantity $k\mathrm{a} - \mathrm{b}$ determine the first order β-function related to the model and its coupling constant λ. If $k\mathrm{a} - \mathrm{b} > 0$ the model is said asymptotically free, if $k\mathrm{a} - \mathrm{b} < 0$, it possesses the so-called Landau ghost with a coupling constant blowing in the UV [51]. Meanwhile, in the case $k\mathrm{a} = \mathrm{b}$ we call the model perturbatively safe at one-loop. It is a striking observation that the more k is large the more likely the quantity $k\mathrm{a} - \mathrm{b}$ is positive. But the quantities a and b themselves are in fact function of k and this makes difficult to know a priori the sign of $\beta(k) = k\mathrm{a}(k) - \mathrm{b}(k)$ as k may vary.

The goal of this section is to show that for the previous renormalizable tensor models Φ^4, $\beta = k\mathrm{a} - \mathrm{b} > 0$. Concerning the renormalizable tensor models Φ^6, the renormalized coupling equations are much more involved and require further loop calculations. It would be very interesting to investigate in general if asymptotic freedom holds for all renormalizable tensor models and therefore this feature is generic. The tower of potentially renormalizable model in rank $d = 3$ prevents us to conclude anything at this stage if we include models with a dynamics which is not Laplacian.

The general procedure that we will use, even though lengthy, turns out to be efficient to get a definite result for the several types of β-functions for all interactions given above. We use the following method:

First, we enlarge the space of couplings and consider for each renormalizable action defined by (71) and (72) as a multiple coupling theory. This means that we give to each interaction term associated with a certain permutation of colors a different coupling. Doing so, we have (forgetting wave function and mass vertices)

– For $k_{\max} = 6$, $\dim G_D = 1$ and $(d, a) \in \{(3, \frac{2}{3}), (4, 1)\}$,

$$S = \sum_{\rho} \frac{\lambda_{6;1;\rho}}{3} S^{\text{int}}_{6;1;\rho} + \sum_{\rho\rho'} \lambda_{6;2;\rho\rho'} S^{\text{int}}_{6;2;\rho\rho} + \sum_{\rho} \frac{\lambda_{4;1;\rho}}{2} S^{\text{int}}_{4;\rho} + \frac{\lambda_{4;2}}{2} \delta_{d,4} S^{\text{int}}_{4;\mathrm{a}}, \tag{149}$$

where the single label $\rho \in \{1, \ldots, d\}$, and the second double index $\rho\rho'$ has to be chosen in all symmetric pairs of color such that $\rho \neq \rho'$. Precisely, $d = 3$, $\rho\rho' \in \{12, 13, 23\}$, whereas for $d = 4$, $\rho\rho' \in \{12, 13, 14, 23, 24, 34\}$;
– For $k_{\max} = 4$, $(d, \dim G_D, a) \in \{(3, 1, \frac{1}{2}), (3, 2, 1), (4, 1, \frac{3}{4}), (4, 1, 1), (5, 1, 1)\}$,

$$S = \sum_{\rho} \frac{\lambda_{4;\rho}}{2} S^{\text{int}}_{4;\rho}\,, \tag{150}$$

with ρ keeping its above meaning.
– For $d = 2$ or matrix models, the renormalizable actions (105) are already in the proper "multi-coupling" form.

Then, at the end, we collapse all couplings of all terms which can be mutually identified up to a permutation of colors to a single value, that is $\lambda_{6;1;\rho} \to \lambda_{6;1}$, $\lambda_{6;2;\rho\rho'} \to \lambda_{6;2}$, and $\lambda_{4;1;\rho} \to \lambda_{4;1}$. This will provide us with the renormalized coupling equation for the models (71) and (72). Importantly, we will concentrate on the maximal valence interaction coupling in this work. The relevant couplings of the Φ^4 type occurring in the $\Phi^{k_{\max}=6}_{d\geq 3}$ models can be simply inferred from this point whereas the Φ^4 couplings occurring in the $\Phi^{k_{\max}=6}_{2}$ matrix models might be very involved and will be not addressed.

7.2. First order β-functions of tensor models.

7.2.1. One-loop β-functions of the Φ^4 models. We simplify in the following the notations and use P for $|P|$, for some momentum (multi-)variable P. Furthermore, in this notation, we recall that P_s^a expands fully as $\sum_{i=1}^D |p_{s,i}|^{2a}$ for the representation of the group $U(1)^D$. We also use the block matrix notation $[1] = 1$ and $\{\check{1}\} = (2, \ldots, d)$. The following formal series will be useful:

$$S^1 := \sum_{P_s} \frac{1}{[P^a_{\check{1}} + \mu^2]^2}\,, \tag{151}$$

where $P^a_{\check{1}} := \sum_{s\in\{\check{1}\}} P^a_s$. The self-energy is expressed as

$$\Sigma(\{b\}) = \Sigma(b_1, \ldots, b_d) = \Sigma(b_{[1]}, b_{\{\check{1}\}}) = \langle \bar{\varphi}_{[1]\{\check{1}\}}\, \varphi_{[1]\{\check{1}\}}\rangle^t_{1PI} \tag{152}$$

where $b_s = (b_{s,1}, \ldots, b_{s,D})$, $D = 1, 2$, $s = 1, \ldots, d$, are external momenta.

We start by evaluating the self-energy as

$$\Sigma(\{b\}) = \sum_{\mathcal{G}_c} K_{\mathcal{G}_c}\, \mathcal{S}_{\mathcal{G}_c}(\{b\}), \tag{153}$$

where the sum is over all amputated 1PI 2-point graphs $\mathcal{G}_c$ that we truncate at one-loop, $K_{\mathcal{G}_c}$ is a combinatorial factor and $\mathcal{S}_{\mathcal{G}_c}(\{b\})$ is the amplitude of the graph. These graphs should be listed in Table 7 for $N_{\text{ext}} = 2$.

Up to color permutation, the graphs which are the most divergent and which will contribute to (153) are tadpoles of the melonic-type T_ρ coined by one particular color $\rho = 1, \ldots, d$ (T_1 has been illustrated in Fig. 16; T_ρ can be obtained by color permutation). Let A_{T_ρ} be the amplitude of T_ρ which necessarily depends on $b_{\rho,i}$, $i \in \{1, \ldots, D\}$. We

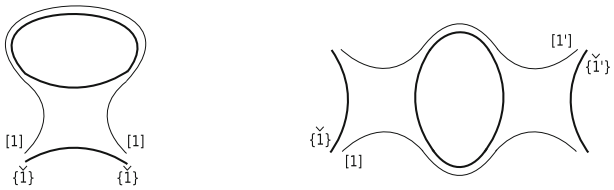

Fig. 16. Tadpole graph T_1 and 4-point graph F_1

fix a particular variable $b_{\rho,1}$ and derivate this amplitude. Note that if $D = 1$, there is no other choice than the one dictated by the color ρ.

The amplitude A_{T_ρ} can be evaluated as

$$A_{T_\rho}(b_\rho) = K_{T_\rho}\left(-\frac{\lambda_{4;\rho}}{2}\right) S_\rho(b_\rho), \quad K_{T_\rho} = 2, \quad S_\rho(b) := \sum_{P_s} \frac{1}{b^a + P^a_{\check{1}} + \mu^2}, \tag{154}$$

such that the wave function renormalization is given by

$$Z = 1 - \partial_{(b_{\rho,1})^a} \Sigma\Big|_{b_{s,i}=0} = 1 - \partial_{(b_{\rho,1})^a} A_{T_\rho}\Big|_{b_{s,i}=0} = 1 - \lambda_{4;\rho} S^1 + O(\lambda_4^2)\,, \tag{155}$$

where S^1 is given in (151) and $O(\lambda_4^2)$ involves all quadratic power of coupling constants.

Next, we must evaluate the $\Gamma_{4;\rho}$ function at 0 external momenta. Formally,

$$\Gamma_4(\{b\}) = \sum_{\mathcal{G}_c} K_{\mathcal{G}_c}\, \mathcal{S}_{\mathcal{G}_c}(\{b\})\,, \tag{156}$$

where the sum runs over all amputated 1PI 4-point graphs which satisfy the first line of Table 7, and the external momentum data of which should reproduce the pattern of the vertex having $\lambda_{4;\rho}$ as coupling constant.

At second order of perturbation, there is a unique way to build these graphs (see Fig. 16). Denote F_ρ such a graph where ρ is the external color index used as well in the propagators. The amplitude of such graph can be written as

$$\begin{aligned} A_{F_\rho}(\{b_\rho\}) &= K_{F_\rho} \frac{1}{2}\left(\frac{-\lambda_{4;\rho}}{2}\right)^2 S'_\rho(b_\rho, b'_\rho), \\ K_{F_\rho} &= 2^3 \qquad S'_\rho(b, b') = \sum_{P_s} \frac{1}{(b^a + P^a_{\check{1}} + \mu^2)} \frac{1}{(b'^a + P^a_{\check{1}} + \mu^2)}. \end{aligned} \tag{157}$$

Hence,

$$\Gamma_{4;\rho}(\{0\}) = -\lambda_{4;\rho} + A_{F_\rho}(\{0\}) = -\lambda_{4;\rho} + \lambda^2_{4;\rho} S^1 + O(\lambda^3). \tag{158}$$

We are in position to calculate the renormalized coupling equation of λ_4. We first set $\lambda_{4;\rho} \to \lambda_4$ in all equations. Using (145), one then gets

$$\lambda_4^{\text{ren}} = -\frac{\Gamma_4(\{0\})}{Z^2} = \lambda_4 + \lambda_4^2 S^1 + O(\lambda_4^3). \tag{159}$$

The β-function at one-loop for all renormalizable Φ^4-models is always fixed and given by

$$\beta = 1. \tag{160}$$

The renormalized coupling equation (159) also exhibits the fact that $\lambda_4^{\text{ren}} > \lambda_4$, for strictly positive coupling $\lambda_4 > 0$. This means that the models are asymptotically free in the UV. The free theory describes non interacting topological d-spheres. Meanwhile going in the other IR direction, the renormalized coupling becomes larger and larger. This generally hints at a phase transition. A widely known example of this kind of theory is certainly QCD where, in the IR, quarks and gluons experience a phase transition for making hadrons. We hope that, for large group distances, the present models may lead to new condensate-type of degrees of freedom (quite different from the basic simplexes used in the initial models) which might be useful to describe interesting geometric properties.

7.2.2. Two- and four-loop β-functions of the Φ^6 models. The computation of the β-functions for the Φ^6 models is inferred from a previous work [58]. The types of graphs relevant for the calculation of the β-function for each model ${}_1\Phi^6_3$ or ${}_1\Phi^6_4$ have been listed in that work. Indeed, the relevant graph construction does not depend much on the characteristics of the models ($\dim G_D, a$) but on the rank d, $k_{\max}$ and on the combinatorics of constructing melonic graphs using Φ^6 interaction. The reduction from $d = 4$ to $d = 3$ is quite immediate.

We introduce the block index notation $[1] = 1$, and depending on the model $[2] = (2, 3)$ and $[3] = 4$ for ${}_1\Phi^6_4$ or $[2] = 2$ and $[3] = 3$ for ${}_1\Phi^6_3$. The following formal sums will be also useful (avoiding multiplication of notations we shall use again S^1):

$$\begin{aligned} S^1 &:= \sum_{p_s, p'_s} \frac{1}{(p_1^{2a} + p_{\check{1}}^{2a} + \mu^2)^2} \frac{1}{(p_1'^{2a} + p_{\check{1}}'^{2a} + \mu^2)}, \\ S^{12} &:= \sum_{p_s, p'_s} \frac{1}{(p_1^{2a} + p_{\check{1}}^{2a} + \mu^2)^2} \frac{1}{(p_1^{2a} + p_{\check{1}}'^{2a} + p_{\check{1}}'^{2a} + \mu^2)}, \end{aligned} \tag{161}$$

where $p_1^{2a} := |p_1|^{2a}$ and $p_{\check{1}}^{2a} := |p_2|^{2a} + \cdots + |p_{d-1}|^{2a}$.

From Lemma 1 in [58], at two loops, the self-energy Σ and wave function renormalization Z compute to

$$\begin{aligned} \Sigma(b_{[1]}, b_{[2]}, b_{[3]}) &= \Sigma^0(b_{[1]}, b_{[2]}, b_{[3]}) + \Sigma'(b_{[2]}, b_{[3]}), \\ \Sigma^0(b_{[1]}, b_{[2]}, b_{[3]}) &= -\lambda_{6;1;1}\tilde{S}^1(b_{[1]}, b_{[1]}) - \sum_{\rho\in\{[2],[3]\}} \Big[\lambda_{6;2;1\rho}\tilde{S}^1(b_{[1]}, b_\rho)\Big] \\ &\quad -\Big[\sum_{\rho\in\{[2],[3]\}} \lambda_{6;2;1\rho}\Big]\tilde{S}^{12}(b_{[1]}) + O(\lambda^2), \end{aligned} \tag{162}$$

$$\begin{aligned} Z &= 1 - \partial_{(b_{[1]})^{2a}}\Sigma^0\Big|_{b_{[s]}=0} = 1 - \Big[2\lambda_{6;1;1} + \sum_{\rho\in\{[2],[3]\}} \lambda_{6;2;1\rho}\Big]S^1 \\ &\quad -\Big[\sum_{\rho\in\{[2],[3]\}} \lambda_{6;2;1\rho}\Big]S^{12} + O(\lambda^2), \end{aligned} \tag{163}$$

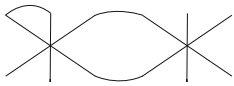

Fig. 17. General form of 1PI 6-point graphs

$$\tilde{S}^1(b,b') := \sum_{p_s,p'_s} \frac{1}{(b^{2a}+p_1^{2a}+p_{\check{1}}^{2a}+\mu^2)} \frac{1}{(b'^{2a}+p_1'^{2a}+p_{\check{1}}'^{2a}+\mu^2)}, \quad (164)$$

$$\tilde{S}^{12}(b) := \sum_{p_s,p'_s} \frac{1}{(b^{2a}+p_1^{2a}+p_{\check{1}}^{2a}+\mu^2)} \frac{1}{(p_1^{2a}+p_1'^{2a}+p_{\check{1}}'^{2a}+\mu^2)},$$

where $\Sigma' = \Sigma - \Sigma^0$ consists in the self-energy remaining part which is independent of the variable $b_{[1]}$ and $O(\lambda^2)$ denotes a sum of O-functions with arguments any quadratic power of the coupling constants $O(\lambda^2_{6;1;\bullet}) + O(\lambda^2_{6;2;\bullet}) + O(\lambda_{6;1;\bullet}\lambda_{6;2;\bullet})$.

1PI amputated 6-point functions truncated at two loops are of the form by Fig. 17 (where we use the most simple representation of the Φ^6-vertex as a vertex with 6 external legs).

The computations are lengthy but we do not need to rederive these. Thus, we use Lemma 2 in [58], in order to get, at two loops, the amputated truncated six-point functions at zero external momenta given as, for $\rho \in \{[1], [2], [3]\}$,

$$\Gamma_{6;1;\rho}(0,\ldots,0) = -\lambda_{6;1;\rho} + \lambda_{6;1;\rho}\Big[6\,\lambda_{6;1;\rho}S^1 + 3\Big[\sum_{\rho'\in\{[1],[2],[3]\}\setminus\{\rho\}} \lambda_{6;2;\rho\rho'}\Big][S^1+S^{12}]\Big] + O(\lambda^3), \quad (165)$$

where S^1 and S^{12} are given by (161) and $O(\lambda^3)$ stands for a sum of O-functions of any cubic power in the coupling constants. On the other hand, for $\rho' \in \{[1], [2], [3]\} \setminus \{\rho\}$, the second function of interest reads

$$\Gamma_{6;2;\rho\rho'}(0,\ldots,0) = -\lambda_{6;2;\rho\rho'} + \lambda_{6;2;\rho\rho'}\Big[2[\lambda_{6;1;\rho}+\lambda_{6;1;\rho'}]S^1$$

$$+\Big[\sum_{\bar{\rho}\in\{[1],[2],[3]\}\setminus\{\rho\}} \lambda_{6;2;\rho\bar{\rho}} + \sum_{\bar{\rho}\in\{[1],[2],[3]\}\setminus\{\rho'\}} \lambda_{6;2;\rho'\bar{\rho}}\Big][S^1+S^{12}]\Big] + O(\lambda^3). \quad (166)$$

The renormalized coupling equation can be evaluated at two-loops by equating all coupling constants $\lambda_{6;1;\rho} = \lambda_{6;1}$ and $\lambda_{6;2;\rho\rho'} = \lambda_{6;2}$. After a straightforward evaluation, one obtains

$$\lambda^{\text{ren}}_{6;1} = -\frac{\Gamma_{6;1}(\{0\})}{Z^3} = \lambda_{6;1} + O(\lambda^3). \quad (167)$$

Thus both models Φ^6 are safe at two-loops in this sector $\lambda_{6;1}$. In order to know the UV behavior of this sector, we need to carry out the computations of the β-function up to four loops. This will be performed after the next paragraph.

Inspecting the second coupling, we have

$$\lambda^{\text{ren}}_{6;2} = -\frac{\Gamma_{6;2}(\{0\})}{Z^3} = \lambda_{6;2} + (d-1)\lambda^2_{6;2}[S^1+S^{12}] + 2\lambda_{6;1}\lambda_{6;2}S^1 + O(\lambda^3). \quad (168)$$

We find that, for $\lambda_{6;1} > 0$ and $\lambda_{6;2} > 0$, the β-function in this sector splits as

$$\beta_{6;2(2)} = (d-1), \qquad \beta_{6;2;(21)} = 2. \tag{169}$$

Thus, we still have $\lambda^{\text{ren}}_{6;2} > \lambda_{6;2}$ and, interestingly, this sector is asymptotically free for both models ${}_1\Phi^6_{3,4}$. Note also that the splitting of the β-function occurs in other (condensed matter) contexts [73]. This simply exhibits the fact that the RG equations of the different couplings are coupled.

The behavior of the coupling constant $\lambda_{6;1}$ still needs to be investigated. Four-loop calculations are required in this case. Note that it has been already established that the coupling constant $\lambda_{6;2}$ tends to 0 in the UV. In order, to determine the behavior of the coupling constant $\lambda_{6;1}$, we can assume that we are far enough in the UV such that $\lambda_{6;2} \sim 0$. Under such circumstances, we do not need to involve vertices of the form $V_{6;2}$.

We use Lemma 3 in [58] and find at four loops the wave function renormalization and $\Gamma_{6;1;\rho}(0,\dots,0)$ function as

$$Z = 1 - 2\lambda_{6;1;1} S^1 + 2\lambda^2_{6;1;1}\Big[2\mathcal{S}^1_{(1)} + 3\mathcal{S}^1_{(2)}\Big] + 2\lambda_{6;1;1}\Big(\sum_{\rho\in\{[2],[3]\}} \lambda_{6;1;\rho}\Big)\Big[2\mathcal{S}^{12}_{(1)} + \mathcal{S}^{12}_{(2)}\Big] + O(\lambda^3) \tag{170}$$

and the sum of truncated amputated six-point functions at four loops satisfies, for any $\rho \in \{[1],[2],[3]\}$,

$$\begin{aligned}\Gamma_{6;1;\rho}(0,\dots,0) = &-\lambda_{6;1;\rho} + 2\cdot 3\,\lambda^2_{6;1;\rho} S^1 - 2\cdot 3\cdot 5\,\lambda^3_{6;1;\rho}\,\mathcal{S}^1_{(2)} \\ &-2\cdot 3\,\lambda^2_{6;1;\rho}\Big[\sum_{\rho'\in\{[1],[2],[3]\}\setminus\{\rho\}} \lambda_{6;1;\rho'}\Big]\mathcal{S}^{12}_{(2)} \\ &-2^2\cdot 5\,\lambda^3_{6;1;\rho}\,\mathcal{S}^1_{(1)} - 2^2\cdot 3\,\lambda^2_{6;1;\rho}\Big[\sum_{\rho'\in\{[1],[2],[3]\}\setminus\{\rho\}} \lambda_{6;1;\rho'}\Big]\mathcal{S}^{12}_{(1)} + O(\lambda^4),\end{aligned} \tag{171}$$

where $O(\lambda^4)$ stands for a function involving a quartic number of couplings and where

$$\begin{aligned}
\mathcal{S}^1_{(1)} &:= \sum_{p_s,p'_s,p''_s,p'''_s}\Big[\frac{1}{(p_1^{2a}+p_{\tilde{1}}^{2a}+\mu^2)^3}\frac{1}{(p_1'^{2a}+p_{\tilde{1}}'^{2a}+\mu^2)}\frac{1}{(p_1''^{2a}+p_{\tilde{1}}''^{2a}+\mu^2)}\frac{1}{(p_1'''^{2a}+p_{\tilde{1}}'''^{2a}+\mu^2)}\Big] \\
\mathcal{S}^1_{(2)} &:= \sum_{p_s,p'_s,p''_s,p'''_s}\Big[\frac{1}{(p_1^{2a}+p_{\tilde{1}}^{2a}+\mu^2)^2}\frac{1}{(p_1'^{2a}+p_{\tilde{1}}'^{2a}+\mu^2)^2}\frac{1}{(p_1''^{2a}+p_{\tilde{1}}''^{2a}+\mu^2)}\frac{1}{(p_1'''^{2a}+p_{\tilde{1}}'''^{2a}+\mu^2)}\Big] \\
\mathcal{S}^{12}_{(1)} &:= \sum_{p_s,p'_s,p''_s,p'''_s}\Big[\frac{1}{(p_1^{2a}+p_{\tilde{1}}^{2a}+\mu^2)^3}\frac{1}{(p_1^{2a}+p_1'^{2a}+p_{\tilde{1}}'^{2a}+\mu^2)}\frac{1}{(p_1^{2a}+p_1''^{2a}+p_{\tilde{1}}''^{2a}+\mu^2)} \\
&\quad\times\frac{1}{(p_1'''^{2a}+p_{\tilde{1}}'''^{2a}+\mu^2)}\Big] \\
\mathcal{S}^{12}_{(2)} &:= \sum_{p_s,p'_s,p''_s,p'''_s}\Big[\frac{1}{(p_1^{2a}+p_{\tilde{1}}^{2a}+\mu^2)^2}\frac{1}{(p_1^{2a}+p_1'^{2a}+p_{\tilde{1}}'^{2a}+\mu^2)}\frac{1}{(p_1^{2a}+p_1''^{2a}+p_{\tilde{1}}''^{2a}+\mu^2)} \\
&\quad\times\frac{1}{(p_1'''^{2a}+p_{\tilde{1}}'''^{2a}+\mu^2)^2}\Big].
\end{aligned} \tag{172}$$

After identifying all couplings, the renormalized coupling equation at four loops becomes

$$\lambda_{6;1}^{\text{ren}} = -\frac{\Gamma_{6;1}(\{0\})}{Z^3} = \lambda_{6;1} + 8\lambda_{6;1}^3 \mathcal{S}_{(1)}^1 + O(\lambda^4), \tag{173}$$

where we used $(S^1)^2 = \mathcal{S}_{(2)}^1$. Hence, the β-function at this order of perturbation reads

$$\beta_{6;1} = 8. \tag{174}$$

Thus the models are asymptotically free in the UV. Similar remarks as in the previous section about the meaning of such free theory hold in the present situation as well. It is also remarkable that, for the Φ^6 tensor models, the maximally divergent graphs with $N_{\text{ext}} = 4$ are graphs without Φ^4 vertices ($V_4 = 0 = V_{4;\text{a}} = V_2$) but only with Φ^6 interaction terms. This immediately implies that at the UV limit, since both $\lambda_{6;1}^{\Lambda}$ and $\lambda_{6;2}^{\Lambda}$ are vanishing, then the renormalized coupling equation for the $\lambda_{4;1}^{\text{ren}}$ reads

$$\lambda_4^{\text{ren}} = \lambda_4, \tag{175}$$

which means that this sector is always safe at all loops. The last sector $\lambda_{4;\text{a}}$ is slightly more subtle as it turns out to be disconnected and can generate divergent amplitudes with only $V_{4;\text{a}}$ vertices [58]. In all situation, it means that we have for both models a UV fixed manifold determined by

$$\lambda_{6;1}^{UV} = 0 = \lambda_{6;2}^{UV}, \qquad \lambda_4^{UV} = k, \qquad \lambda_{4;\text{a}}^{UV} = 0, \tag{176}$$

for some arbitrary k. Adding small perturbations around this line implies that the coupling constants $\lambda_{6;1}^{\text{ren}}$ and $\lambda_{6;2}^{UV}$ grow in the IR.

7.3. First order β-functions of matrix models $\Phi_2^{4,6}$. We now turn our attention to the renormalizable matrix models and their β-function at small number of loops. Consider then the ${}_{\dim G_D}\Phi_2^{4,6}$ models with their list of all divergent graphs. We will focus on the main interactions with maximal valence $k_{\max} = 4$ and 6.

7.3.1. One-loop β-function of Φ_2^4 models. We discuss here the Φ^4 models such that

$$({}_1\Phi_2^4, a = \frac{1}{4}), \quad ({}_2\Phi_2^4, a = \frac{1}{2}), \quad ({}_3\Phi_2^4, a = \frac{3}{4}), \quad ({}_4\Phi_2^4, a = 1), \tag{177}$$

with ribbon-like propagator and 4-valent vertex represented as in Fig. 10 and aim at computing the renormalized coupling equation

$$\lambda_4^{\text{ren}} = -\frac{\Gamma_4(\{0\})}{Z^2}. \tag{178}$$

We will establish that the β-functions at one-loop of the models (177) are all vanishing. This is strongly related with the same property of the GW model which holds at all orders.

Let us introduce the formal sum S^1 with now a different content given by

$$S^1 = \sum_P \frac{d_f(P)}{(P^a + \mu^2)^2}, \tag{179}$$

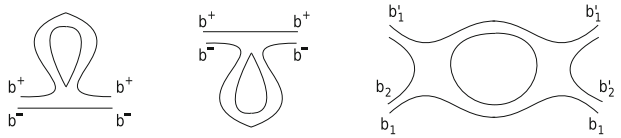

Fig. 18. Tadpole graphs $T^{\pm}$ and a 4-point graph G_4

where according to the group nature, $d_f(P)$ is defined such that:

- if $G_D = U(1)^D$ then $d_f(P) = 1$;
- if $G = SU(2)$ then $d_f(P) = 2P + 1$, $P \in \frac{1}{2}\mathbb{N}$ (this can happen only for the model $({}_3\Phi_2^4, a = \frac{3}{4})$ for the choice $G_D = SU(2)$).

Evaluating the self-energy at one-loop, the tadpole graphs in Fig. 18, should contribute. These are generally named as the tadpole up (+) and down (−). We have at one-loop, for external momenta $b_{\epsilon=\pm}$,

$$\Sigma(b_+, b_-) = \sum_{\epsilon=\pm} A_{T^\epsilon}(b_\epsilon),\ A_{T^\epsilon}(b_\epsilon) = \frac{-\lambda_4}{2} K_{T^\epsilon} \tilde{S}^1(b_\epsilon),\ \tilde{S}^1(b) := \sum_P \frac{d_f(P)}{b^a + P^a + \mu^2}, \tag{180}$$

with $K_{T^\epsilon} = 2$. One therefore infers the wave function renormalization as

$$Z = 1 - \partial_{b_+^a} \Sigma|_{b_\epsilon=0} = 1 - \lambda_4 S^1 + O(\lambda_4^2), \tag{181}$$

where S^1 is given by (179). Next, we focus on 1PI amputated 4-point functions and evaluate Γ_4 at low external momenta. There is a single planar connected graph with one connected component of the boundary, it is given by G_4 in Fig. 18. Computing the amplitude associated with this graph and inserting the result in Γ_4 yields

$$\Gamma_4(\{0\}) = -\lambda_4 + \frac{1}{2!}\left(\frac{-\lambda_4}{2}\right)^2 K_{G_4} S^1 + O(\lambda_4^3) = -\lambda_4 + 2\lambda_4^2 S^1 + O(\lambda_4^3), \tag{182}$$

where we use the fact that the combinatorial factor associated with that graph is $K_{G_4} = 2^4$. The renormalized coupling constant equation is straightforward and given by

$$\lambda_4^{\text{ren}} = \lambda_4. \tag{183}$$

Thus, the β-function is vanishing at one-loop

$$\beta_4 = 0. \tag{184}$$

In fact, we can see that the matrix models (177) reproduce the same features as the complex GW model. At small number of loops, in the derivations of the wave function renormalization, the graph amplitude which may very well vary from one model to the other, keeps at least its overall form. A similar fact happens in the calculation of the 4-point functions. All graphs which should be involved in calculation of β-function of the GW model should appear in the β-function of the present class of models with the same combinatorial factor.

We must emphasize that this vanishing β-function should be strongly correlated with a recent breakthrough concerning the solvability of the GW model [63]. We will focus

on one result in that work that it is useful for the present study. Consider real matrices M_{ab}, where a and b belong to a set I of discrete indices (though the following is valid for continuous indices, we will only discuss the discrete case). We can define a product on these $(MN)_{ab} = \sum_{c\in I} \mu_c M_{ac} N_{cb}$, for a constant weight μ_c. We can also introduce a trace $\mathrm{tr}M = \sum_a \mu_a M_{aa}$ with a quartic interaction of the form $S = V\mathrm{tr}(MEM + (M)^4)$, with V a volume factor, E kinetic term which is not the identity operator but an unbounded self-adjoint operator on an Hilbert space with compact resolvent so that MEM is traceclass. Hence, one must restrict the set of matrices M. Theorem 3.2 of [63] states that the model defined by S has a vanishing β-function. This result holds at the non perturbative level.

The model $({}_1\Phi^4_2, a = \frac{1}{4})$ fits in the above category of models for a suitable set of matrices φ_{mn}. The fact that $\beta_4 = 0$ at all orders for this case is a simple corollary of Theorem 3.2 of [63]. For the other models written in (177), the group dimension is greater than 2, and the fields φ are not really matrices but implicitly tensors (see Remark 1). But we have also seen that the GW model in 4D may be written in terms of tensors, so this might not be a great issue for applying that theorem to the rest of these models. However, using the representation of the group $SU(2)$, we obtain face amplitude contributions of the form $d_f(P)$ which modifies the overall amplitude of any N-point function. One must carefully check if these features may or not affect that theorem.

In any case, we conjecture that the models have all a vanishing β-function at all orders or perturbation. At the non perturbative level, this could be achieved using the same techniques developed in [71,72]. If this statement is true, all these models might be asymptotically safe which means that they have a non trivial fixed point in the UV and Theorem 3.2 of [63] would be valid on a larger domain from matrices to tensors.

7.3.2. Two-loop β-function of the Φ^6_2 models. We are now interested in the UV behavior of the models

$$({}_1\Phi^6_2, a = \frac{1}{3}), \quad ({}_2\Phi^6_2, a = \frac{2}{3}), \quad ({}_3\Phi^6_2, a = 1). \tag{185}$$

The vertices of these models are 6-valent and we will use instead a simplified representation for these as given in Fig. 19. One must pay attention to the fact that, although this simplified vertex notation does not seem to be cyclic, there is no way to distinguish pairs of external lines obtained from one another after a cyclic permutation. In fact, this simplified notation is not canonical in the sense that it can be found (easily) a distinct simplified graph encoding the same vertex. However, introducing this notation will be enough for capturing the essential properties that we want to discuss.

Our goal is to compute at two loops the renormalized coupling equation

$$\lambda_6^{\mathrm{ren}} = -\frac{\Gamma_6(\{0\})}{Z^3}. \tag{186}$$

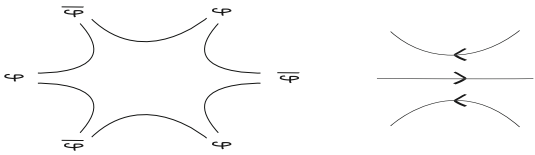

Fig. 19. The Φ^6 vertex and its simplified representation

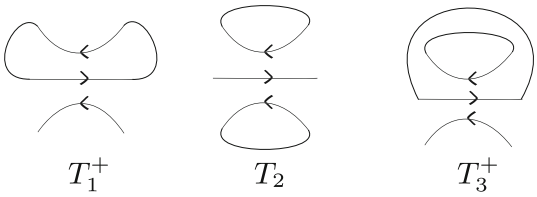

Fig. 20. Tadpoles graphs

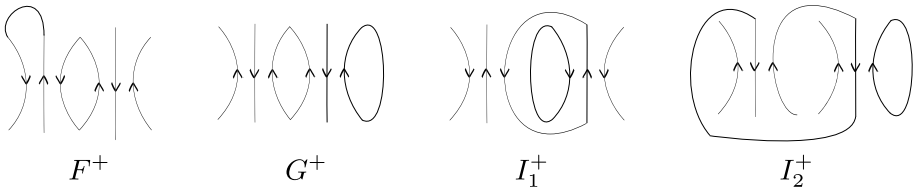

Fig. 21. 1PI 6-point graphs contributing to Γ_6

We will use also the same anterior compact notation for the momentum P^a and denote S^1 and S^{12} now as the formal sums

$$S^1 = \sum_{P_1,P_2} \frac{d_f(P_1)d_f(P_2)}{(P_1^a+\mu^2)^2(P_2^a+\mu^2)}, \qquad S^{12} = \sum_{P_1,P_2} \frac{d_f(P_1)d_f(P_2)}{(P_1^a+\mu^2)^2(P_1^a+P_2^a+\mu^2)}, \tag{187}$$

where as usual $d_f(P_s)$ depends on the group manifold.

At two loops, the wave function renormalization is evaluated from the self-energy which includes the amplitudes associated with the tadpole graphs $\{T_1^{\pm}, T_2, T_3^{\pm}\}$; T_1^+, T_2 and T_3^+ appear in Fig. 20, and T_1^- and T_3^- are obtained either by flipping (top-down) the graphs T_1^+ and T_3^+, respectively, or by conserving the same graphs and switching the orientation of the arrows.

The self-energy $\Sigma(b_+, b_-)$ splits in two sums: one including the external variable b_+ which is $\Sigma^0(b_+, b_-)$ and a remainder. We have

$$\Sigma^0(b_+, b_-) = A_{T_1^+}(b_+, b_-) + A_{T_2}(b_+, b_-) + A_{T_3^+}(b_+, b_-), \tag{188}$$

where $A_{\mathcal{G}}$ is the graph amplitude associated with the graph $\mathcal{G}$. By direct evaluation, using the so far routine, we arrive at

$$Z = 1 - \partial_{b_1^a}\Sigma^0|_{b_s=0} = 1 - \lambda_6(3S^1 + S^{12}) + O(\lambda^2), \tag{189}$$

where S^1 and S^{12} are given by (187).

1PI amputated 6-point functions are once again of the rough form given by Fig. 17.

The amplitudes contributing to Γ_6 are associated to the graphs $\{F^{\pm}, G^{\pm}, I_{1,2}^{\pm}\}$ of the form are listed in Fig. 21 (note that F^-, G^- and $I_{1,2}^-$ are obtained by reversing the orientations of their (+)-partner). At this order of perturbation, the amplitude of any graph $\mathcal{G}$ at low external momenta is

$$A_{\mathcal{G}}(\{0\}) = \frac{1}{2!}\left(\frac{-\lambda_6}{3}\right)^2 K_{\mathcal{G}}\widetilde{S}_{\mathcal{G}}(\{0\}), \tag{190}$$

where $\widetilde{S}_{\mathcal{G}}(\{b\})$ stands for a formal sum and $K_{\mathcal{G}}$ is the combinatorial coefficient associated with each of the significant graphs. It can be shown that

$$\begin{aligned} &K_{F^{\pm}} = 3^3 \cdot 2^2, \quad \widetilde{S}_{F^{\pm}}(\{0\}) = S^1; \qquad K_{G^{\pm}} = 3^3 \cdot 2, \quad \widetilde{S}_{G^{\pm}}(\{0\}) = S^1; \\ &K_{I^{\pm}_{1,2}} = 3^3 \cdot 2, \quad \widetilde{S}_{G^{\pm}}(\{0\}) = S^{12}, \end{aligned} \tag{191}$$

where S^1 and S^{12} are still found in (187). A straightforward evaluation yields

$$\Gamma_6(\{0\}) = -\lambda_6 + \sum_{\mathcal{G} \in \{F^{\pm}, G^{\pm}, I^{\pm}_{1,2}\}} A_{\mathcal{G}}(\{0\}) + O(\lambda^3) = -\lambda_6 + 6\lambda_6^2(3S^1 + 2S^{12}) + O(\lambda^3). \tag{192}$$

We are in position to evaluate the first order renormalized coupling equation. One has

$$\lambda_6^{\text{ren}} = \lambda_6 - 9\lambda_6^2(S^1 + S^{12}) + O(\lambda^3). \tag{193}$$

The two-loop β-function of this coupling constant is

$$\beta_6 = -9. \tag{194}$$

Clearly, from (193) and considering positive coupling constant $\lambda_6 > 0$, the models possess a Landau ghost. In other words, the coupling constant blows in the UV. This matrix models have the same behavior as the ordinary scalar Φ^4 theory in 4D.

8. Concluding Remarks

We have investigated the renormalization analysis of field theories defined with rank $d \geq 2$ tensors defined on representation indices of $G_D \in \{U(1)^D, SU(2)^D\}$. The actions of the models considered are defined with a general kinetic term written in momentum space and which involves a propagator of the form $\frac{1}{p^{2a}+\mu^2}$, where p is the eigenvalue of the Laplacian operator acting on the group background G_D, a a parameter free to take any value in $(0, 1]$ and μ is a mass. The limiting case $a = 1$ yields the ordinary Laplacian dynamics. Our fields are simply random tensors which are not subjected to any condition but integrability. This is in contrast with another type of TGFTs enforcing the so-called gauge invariance on tensors [21] that we did not consider in this work. Within the present framework, we find that there are several just-renormalizable models in any rank. In particular, under the above conditions, we successfully prove that

(A) For the rank $d \geq 3$ case:
- there are 6 just-renormalizable models with rank $d \geq 3$, ${}_1\Phi^6_{3,4}$, ${}_2\Phi^4_3$, ${}_1\Phi^4_{3,4,5}$, the maximal valence of the vertex is 6;
- there is no just-renormalizable tensor model with rank $d \geq 6$,
- there is no just-renormalizable tensor model defined with a group dimension $\dim G_D \geq 3$; in particular there is no just-renormalizable model defined on $G = SU(2)$,
- there is a tower of tensor models in rank $d = 3$ with group $G = U(1)$ which can be potentially just-renormalizable; a model in the tower is determined by the maximal valence $k_{\max} \geq 4$ of its vertices,
- all proved just-renormalizable models are so far asymptotically free in the UV,

Table 8. Updated list of renormalizable models and their features (AF ≡ asymptotically free; LG ≡ existence of a Landau ghost; $\text{AS}^{(\ell)}$ asymptotically safe at ℓ-loops)

TGFT (type)	G_D	$\Phi^{k_{\max}}$	d	a	Renormalizability	UV behavior
	$U(1)$	Φ^6	4	1	Just-	AF
	$U(1)$	Φ^4	3	$\frac{1}{2}$	Just-	AF
	$U(1)$	Φ^6	3	$\frac{2}{3}$	Just-	AF
	$U(1)$	Φ^4	4	$\frac{3}{4}$	Just-	AF
	$U(1)$	Φ^4	5	1	Just-	AF
	$U(1)^2$	Φ^4	3	1	Just-	AF
	$U(1)$	Φ^{2k}	3	1	Super-	–
gi-	$U(1)$	Φ^4	6	1	Just-	AF
gi-	$U(1)$	Φ^6	5	1	Just-	AF
gi-	$SU(2)^3$	Φ^6	3	1	Just-	?
gi-	$U(1)$	Φ^{2k}	4	1	Super-	–
gi-	$U(1)$	Φ^4	5	1	Super-	–
Matrix	$U(1)$	Φ^{2k}	2	$\frac{1}{2}(1-\frac{1}{k})$	Just-	$(k=2, \text{AS}^{(\infty)})$; $(k=3, \text{LG})$
Matrix	$U(1)^2$	Φ^{2k}	2	$1-\frac{1}{k}$	Just-	$(k=2, \text{AS}^{(1)})$; $(k=3, \text{LG})$
Matrix	$U(1)^3$ or $SU(2)$	Φ^6	2	1	Just-	LG
Matrix	$U(1)^3$ or $SU(2)$	Φ^4	2	$\frac{3}{4}$	Just-	$\text{AS}^{(1)}$
Matrix	$U(1)^4$	Φ^4	2	1	Just-	$\text{AS}^{(1)}$
Matrix	$U(1)$	Φ^{2k}	2	$\frac{1}{2}$	Super-	–
Matrix	$U(1)^2$	Φ^{2k}	2	1	Super-	–

- the tower $({}_1\Phi^k_3, a=1)$, for all $k \geq 4$, defines super-renormalizable tensor models. More super-renormalizable models $\Phi^{k'_{\max}}$ can be found from just-renormalizable models $\Phi^{k_{\max}}$ by taking $4 \leq k'_{\max} < k_{\max}$, and keeping the same remaining parameters;

(B) For the $d=2$ or matrix models case:
- there are 6 plus two towers of just-renormalizable models,
- there is no just-renormalizable model defined on a group with dimension $\dim G_D \geq 7$,
- all Φ^4 models have a vanishing β-function at one-loop which is strongly reminiscent of the vanishing β-function at all orders of the GW model in 4D; we conjecture that, indeed, these models are asymptotically safe at all loops in the UV,
- all Φ^6 models have a Landau pole in the UV,
- the tower $(_{\dim G_D}\Phi^k_2, a)$, with $(\dim G_D, a) \in \{(1, \frac{1}{2}), (2, 1)\}$, for all $k \geq 4$, defines super-renormalizable matrix models. Once again, apart from this class of models, one can build several other super-renormalizable models $\Phi^{k'_{\max}}$ from just-renormalizable models $\Phi^{k_{\max}}$ by taking $4 \leq k'_{\max} < k_{\max}$, and keeping the same remaining parameters of the model.

We can update Table 1 as Table 8.

The tower of rank $d=3$ models which might be just-renormalizable addresses a new combinatoric issue which is the classification of all melonic interactions of this rank according to some criteria. This problem can be addressed in any rank $d \geq 3$, of course, for its own combinatoric purpose. This deserves to be understood in order to complete the list of just-renormalizable models in rank $d=3$ as well as to check whether or not asymptotic freedom is a genuine feature of tensor models in rank $d \geq 3$.

Finally, the present investigation pertains to the "discrete to continuum" approach for quantum gravity. To that extent, one might scrutinize all UV asymptotically free theories issued from this work as potentially interesting candidates for describing new degrees of freedom after a likely phase transition in the IR.

Acknowledgements. Research at Perimeter Institute is supported by the Government of Canada through Industry Canada and by the Province of Ontario through the Ministry of Research and Innovation.

Appendix

Appendix A: Face Amplitude Expansion and the Euler Maclaurin Formula

We provide in this appendix further details on the face amplitude expansions (29) and (30) for arbitrary $a \in (0, 1]$ and small $A \sim M^{-i_\ell}$, $A > 0$.

Let us first consider $h_n(x) = x^n e^{-Ax^a}$, with $x \geq 0$, $n \in \mathbb{N}$, and the sum $\sum_{p=0}^{\infty} h_n(p)$. Using the Euler–Maclaurin formula, we have, for a finite integer $q \geq 1$,

$$\sum_{p=1}^{q} h_n(p) = \int_1^q h_n(p)dp + R_n(q),$$

$$R_n(q) = -B_1(h_n(1) + h_n(q)) + \sum_{k=1}^{\infty} \frac{B_{2k}}{(2k!)}(h_n^{(2k-1)}(q) - h_n^{(2k-1)}(1)), \quad \text{(A.1)}$$

where B_k are Bernoulli numbers. A rapid checking shows that

$$h_n'(x) = (x^n e^{-Ax^a})' = x^{-1+n}(n - Aax^a)h_0(x), \ldots,$$
$$h_n^{(m)}(x) = x^{-m+n}(nF_n(m) + G_{n,m}(a, Ax^a))h_0(x), \quad \text{(A.2)}$$

where $F_n(m) = \prod_{l=1}^{m-1}(n - l)$ and $G_{n,m}$ is polynomial in the variable Ax^a so that the remainder R_n is of the form

$$R_n(q) = -B_1(e^{-A} + q^n e^{-Aq^a}) + \sum_{k=1}^{\infty} \frac{B_{2k}}{(2k!)}[q^{-(2k-1)+n}(nF_n(2k-1) + G_{n,2k-1}(a, Ax^a))h_0(q) - (nF_n(2k-1) + G_{n,2k-1}(a, A))h_0(1)]. \quad \text{(A.3)}$$

At the limit $q \to \infty$, $h_n^{(k)}(q)$ is clearly exponentially suppressed by presence of $h_0(q) \to 0$, we obtain

$$\lim_{q\to\infty} R_n(q) = -B_1(1 + O(A)) - \sum_{k=1}^{\infty} \frac{B_{2k}}{(2k!)}(nF_n(2k-1) + G_{n,2k-1}(a, A))h_0(1) = -\tilde{B}_n + O(A), \quad \text{(A.4)}$$

with $\tilde{B}_n$ some constant (note that the sum in k over $nF_n(2k-1)$ is necessarily finite because at some order k $F_n(k) = 0$). On the other hand, for any A, the following integral is exact:

$$\lim_{q\to\infty} \int_1^q h_n(p)dp = \frac{1}{a}\Gamma[\frac{1+n}{a}, A]\, A^{-\frac{1+n}{a}} = \frac{1}{a}A^{-\frac{1+n}{a}}\Gamma[\frac{1+n}{a}] - \frac{1}{1+n} + O(A), \quad \text{(A.5)}$$

where $\Gamma[\cdot,\cdot]$ denotes the incomplete Gamma function and $\Gamma[\cdot]$ stands for the Euler gamma function. Finally, one obtains

$$\sum_{p=1}^{\infty} h_n(p) = \lim_{q\to\infty}\sum_{p=1}^{q} h_n(p) = \frac{1}{a}A^{-\frac{1+n}{a}}\Gamma[\frac{1+n}{a}] - \frac{1}{1+n} - \tilde{B}_n + O(A)$$
$$= c_{a,n}A^{-\frac{1+n}{a}}(1+O(A^{\frac{1+n}{a}})), \tag{A.6}$$

with some constant $c_{a,n} = \Gamma[(1+n)/a]/a$.

We are now in position to specifically address (29) and (30). Equation (A.6) implies at $n = 0$ the following relation

$$\sum_{p=0}^{\infty} h_0(p) = 1 + \sum_{p=1}^{\infty} e^{-Ap^a} = \frac{1}{a}A^{-\frac{1}{a}}\Gamma[\frac{1}{a}] - \tilde{B}_0 + O(A) = c_{a,0}A^{-\frac{1}{a}}(1+O(A^{\frac{1}{a}})) \tag{A.7}$$

which implies (29).

Second, consider the following sum $\sum_{p\in\frac{1}{2}N}(2p+1)^2 e^{-A'p^a}$ in relation with (30) and that expands as:

$$\sum_{p\in\frac{1}{2}N}(2p+1)^2 e^{-A'p^a} = \sum_{p=1}^{\infty} p^2 e^{-Ap^a} + 2\sum_{p=1}^{\infty} p e^{-Ap^a} + \sum_{p=0}^{\infty} e^{-Ap^a}, \tag{A.8}$$

where $A = A'/2^a$. For each resulting sum, we use (A.6) at $n = 2, n = 1$ and $n = 0$, respectively, and get

$$\sum_{p\in\frac{1}{2}N}(2p+1)^2 e^{-A'p^a} = (\frac{1}{a}A^{-\frac{3}{a}}\Gamma[\frac{3}{a}] - \frac{1}{3} - \tilde{B}_2) + 2(\frac{1}{a}A^{-\frac{2}{a}}\Gamma[\frac{2}{a}] - \frac{1}{2} - \tilde{B}_1)$$
$$+\frac{1}{a}A^{-\frac{1}{a}}\Gamma[\frac{1}{a}] - \tilde{B}_0 + O(A)$$
$$= c_{a,3}A^{-\frac{3}{a}}(1+O(A^{\frac{1}{a}})) \tag{A.9}$$

which implies (30).

Appendix B: On Potentially Renormalizable Real Matrix Models

We make in this section additional comments on real matrix models which were not analyzed in Sect. 5. Due to the occurrence of an odd valence of interactions, these models could be defined via real matrix fields. These are

$$({}_1\Phi_2^{2+\gamma>2}, a = \frac{\gamma}{2(2+\gamma)} \leq \frac{1}{2}), \quad ({}_2\Phi_2^{2+\gamma>4}, a = \frac{\gamma}{2+\gamma} \geq \frac{1}{2}), \quad ({}_2\Phi_2^3, a = \frac{1}{3}),$$
$$({}_3\Phi_2^{3,5}, a = \frac{1}{2}, \frac{9}{10}), \quad ({}_4\Phi_2^3, a = \frac{2}{3}), \quad ({}_5\Phi_2^3, a = \frac{5}{6}), \quad ({}_6\Phi_2^3, a = 1), \tag{B.1}$$

where $2+\gamma$ should be an odd integer.

The interaction for these models are of the form

$$S_k^{\text{int}} = \sum_{P_{[I]}} \text{tr}\Big[(\varphi_{[I]})^k\Big] = \sum_{P_{[I]}} \varphi_{12}\, \varphi_{1'2}\, \varphi_{1'2'}\, \varphi_{1''2'} \dots \varphi_{1'''2'''}\, \varphi_{12'''}, \tag{B.2}$$

where, this time, we now allow k to take odd integer values greater than 2. Given a real matrix model ${}_{\dim G_D}\Phi_2^{k_{\max}}$, a cut-off Λ in momentum space, the total interaction may be written

$$S^\Lambda = \sum_{k=3}^{k_{\max}} \frac{\lambda_k^\Lambda}{k} S_k^{\text{int}} + CT_{2;1}^\Lambda + CT_{2;2}^\Lambda S_{2;2}. \tag{B.3}$$

Note that S^Λ includes even and odd valence interaction terms.

The next stage is to list all primitively divergent graphs. For this purpose, we adopt the same method of Sect. 5 and write the divergence degree of a connected graph $\mathcal{G}$, with $N_{\text{ext}} \geq 1$ external leg(s), $C_{\partial\mathcal{G}} \geq 1$ and $V_2 = V_{2;1}$ number of mass vertices as

$$\begin{aligned}
\omega_{\text{d}}(\mathcal{G}) &= -2\dim G_D g_{\tilde{\mathcal{G}}} - P_a(\mathcal{G}),\\
P_a(\mathcal{G}) &= \dim G_D (C_{\partial\mathcal{G}} - 1) + \frac{1}{2}\Big[(\dim G_D - 2a) N_{\text{ext}} - 2\dim G_D\Big]\\
&\quad + \frac{1}{2}\sum_{k=2}^{k_{\max}-1} \Big[2\dim G_D + (2a - \dim G_D)k\Big] V_k,
\end{aligned}$$

where the sum $\sum_{k=2}^{k_{\max}-1}$ is performed over even and odd integers. This is in contrast with the complex case where only even integers were considered in this sum.

In the same vein, $N_{\text{ext}} > k_{\max}$ will give $\omega_{\text{d}}(\mathcal{G}) < 0$ and $N_{\text{ext}} = k_{\max}$ will give $\omega_{\text{d}}(\mathcal{G}) = 0$ if and only if $g_{\tilde{\mathcal{G}}} = 0$, $C_{\partial\mathcal{G}} = 1$, $V_k = 0$, for all k.

– If $N_{\text{ext}} = k_{\max} - q$, where $1 \leq q \leq k_{\max} - 2$, one gets

$$\begin{aligned}
P_a(\mathcal{G}) &= \dim G_D (C_{\partial\mathcal{G}} - 1) + \frac{1}{2}\Big[(\dim G_D - 2a)(k_{\max} - q) - 2\dim G_D\Big]\\
&\quad + \frac{1}{2}\sum_{k=2}^{k_{\max}-1} \Big[2\dim G_D + (2a - \dim G_D)k\Big] V_k\\
&= \dim G_D (C_{\partial\mathcal{G}} - 1) - \frac{1}{2}(\dim G_D - 2a)\left(q - \sum_{k=1}^{k_{\max}-2} k V_{k_{\max}-k}\right).
\end{aligned} \tag{B.4}$$

Using the same arguments as in Sect. 5.1, we must have $C_{\partial\mathcal{G}} = 1$ and $g_{\tilde{\mathcal{G}}} = 0$ in all cases. Then the analysis of divergent graphs with $\omega_{\text{d}}(\mathcal{G}) = -P_a(\mathcal{G}) \geq 0$ can be also recast in terms of a partition of q and $q - q_1$ for an integer $q_1 \leq q$. We clearly see that the number of primitively divergent configurations can be listed according to these partitions.

– If $N_{\text{ext}} = 1$,

$$P_a(\mathcal{G}) = \dim G_D (C_{\partial\mathcal{G}} - 1) - \frac{1}{2}(\dim G_D - 2a)\left(k_{\max} - 1 - \sum_{k=1}^{k_{\max}-2} k V_{k_{\max}-k}\right). \tag{B.5}$$

Then, it may exist some configurations such that $V_{k_{\max}-k} = 0$ for all $k = 1, \ldots, k_{\max} - 2$. Having $N_{\text{ext}} = 1$ such that $C_{\partial\mathcal{G}} = 1$, we infer

$$\omega_{\text{d}}(\mathcal{G}) = -2 \dim G_D g_{\tilde{\mathcal{G}}} + \frac{1}{2}(\dim G_D - 2a)(k_{\max} - 1). \tag{B.6}$$

Therefore it may exist 1-point function configurations which are divergent. Indeed, take the planar tadpole of the $({}_1\Phi_2^3, a = \frac{1}{6})$ model. It diverges as $\Lambda^{\frac{2}{3}}$. Thus (B.6) could generate a new type of anomalous terms of the vector form. A non-invariant interaction vertex which could be introduced is of the form $S_1^{\text{int}} = \text{tr}(\varphi) = \sum_a \varphi_{aa}$. Another way to proceed is to combine both vector and matrix fields in the initial action. One then has to consider this situation with all the care needed by performing the multi-scale analysis from the beginning for this new class of mixed rank models ((vector+matrix)-models).

Appendix C: Primitively Divergent Graphs for the $(_{\dim G_D}\Phi_2^8, a)$ Model

We now provide a complete application of the method of finding primitively divergent graphs for the nontrivial order $k_{\max} = 8$ in the matrix model $(_{\dim G_D}\Phi_2^8, a)$.

It can be simply proved that $N_{\text{ext}} > 8$ yields a convergent amplitude. $N_{\text{ext}} = 8$ leads to a log–divergent amplitude if and only if $g_{\tilde{\mathcal{G}}} = 0$, and $V_6 = V_4 = V_{2;1} = 0$ and $C_{\partial\mathcal{G}} = 1$.

– For $N_{\text{ext}} = 6$, we can write

$$\begin{aligned} P_a(\mathcal{G}) &= \dim G_D(C_{\partial\mathcal{G}} - 1) + \frac{1}{2}\Big[2\dim G_D + (2a - \dim G_D)(8-2)\Big](V_6 - 1) \\ &\quad + \frac{1}{2}\Big[2\dim G_D + (2a - \dim G_D)(8-4)\Big]V_4 \\ &\quad + \frac{1}{2}\Big[2\dim G_D + (2a - \dim G_D)(8-6)\Big]V_{2;1} \\ &= \dim G_D(C_{\partial\mathcal{G}} - 1) - \frac{1}{2}(\dim G_D - 2a)\Big(-2(V_6 - 1) - 4V_4 - 6V_{2;1}\Big). \end{aligned} \tag{C.1}$$

(8j) Seeking solution of $P_a(\mathcal{G}) = 0$, we have $V_6 = 1$, $V_4 = 0 = V_{2;1}$ and $C_{\partial\mathcal{G}} = 1$, giving log–divergent graphs if $g_{\tilde{\mathcal{G}}} = 0$.

(8l) Solutions of $P_a(\mathcal{G}) = (2a - \dim G_D)$ are given by $C_{\partial\mathcal{G}} = 1$, $V_6 = 0$, $V_4 = 0 = V_{2;1}$. This case gives divergent graphs with $\omega_{\text{d}}(\mathcal{G}) = \dim G_D - 2a$, if $g_{\tilde{\mathcal{G}}} = 0$.

– For $N_{\text{ext}} = 4$, we have

$$\begin{aligned} P_a(\mathcal{G}) &= \dim G_D(C_{\partial\mathcal{G}} - 1) + \frac{1}{2}\Big[2\dim G_D + (2a - \dim G_D)(8-2)\Big]V_6 \\ &\quad + \frac{1}{2}\Big[2\dim G_D + (2a - \dim G_D)(8-4)\Big](V_4 - 1) \\ &\quad + \frac{1}{2}\Big[2\dim G_D + (2a - \dim G_D)(8-6)\Big]V_{2;1} \\ &= \dim G_D(C_{\partial\mathcal{G}} - 1) - \frac{1}{2}(\dim G_D - 2a)\Big(-2V_6 - 4(V_4 - 1) - 6V_{2;1}\Big). \end{aligned} \tag{C.2}$$

(8m) Solving $P_a(\mathcal{G}) = 0$ yields a log–divergent amplitude if $g_{\tilde{\mathcal{G}}} = 0$ and if
  (8m1) $V_4 = 1, V_{2;1} = 0, V_6 = 0, C_{\partial\mathcal{G}} = 1$;
  (8m2) $V_4 = 0, V_{2;1} = 0, V_6 = 2, C_{\partial\mathcal{G}} = 1$ (corresponding to the partition of 4/2=2=1+1);
(8n) Solving $P_a(\mathcal{G}) = (2a - \dim G_D)$ yields a divergent amplitude with $\omega_{\mathrm{d}}(\mathcal{G}) = \dim G_D - 2a$ if $g_{\tilde{\mathcal{G}}} = 0$ and if $V_4 = 0, V_{2;1} = 0, C_{\partial\mathcal{G}} = 1$, and $V_6 = 1$ (corresponding to the trivial partition of 1=1+0);
(8o) Solving $P_a(\mathcal{G}) = 2(2a - \dim G_D)$ yields a divergent amplitude with $\omega_{\mathrm{d}}(\mathcal{G}) = 2(\dim G_D - 2a)$ if $g_{\tilde{\mathcal{G}}} = 0$ and if $V_4 = 0, V_{2;1} = 0, C_{\partial\mathcal{G}} = 1$, and $V_6 = 0$.
– For $N_{\mathrm{ext}} = 2$, it can be written

$$P_a(\mathcal{G}) = \dim G_D (C_{\partial\mathcal{G}} - 1) - \frac{1}{2}(\dim G_D - 2a)\Big(- 2V_6 - 4V_4 - 6(V_{2;1} - 1)\Big). \tag{C.3}$$

(8p) Solving $P_a(\mathcal{G}) = 0$ yields a log–divergent amplitude if $g_{\tilde{\mathcal{G}}} = 0$ and if
  (8p1) $V_{2;1} = 1, V_6 = 0, V_4 = 0, C_{\partial\mathcal{G}} = 1$;
  (8p2) $V_{2;1} = 0, V_6 = 3, V_4 = 0, C_{\partial\mathcal{G}} = 1$ (corresponding to the partition of 3=1+1+1);
  (8p3) $V_{2;1} = 0, V_6 = 1, V_4 = 1, C_{\partial\mathcal{G}} = 1$ (corresponding to the partition of 3=1+2);
(8q) Solving $P_a(\mathcal{G}) = (2a - \dim G_D)$ yields a divergent amplitude with $\omega_{\mathrm{d}}(\mathcal{G}) = \dim G_D - 2a$ if $g_{\tilde{\mathcal{G}}} = 0$ and if
  (8q1) $V_{2;1} = 0, V_6 = 2, V_4 = 0, C_{\partial\mathcal{G}} = 1$ (corresponding to the partition of 2=1+1);
  (8q2) $V_{2;1} = 0, V_6 = 0, V_4 = 1, C_{\partial\mathcal{G}} = 1$ (corresponding to the trivial partition of 2=2+0);
(8r) Solving $P_a(\mathcal{G}) = (2a - \dim G_D)2$ yields a divergent amplitude with $\omega_{\mathrm{d}}(\mathcal{G}) = 2(\dim G_D - 2a)$ if $g_{\tilde{\mathcal{G}}} = 0$ and if $V_{2;1} = 0, V_6 = 1, V_4 = 0, C_{\partial\mathcal{G}} = 1$ (corresponding to the partition of 1=1+0);
(8r) Solving $P_a(\mathcal{G}) = (2a - \dim G_D)3$ yields a divergent amplitude with $\omega_{\mathrm{d}}(\mathcal{G}) = 3(\dim G_D - 2a)$ if $g_{\tilde{\mathcal{G}}} = 0$ and if $V_{2;1} = 0, V_6 = 0, V_4 = 0, C_{\partial\mathcal{G}} = 1$.

Table 9 gives the list of primitively divergent graph for the ${}_{\dim G_D}\Phi^8_2$ models.

Table 9. List of primitively divergent graphs of matrix models ${}_{\dim G_D}\Phi^8_2$

N_{ext}	$V_{2;1}$	V_4	V_6	$C_{\partial\mathcal{G}} - 1$	$g_{\tilde{\mathcal{G}}}$	$\omega_{\mathrm{d}}(\mathcal{G})$
8	0	0	0	0	0	0
6	0	0	0	0	0	$\dim G_D - 2a$
6	0	0	1	0	0	0
4	0	0	0	0	0	$2(\dim G_D - 2a)$
4	0	0	1	0	0	$\dim G_D - 2a$
4	0	1	0	0	0	0
4	0	0	2	0	0	0
2	0	0	0	0	0	$3(\dim G_D - 2a)$
2	0	0	1	0	0	$2(\dim G_D - 2a)$
2	0	1	0	0	0	$\dim G_D - 2a$
2	0	0	2	0	0	$\dim G_D - 2a$
2	1	0	0	0	0	0
2	0	1	1	0	0	0
2	0	0	3	0	0	0

References

1. Di Francesco, P., Ginsparg, P.H., Zinn-Justin, J.: 2-D Gravity and random matrices. Phys. Rep. **254**, 1 (1995). [arxiv:hep-th/9306153]
2. Ambjorn, J., Durhuus, B., Jonsson, T.: Three-dimensional simplicial quantum gravity and generalized matrix models. Mod. Phys. Lett. A **6**, 1133 (1991)
3. Gross, M.: Tensor models and simplicial quantum gravity in $>$ 2-D. Nucl. Phys. Proc. Suppl. **25**, 144 (1992)
4. Sasakura, N.: Tensor model for gravity and orientability of manifold. Mod. Phys. Lett. A **6**, 2613 (1991)
5. Konopka, T., Markopoulou, F., Smolin, L.: Quantum Graphity. hep-th/0611197
6. 't Hooft, G.: A planar diagram theory for strong interactions. Nucl. Phys. B **72**, 461 (1974)
7. Kazakov, V.A.: Bilocal regularization of models of random surfaces. Phys. Lett. B **150**, 282 (1985)
8. David, F.: A model of random surfaces with nontrivial critical behavior. Nucl. Phys. B **257**, 543 (1985)
9. Knizhnik, V.G., Polyakov, A.M., Zamolodchikov, A.B.: Fractal structure of 2D quantum gravity. Mod. Phys. Lett. A **3**, 819 (1988)
10. David, F.: Conformal field theories coupled to 2D gravity in the conformal gauge. Mod. Phys. Lett. A **3**, 1651 (1988)
11. Distler, J., Kawai, H.: Conformal field theory and 2D quantum gravity or who's afraid of Joseph Liouville? Nucl. Phys. B **321**, 509 (1989)
12. Duplantier, B.: Conformal Random Geometry. In: Bovier, A., Dunlop, F., den Hollander, F., van Enter, A., Dalibard, J. (eds.) Les Houches, Session LXXXIII, 2005. Mathematical Statistical Physics, pp. 101–217. Elsevier B. V., Amsterdam (2006). [arXiv:math-ph/0608053]
13. Duplantier, B.: The Hausdorff dimension of two-dimensional quantum gravity. arXiv:1108.3327 [math-ph]
14. Duplantier, B., Sheffield, S.: Schramm Loewner evolution and Liouville quantum gravity. Phys. Rev. Lett. **107**, 131305 (2011). [arXiv:1012.4800 [math-ph]]
15. Miermont, G.: The Brownian map is the scaling limit of uniform random plane quadrangulations. Acta Math. **210**, 319–401 (2013). [arXiv:1104.1606 [math.PR]]
16. Curien, N., Le Gall, J.-F., Miermont, G.: The Brownian Cactus I. Scaling limits of discrete cactuses. Ann. Inst. H. Poincaré Probab. Stat. **49**, 307–609 (2013). [arXiv:1102.4177 [math.PR]]
17. Le Gall, J.-F., Miermont, G.: Scaling limits of random trees and planar maps. In: Probability and Statistical Physics in Two or More Dimensions (Búzios, 2010), Clay Mathematics Proceedings, vol. 15, pp. 155–211. American Mathematical Society, Providence (2012) arXiv:1101.4856 [math.PR]
18. Le Gall, J.-F., Miermont, G.: Scaling limits of random planar maps with large faces. Ann. Probab. **39**, 1–69 (2011). arXiv:0907.3262 [math.PR]
19. Boulatov, D.V.: A model of three-dimensional lattice gravity. Mod. Phys. Lett. A **7**, 1629 (1992). [hep-th/9202074]
20. Ooguri, H.: Topological lattice models in four-dimensions. Mod. Phys. Lett. A **7**, 2799 (1992). [hep-th/9205090]
21. Oriti, D.: The group field theory approach to quantum gravity. In: Oriti, D. (ed.) Approaches to Quantum Gravity: Toward a New Understanding of Space, Time and Matter, pp 310–331. Cambridge University Press, Cambridge (2009). [gr-qc/0607032]
22. Oriti, D.: A quantum field theory of simplicial geometry and the emergence of spacetime. J. Phys. Conf. Ser. **67**, 012052 (2007). [hep-th/0612301]
23. Gurau, R.: The 1/N expansion of colored tensor models. Annales Henri Poincare **12**, 829 (2011). [arXiv:1011.2726 [gr-qc]]
24. Gurau, R., Rivasseau, V.: The 1/N expansion of colored tensor models in arbitrary dimension. Europhys. Lett. **95**, 50004 (2011). [arXiv:1101.4182 [gr-qc]]
25. Gurau, R.: The complete 1/N expansion of colored tensor models in arbitrary dimension. Annales Henri Poincare **13**, 399 (2012). [arXiv:1102.5759[gr-qc]]
26. Gurau, R.: Colored group field theory. Commun. Math. Phys. **304**, 69 (2011). [arXiv:0907.2582 [hep-th]]
27. Gurau, R.: Topological graph polynomials in colored group field theory. Annales Henri Poincare **11**, 565 (2010). [arXiv:0911.1945 [hep-th]]
28. Gurau, R.: Lost in translation: topological singularities in group field theory. Class. Quantum Gravity **27**, 235023 (2010). [arXiv:1006.0714 [hep-th]]
29. Gurau, R., Ryan, J.P.: Colored tensor models—a review. SIGMA **8**, 020 (2012). [arXiv:1109.4812 [hep-th]]
30. Bonzom, V., Gurau, R., Riello, A., Rivasseau, V.: Critical behavior of colored tensor models in the large N limit. Nucl. Phys. B **853**, 174 (2011). [arXiv:1105.3122 [hep-th]]
31. Gurau, R., Ryan, J.P.: Melons are branched polymers. Annates Henri Poincaré (to appear, 2014). arXiv:1302.4386 [math-ph]

32. Gurau, R.: The 1/N expansion of tensor models beyond perturbation theory. Commun. Math. Phys., online first. doi:10.1007/s00220-014-1907-2, arXiv:1304.2666 [math-ph]
33. Bonzom, V., Gurau, R., Rivasseau, V.: The ising model on random lattices in arbitrary dimensions. Phys. Lett. B **711**, 88 (2012). [arXiv:1108.6269 [hep-th]]
34. Benedetti, D., Gurau, R.: Phase transition in dually weighted colored tensor models. Nucl. Phys. B **855**, 420 (2012). [arXiv:1108.5389[hep-th]]
35. Gurau, R.: The double scaling limit in arbitrary dimensions: a toy model. Phys. Rev.D **84**, 124051 (2011). [arXiv:1110.2460 [hep-th]]
36. Gurau, R.: A generalization of the Virasoro algebra to arbitrary dimensions. Nucl. Phys. B **852**, 592 (2011). [arXiv:1105.6072 [hep-th]]
37. Gurau, R.: The Schwinger Dyson equations and the algebra of constraints of random tensor models at all orders. Nucl. Phys. B **865**, 133 (2012). [arXiv:1203.4965 [hep-th]]
38. Gurau, R.: Universality for random tensors. accepted for pubilcation by Annales de l'Institut Henri Poincaré (B) Probability and Statistics, arXiv:1111.0519[math.PR]
39. Gurau, R.: A review of the large N limit of tensor models. arXiv:1209.4295 [math-ph]
40. Gurau, R.: A review of the 1/N expansion in random tensor models. In: Proceedings ot the 17th International Congress on Mathematical Physics (ICMP12). arXiv:1209.3252 [math-ph]
41. Bonzom, V., Gurau, R., Rivasseau, V.: Random tensor models in the large N limit: uncoloring the colored tensor models. Phys. Rev. D **85**, 084037 (2012). [arXiv:1202.3637 [hep-th]]
42. Gordan, P.: Beweis, dass jede Covariante und Invariante einer binären Form eine ganze Function mit numerischen Coefficienten einer endlichen Anzahl solcher Formen ist. J. Reine Angew. Math. **69**, 323–354 (1868). (Available at the Gottinger DigitalisierungsZentrum (GDZ), at http://gdz.sub.uni-goettingen.de/en/gdz/.)
43. Abdesselam, A.: On the volume conjecture for classical spin networks. J. Knot Theory Ramif. **21** (3), 1250022 (2012)
44. Ben Geloun, J., Rivasseau, V. A renormalizable 4-dimensional tensor field theory. Commun. Math. Phys. **318**, 69 (2013). [arXiv:1111.4997[hep-th]]
45. Ben Geloun, J., Rivasseau, V.: Addendum to 'A Renormalizable 4-Dimensional Tensor Field Theory'. Commun. Math. Phys. **322**, 957 (2013). [arXiv:1209.4606 [hep-th]]
46. Rivasseau, V.: Towards renormalizing group field theory. PoS C **NCFG2010**, 004 (2010). [arXiv:1103.1900 [gr-qc]]
47. Rivasseau, V.: Quantum gravity and renormalization: the tensor track. AIP Conf. Proc. **1444**, 18 (2011). [arXiv:1112.5104 [hep-th]]
48. Rivasseau, V.: The tensor track: an update. arXiv:1209.5284 [hep-th]
49. Grosse, H., Wulkenhaar, R.: Renormalisation of phi**4 theory on noncommutative R**4 in the matrix base. Commun. Math. Phys. **256**, 305 (2005). [hep-th/0401128]
50. Rivasseau, V.: Non-commutative renormalization. In: Duplantier, B., Rivasseav, V. (eds.) Quantum Spaces (séininaire Poincaré X), pp. 19–107. Bikhäuser, Basel (2007) arXiv:0705.0705 [hep-th]
51. Rivasseau, V.: From perturbative to constructive renormalization. Princeton series in Physics. Princeton University Press, Princeton (1991)
52. Ben Geloun, J., Magnen, J., Rivasseau, V.: Bosonic colored group field theory. Eur. Phys. J. C **70**, 1119 (2010). [arXiv:0911.1719 [hep-th]]
53. Ben Geloun, J., Krajewski, T., Magnen, J., Rivasseau, V.: Linearized group field theory and power counting theorems. Class. Quantum Gravity **27**, 155012 (2010). [arXiv:1002.3592 [hep-th]]
54. Ben Geloun, J., Gurau, R., Rivasseau, V.: EPRL/FK group field theory. Europhys. Lett. **92**, 60008 (2010). [arXiv:1008.0354 [hep-th]]
55. Ben Geloun, J., Bonzom, V.: Radiative corrections in the Boulatov–Ooguri tensor model: the 2-point function. Int. J. Theor. Phys. **50**, 2819 (2011). [arXiv:1101.4294 [hep-th]]
56. Ben Geloun, J., Samary, D.O.: 3D tensor field theory: renormalization and one-loop β-functions. Annales Henri Poincare **14**, 1599 (2013). [arXiv:1201.0176 [hep-th]]
57. Ben Geloun, J., Livine, E.R.: Some classes of renormalizable tensor models. J. Math. Phys. **54**, 082303 (2013). [arXiv:1207.0416 [hep-th]]
58. Ben Geloun, J.: Two and four-loop β-functions of rank 4 renormalizable tensor field theories. Class. Quantum Gravity **29**, 235011 (2012). [arXiv:1205.5513 [hep-th]]
59. Carrozza, S., Oriti, D., Rivasseau, V.: Renormalization of tensorial group field theories: Abelian U(1) models in four dimensions. Commun. Math. Phys. **327**, 603 (2014). [arXiv:1207.6734 [hep-th]]
60. Samary, D.O., Vignes-Tourneret, F.: Just renormalizable TGFT's on $U(1)^d$ with gauge invariance. Commun. Math. Phys. **329**(2), 545–578 (2014). [arXiv:1211.2618 [hep-th]]
61. Carrozza, S., Oriti, D., Rivasseau, V.: Renormalization of an SU(2) tensorial group field theory in three dimensions. Commun. Math. Phys. (to appear, 2014). [arXiv:1303.6772 [hep-th]]

62. Samary, D.O.: Beta functions of $U(1)^d$ gauge invariant just renormalizable tensor models. Phys. Rev. D **88**, 105003 (2013). [arXiv:1303.7256 [hep-th]]
63. Grosse, H., Wulkenhaar, R.: Self-dual noncommutative ϕ^4-theory in four dimensions is a non-perturbatively solvable and non-trivial quantum field theory. Commun. Math. Phys. **329**(3), 1069–1130 (2014) arXiv:1205.0465 [math-ph]
64. Avohou, R.C., Ben Geloun, J., Hounkonnou, M.N.: A polynomial invariant for rank 3 weakly-colored stranded graphs. arXiv:1301.1987 [math.CO]
65. Ryan, J.P.: Tensor models and embedded Riemann surfaces. Phys. Rev. D **85**, 024010 (2012). [arXiv:1104.5471 [gr-qc]]
66. Bollobas, B., Riordan, O.: A polynomial of graphs on surfaces. Math. Ann. **323**, 81–96 (2002)
67. Kontsevich, M.: Intersection theory on the moduli space of curves and the matrix Airy function. Commun. Math. Phys. **147**, 1–23 (1992)
68. Rivasseau, V.: The Tensor Track, III. Fortschr. Phys. **62**(2), 81–107 (2014) arXiv:1311.1461 [hep-th]
69. Gallavotti, G., Nicolo, F.: Renormalization theory in four-dimensional scalar fields. I. Commun. Math. Phys. **100**, 545 (1985)
70. Ben Geloun, J., Ramgoolam, S.: Counting tensor model observables and branched covers of the 2-sphere. Ann. Inst. Henri Poincaré, D **1**(1), 77–138 (2014) arXiv:1307.6490 [hep-th]
71. Disertori, M., Gurau, R., Magnen, J., Rivasseau, V.: Vanishing of beta function of non commutative phi**4(4) theory to all orders. Phys. Lett. B **649**, 95 (2007). [hep-th/0612251]
72. Ben Geloun, J., Gurau, R., Rivasseau, V.: Vanishing beta function for Grosse–Wulkenhaar model in a magnetic field. Phys. Lett. B **671**, 284 (2009). [arXiv:0805.4362 [hep-th]]
73. Feldman, J., Trubowitz, E.: The flow of an electron–phonon system to the superconducting state. Helvetica Physica Acta **64**, 214 (1991)

Communicated by A. Connes